Supersymmetric Orientifolds with D-branes at Angles

Dissertation
zur
Erlangung des Doktorgrades (Dr. rer. nat.)
der
Mathematisch-Naturwissenschaftlichen Fakultät
der
Rheinischen Friedrich-Wilhelms-Universität Bonn

vorgelegt von

Ralph Schreyer

aus
Remagen

Bonn, November 2001

Angefertigt mit Genehmigung der Mathematisch-Naturwissenschaftlichen Fakultät der Rheinischen Friedrich-Wilhelms-Universität Bonn

1. Referent:	Prof. Dr. Hans-Peter Nilles
2. Referent:	Prof. Dr. Herbert K. Dreiner
Tag der Promotion:	21. Dezember 2001

Abstract

We show the construction and detailed calculation of $\mathcal{N}=1$ supersymmetric orientifold compactifications of type IIB string theory to six dimensions and type IIA string theory to four dimensions. The orbifold group in the six dimensional models is $\mathbb{Z}_N$ and in the four dimensional models $\mathbb{Z}_N \times \mathbb{Z}_M$. In addition, worldsheet parity Ω in combination with the complex conjugation $\mathcal{R}$ in the compact directions, which are chosen to be direct products of two-tori, is modded out. This naturally leads to the inclusion of D-branes intersecting at angles in the compact directions. Gauge theories are known to live on the worldvolume of D-branes and chiral fermions are expected to be localized at the intersection points. This opens up the possibility to construct new phenomenologically interesting compactifications of string theory. However, the four dimensional models under consideration lead to non-chiral spectra. This is a consequence of the symmetric choice of placing the D-branes on top of the orientifold fixed planes. Nevertheless, a generalization of our model presented in the recent literature has led to a $\mathcal{N}=1$ supersymmetric compactification to four dimensions including the SM gauge group and three families of chiral fermions. As a more formal aspect, we focus on the case of $\mathbb{Z}_2$ in the six dimensional and $\mathbb{Z}_2 \times \mathbb{Z}_2$ in the four dimensional $\Omega\mathcal{R}$ orientifolds to explicitely present models T-dual to known Ω orientifolds. The equivalence of the massless spectra is verified. In addition to the standard consistency conditions from tadpole cancellation, we obtain constraints for some of the models from worldsheet duality using the boundary state formalism.

Acknowledgements

First of all, I would like to thank Prof. Hans-Peter Nilles for supporting and guiding me during the four years I spent in his group. The atmosphere was always inspiring and open minded and provided me with an insight into scientific life.
I would like to thank the Fritz-ter-Meer-Stiftung and the Richard-Winter-Stiftung for financial support.
I am very thankful to Gabriele Honecker and Dr. Stefan Förste for a fruitful collaboration during the last years and numberless hours of instructive discussions in our offices. In addition, I would like to thank both of them and Martin Walter for proofreading.
Furthermore, I am very grateful to Jan O. Conrad for patiently introducing me into the world of orbifold constructions (and FreeBSD) and to Andreas Wißkirchen who keeps many things going in our institute.
Many thanks to the numerous members of Hans-Peter Nilles' group for always having an open ear for questions and simply having a good time.
All this would not have been possible without the support and love from my parents Theresia and Gerold, my sister Yvonne, my partner in life Angela and my family and friends.

Contents

Chapter 1

Introduction

In this thesis, we present orientifold compactifications of type II superstring theories with D-branes intersecting at angles. Before specifying these terms, we would like to review some of the important developments in string theory, thereby focussing on orientifolds, in order to put this thesis in a proper context.

Quantum field theories in general and especially the standard model of elementary particles (SM) appear to be incompatible with general relativity. String theory overcomes this problem by viewing the elementary particles as one dimensional extended objects ('strings'), leading to several consistent perturbative descriptions in ten dimensional spacetime, namely the type IIA, type IIB, type I $SO(32)$, heterotic $SO(32)$ and heterotic $E_8 \times E_8$ superstring theories. For introductory textbooks consider [49, 50, 67, 68, 63]. The type II theories [46, 76] are $\mathcal{N} = 2$ supersymmetric, whereas the others are $\mathcal{N} = 1$ supersymmetric in ten dimensions. Among these theories, only type IIA theory is non-chiral. Crucial for the development of string theory was the result that the type I $SO(32)$ theory is free of anomalies [48] and the formulation of the heterotic theories [53, 51, 52], because now gauge groups came into play which comprised the SM gauge group. In the following years, the focus was on compactifying these theories to $\mathcal{N} = 1$ supersymmetric theories in four dimensions, either by compactification on Calabi-Yau spaces [25, 81] or on orbifolds [34, 35]. One is interested in keeping $\mathcal{N} = 1$ supersymmetry in four dimensions, because this is a possible solution of the hierarchy problem[1]. Orbifold compactifications of the heterotic $E_8 \times E_8$ superstring turned out to be phenomenologically interesting, because in these setups $\mathcal{N} = 1$ supersymmetric models in four dimensions with three generations of chiral fermions and a gauge group close to the SM were found [59, 38, 39]. For a long period of time it was common sense that the five superstring theories are distinct, that the heterotic $E_8 \times E_8$ theory might be realized in nature and that it remains to find the correct vacuum and the reason

[1]Nevertheless, a fully realistic theory has to provide mechanisms to break supersymmetry in the end.

for this vacuum to be implemented.

This picture changed dramatically when the assumed distinct string theories were found to be connected by a web of dualities. E.g. type IIA and type IIB as well as the heterotic $SO(32)$ and $E_8 \times E_8$ theories are T-dual to each other [32, 45]. The $SO(32)$ type I and heterotic theories are conjectured to be related by a strong/weak coupling dualtity [84, 72]. The deeper reason for these dualities is seen in the conjecture that all known superstring theories are ten dimensional perturbative descriptions of an underlying eleven dimensional theory, called M-theory [83]. M-theory itself is still unknown, but its low energy limit is described by eleven dimensional supergravity [27, 64]. The link to eleven dimensions comes about because eleven dimensional supergravity seems to arise as the low energy limit in the strong coupling region of type IIA string theory [82, 84]. In a similar fashion, the strong coupling region of the heterotic $E_8 \times E_8$ theory seems to be governed by eleven dimensional supergravity on an interval, where each of the E_8 gauge groups is restricted to a ten dimensional boundary [57, 56, 26]. Interesting phenomenological implications are discussed in [65, 66].

In these recent developments, D-branes [69, 70, 13] have played an important role. D-branes[2] can be defined by the fact that open strings can end upon them, which is equivalent to impose Dirichlet boundary conditions on the ends of open strings, which in turn can be viewed as topological defects. In this sense, namely as backgrounds for open string compactifications, D-branes were already discussed in [73, 54, 32], but in these early studies their status of intrinsic non-perturbative excitations was not fully appreciated. Dp-branes carry Ramond-Ramond (RR) charges and thus couple naturally to $p+1$ RR forms. Since fundamental strings do not provide RR sources and since they are the only quanta of string perturbation theory, Dp-branes must arise as non-perturbative solitonic solutions. For a presentation of branes from the viewpoint as solitonic solutions of supergravity theories (p-branes), consider e.g. [36]. Note, that the heterotic theories do not contain any RR forms and therefore no D-branes. The reason why D-branes are so important in establishing various dualities lies in the fact that Dp-branes, which naturally couple to the $p+1$ forms of the underlying theory, are BPS states and therefore are stable under duality transformations, such that they provide strong arguments for the conjectured dualities. For stable non-BPS states, consider e.g. [78]. There are many other important applications of D-branes, which in principle rely on the fact that D-branes reveal relations between supersymmetric gauge theories, which naturally live on their worldvolumes, and geometry.

Let us sketch the connection between type I string theory, which has $SO(32)$ as a gauge group and type IIB, which has no non-abelian gauge group. This connection can be established by the use of D-branes. Type IIB is invariant

[2]D-branes are extended objects with a $p+1$ dimensional worldvolume, i.e. p spatial and one time dimension and therefore are often denoted by Dp-branes.

under the worldsheet parity Ω, which interchanges the left and the right movers of the closed strings. If we mod out Ω, we obtain a theory of unoriented closed strings, which is inconsistent because its partition function diverges. This inconsistency can be viewed in another way: There exists an extended object which is invariant under Ω, the so called 'orientifold fixed plane' (O-plane). This O-plane is extended in the whole ten dimensional space time and therefore called O9-plane. It carries a physical charge which has to be cancelled to render the theory consistent. This can be achieved by adding 32 D9-branes, which fill the whole spacetime, as well. N D-branes lying on top of each other generate a gauge group $U(N)$ on their shared worldvolume. But Ω gives rise to a projection condition, such that we end up with $SO(32)$ as a gauge group. Remember, that D-branes are defined by the fact that open strings can end upon them. Putting all this together, we end up with an $\mathcal{N}=1$ supersymmetric (Ω projects out half of the supersymmetries) theory of unoriented closed and open strings with $SO(32)$ as a gauge group, i.e. type I string theory. We can summarize this paragraph as follows: Type I theory is an orientifold of type IIB theory with a certain background of D-branes. Now we have established the connection to the terms 'orientifolds' and 'D-branes' in the title of this work. Therefore we stop to describe the general development in string theory and mainly concentrate on the various orientifold and orbifold compactifications of type I and type II theories containing D-branes in the following.

The fact that gauge theories live on the worldvolume of D-branes, as mentioned above, served as a new starting point on the way to construct phenomenologically interesting compactifications of string theory. After some early publications on orientifold constructions [75, 73, 47, 55, 17, 18], the six dimensional $\Omega \times \mathbb{Z}_2$ orientifold of type IIB presented in [44] clarified the role of D-branes in these models and triggered the development in this field. For consistency, i.e. to satisfy the so called 'tadpole cancellation conditions', the model contains 16 D9- and 16 D5-branes, leading to a maximal gauge group of $U(16) \times U(16)$ if all D5-branes are placed on one fixed point. Moving away the D5-branes from the fixed points (in a manner compatible with the symmetries of the theory) higgses the factor of the gauge group which corresponds to the D5-branes. In [43], the orbifold group is generalized to $\mathbb{Z}_N$. Similar models are discussed in [30, 31]. All these models are $\mathcal{N}=1$ supersymmetric in six dimensions. In [15] a four dimensional $\mathcal{N}=1$ supersymmetric $\Omega \times \mathbb{Z}_2 \times \mathbb{Z}_2$ orientifold of type IIB is constructed. In [85] the generalization to the orbifold group $\mathbb{Z}_N \times \mathbb{Z}_M$ is performed and in [1] a systematic discussion of four dimensional $\mathcal{N}=1$ orientifolds of type IIB is presented, consider also the references therein. Further supersymmetric orientifolds in four dimensions are presented in [6, 62, 60]. Some of the models are chiral and the tadpole cancellation conditions turn out to be very restrictive. In [1] the relationship between tadpole and anomaly cancellation in these type IIB models is discussed and [28] includes non-abelian Wilson lines to obtain a model with three generations of chiral fermions. However, the gauge groups and the matter content of all these models are still far away from the SM (or rather the minimal supersymmetric SM, the MSSM).

In [5] six and four dimensional type IIB orientifolds including D-branes and anti-D-branes have been constructed. Due to the presence of the anti-D-branes, supersymmetry is completely broken at the string scale. To avoid the reintroduction of the hierarchy problem, the string scale is lowered to about a TeV by the approach of large compact dimensions [9, 11, 33, 10]. In [4], type IIB orientifolds with D- and anti-D-branes are presented which lead to models remarkably close to the SM. However, in these kinds of models, there exist moduli which could drive the configuration into regions where tachyons develop in the open string sector. Therefore one has to take care of the stability of these models and runs into the unsolved problems of either providing suitable potentials for the moduli or considering tachyon condensation [77, 79, 80]. Nevertheless, these models provide first examples of SM-like compactifications of type I theory. First attempts to discuss the issue of stability in these kinds of orientifolds are presented in [8, 74].

In the following paragraphs, we would like to consider type II compactifications with D-branes intersecting at angles. The models presented in this thesis are members of this class. In [14], it is observed that D-branes intersecting at angles may give rise to chiral fermions living at the intersection points. If the intersecting D-branes are not related by any symmetry of the underlying theory, the fermions living at the intersection points are charged under the bifundamental representation of the gauge groups on the corresponding D-branes. Apart from that, the multiplicity of the intersection points may serve as a natural explanation for the replication of families. These features opened a new way for the construction of phenomenologically interesting stringtheoretical models and constituted the main motivation for our studies.

In [20, 7], six dimensional $\mathcal{N} = 1$ supersymmetric $\Omega\mathcal{R} \times \mathbb{Z}_N$ orientifolds of type IIB with D7-branes at angles are introduced. The additional operation $\mathcal{R}$ in the orientifold group is the complex conjugation in the compact space. This implies that the O-planes are now O7-planes intersecting at angles and thus the most obvious way to cancel the tadpoles is to include D7-branes on top of the O7-planes. This means that the intersection angles in these models appear naturally, which otherwise have to be introduced by hand.

In chapter 2 of this thesis, we present the detailed calculations of all these models. Special emphasis is put on the case of $\mathbb{Z}_2$, which has not been explicitely discussed in [20, 7]. For a particular choice of the lattices in the compact directions, this model is T-dual to [44] and we check that the massless spectra are the same. As explained above, dualities are an important and powerful concept in the recent developments in string theory and with the explicit construction of a model T-dual to [44] we hope to shed some light on this aspect. For $\mathbb{Z}_{3,4,6}$, the

$\Omega\mathcal{R}$ orientifolds are T-dual to asymmetric Ω orientifolds, see [7, 21] for details.

As mentioned above, our main motivation is to construct phenomenologically interesting models and therefore, of course, we have to discuss compactifications to four dimensions. The authors of [19] present four dimensional $\mathcal{N} = 1$ supersymmetric $\Omega\mathcal{R} \times \mathbb{Z}_N$ orientifolds, now of type IIA with D6-branes at angles on top of the orientifold planes. Inspired by these constructions, in [41] we presented four dimensional $\mathcal{N} = 1$ supersymmetric $\Omega\mathcal{R} \times \mathbb{Z}_N \times \mathbb{Z}_M$ type IIA orientifolds with D6-branes at angles. The detailed calculations for these models are shown in chapter 3. In the case of $\mathbb{Z}_2 \times \mathbb{Z}_2$, again for some special choice of the lattices in the compact directions, our model is T-dual to the model presented in [15]. We explicitely verify the equivalence of the massless spectra. With the construction of this model, we give another explicit example for T-duality. However, from the phenomenological point of view, these models could only serve as a first step, because the spectra are non-chiral and the gauge groups are quite restricted. The reason for this lies in the symmetric choice of positioning the D-branes on top of the O-planes.

The authors of [22, 23] try to solve this problem by considering similar models, but now with D-branes at arbitrary angles. They obtain four (and six) dimensional models with three generations of chiral fermions and gauge groups quite close to the SM. In [40], we consider a hybrid approach. We construct four dimensional $\Omega\mathcal{R} \times \mathbb{Z}_N$ orientifolds, where the D6-branes intersect at arbitrary angles in two of the six compact dimensions and the orbifold group acts in the remaining four compact dimensions. In this setup, we obtain chiral fermions and, in the case of $\mathbb{Z}_2$, give an explicit example which encloses the SM gauge group. In these setups all supersymmetries are broken and tachyons appear in the spectrum, such that one again has to examine the stability of these models. This analysis, together with a systematic study of a whole class of SM-like models and their phenomenological properties is performed in [24]. Similar models are discussed in [58]. At first sight, all these models do not allow large compact dimensions and thus suffer from the hierarchy problem. However, in [40] we point out that there might be a way out by taking into account the Fischler-Susskind mechanism [37] due to the non-vanishing NSNS tadpoles. An interesting link between tachyon condensation and the Higgs mechanism has been proposed in [3, 2], where non-supersymmetric toroidal compactifications of type IIB with D4-branes intersecting in two of the compact directions are presented. In the remaining compact directions, which can be chosen to be large to obtain a string scale of about a TeV, the D4-branes are sitting at singular points. Interestingly, some of the tachyons which appear in the spectrum carry the quantum numbers of the Higgs particle and the condensation of these tachyons may give rise to spontaneous symmetry breaking. However, much work has to be done for this mechanism to be understood properly.

Now we turn back to the supersymmetric $\Omega\mathcal{R}$ orientifolds. As mentioned above, our four dimensional $\mathcal{N} = 1$ supersymmetric $\Omega\mathcal{R} \times \mathbb{Z}_N \times \mathbb{Z}_M$ type IIA orientifolds with D6-branes at angles [41] lead to non-chiral spectra. Nevertheless, this work can be seen as an important contribution on the way towards phenomenologically relevant supersymmetric compactifications of type IIA theory using D-branes intersecting at angles. In a recent paper [29], our $\mathbb{Z}_2 \times \mathbb{Z}_2$ model which is discussed in each detail in section 3.2, is generalized by taking into account D6-branes not aligned with the orientifold planes. In this way, four dimensional $\mathcal{N} = 1$ supersymmetric models containing three families of chiral fermions and the SM gauge group are constructed.

As already mentioned above, a more formal aspect of D-branes is discussed in this thesis by explicitely constructing the models T-dual to [44] in the six dimensional case of $\mathbb{Z}_2$ and to [15] in the four dimensional case of $\mathbb{Z}_2 \times \mathbb{Z}_2$. Another important formal aspect is worldsheet duality, i.e. the equivalence of viewing the Klein bottle, the annulus and the Möbius strip diagrams as 1-loop or as tree channel diagrams, respectively. These diagrams contribute to the exchange of RR closed strings between D-branes and O-planes, which has to vanish for the orientifold construction to be consistent [48, 71]. The resulting conditions are called tadpole cancellation conditions. The easiest and standard way to obtain these conditions is to calculate the 1-loop amplitudes, perform the modular transformation to the tree channel and extract the contributions to the RR exchange. Because of worldsheet duality, the same result should be obtained if one calculates the amplitudes directly in the tree channel. To perform the direct tree channel calculation, one has to introduce the boundary state formalism [71, 42]. Now, a possible mismatch between the results from these two approaches may be due to the fact that all these methods are perturbative methods and that we miss contributions from non-perturbative states. This does not mean that the models where we obtain such a mismatch do not exist, but rather the perturbative description of these models is simply not valid and therefore, since we are still lacking the corresponding non-perturbative methods, we have to discard them [20]. As we will see, this violation of perturbative worldsheet duality will happen for some of the models and therefore imposes a constraint in addition to the tadpole cancellation conditions.

The contents of this thesis are organized as follows:

In chapter 2, we present the detailed calculations of the six dimensional $\mathcal{N} = 1$ supersymmetric $\Omega\mathcal{R} \times \mathbb{Z}_N$ orientifolds with D7-branes on top of the O7-planes. We begin with the general setup and review some important facts of orientifold constructions. Then we show the construction of the $\mathbb{Z}_2$ case in each detail, which is an explicit T-dual description of the model presented in [44]. The $\mathbb{Z}_2$ case has not been discussed in [20] and only briefly mentioned in [7]. Technical details necessary for the calculation of the 1-loop amplitudes are collected in appendix A and for the direct calculation of the tree channel amplitudes in appendix B. In appendix B, we also give a short introduction into the boundary state formalism, thereby focussing on the construction of the crosscap states. The cases $\mathbb{Z}_{3,4,6}$ have already been presented in the literature [20, 7] in more or less detail, but for completeness we collect the detailed calculations and results in appendix C.

Equipped with the technical knowledge, in chapter 3 we discuss all possible four dimensional $\mathcal{N} = 1$ supersymmetric $\Omega\mathcal{R} \times \mathbb{Z}_N \times \mathbb{Z}_M$ orientifolds with D6-branes on top of the O6-planes. This is an extended representation of the work we published in [41]. The case of $\mathbb{Z}_2 \times \mathbb{Z}_2$ is another explicit T-dual construction of a model already presented in the literature [15].

We end by giving a short summary and conclusions in chapter 4.

Parts of this thesis are published in

- [41]: S. Förste, G. Honecker and R. Schreyer, *Supersymmetric $\mathbb{Z}_N \times \mathbb{Z}_M$ orientifolds in 4d with D-branes at angles*, Nucl. Phys **B593** (2001), 127-154, hep-th/0008250.

Chapter 2

Six dimensional $\Omega\mathcal{R} \times \mathbb{Z}_N$ orientifolds

In this chapter, we present the construction of $\mathcal{N} = 1$ supersymmetric $\Omega\mathcal{R} \times \mathbb{Z}_N$ orientifolds of Type IIB in six dimensions with D7-branes at angles [20, 7]. The four compact dimensions are chosen to be a product of two-tori, where the orbifold group $\mathbb{Z}_N$ acts upon. The worldsheet parity Ω is accompanied by a reflection $\mathcal{R}$ of two of the four compact directions. We present a detailed calculation of all these models. Since the case of $\mathbb{Z}_2$ is only briefly mentioned in the literature, we will mainly concentrate on this case in the following. The detailed calculations and results for the cases $\mathbb{Z}_{3,4,6}$ are collected in appendix C for completeness.

2.1 The general setup

The models discussed in this chapter are six dimensional. The non-compact coordinates are called X^μ, where $\mu = 0, \ldots, 5$. We describe the four compact directions by two complex coordinates

$$Z^1 = X^6 + iX^7\,, \quad Z^2 = X^8 + iX^9\,. \tag{2.1}$$

We always choose the compact space to be a product of two two-tori $T_1 \times T_2$, where each T_i is described by the complex coordinate Z^i. The orientifold group is taken to be $G + \Omega\mathcal{R}G$, where the spacetime symmetry group (or orbifold group) is $G = \mathbb{Z}_N$, with $N \in \{2, 3, 4, 6\}$. The orbifold group acts on the compact coordinates as the rotation

$$\Theta : \quad Z^i \;\longrightarrow\; e^{2\pi i v_i} Z^i\,, \tag{2.2}$$

with $\Theta^N = \mathbb{1}$ and $i = 1, 2$ and $\vec{v} = \frac{1}{N}(1, -1)$, i.e. the geometry preserves $\mathcal{N} = 1$ supersymmetry in six dimensions. Ω is the well-known worldsheet parity which changes the orientation of the worldsheet, or, equivalently, interchanges left and right movers in the mode expansions of the closed string. Ω is accompanied by the reflection $\mathcal{R}$ of the 7th and 9th direction, expressed in complex coordinates

$$\mathcal{R}: \quad Z^i \quad \longrightarrow \quad Z^{\bar{i}}\,, \tag{2.3}$$

i.e. the complex conjugation ($\bar{i} = \bar{1}, \bar{2}$). Now we address the question of how this construction is related to other orientifold models. $\Omega\mathcal{R}$ is related to Ω by applying T-duality in the 7th and 9th direction, i.e.

$$T: \quad X_L^{7,9} + X_R^{7,9} \quad \longrightarrow \quad X_L^{7,9} - X_R^{7,9}\,, \tag{2.4}$$

expressed in complex coordinates

$$T: \quad Z_L^i + Z_R^i \quad \longrightarrow \quad Z_L^i + Z_R^{\bar{i}}\,. \tag{2.5}$$

Thus, the orbifold action $\hat{\Theta}$ becomes asymmetric on the T-dual torus, namely

$$\hat{\Theta} \equiv T\Theta T^{-1}: \quad Z_L^i + Z_R^i \quad \longrightarrow \quad e^{2\pi i v_i} Z_L^i + e^{-2\pi i v_i} Z_R^i\,. \tag{2.6}$$

i.e. in the cases $\mathbb{Z}_{3,4,6}$ T-duality in the 7th and 9th direction leads to Ω orientifolds with an asymmetric orbifold action. In [21], this T-duality is used to study the D-brane content of these asymmetric orientifolds. In the case of $\mathbb{Z}_2$, the orbifold action remains symmetric, of course, and the T-dual model should be the one presented in [44]. The gauging of the orientifold group creates orientifold fixed planes (O-planes). The location of these planes is given by sets of points fixed under the elements of $\Omega\mathcal{R} \times \mathbb{Z}_N$. These fixed planes carry RR charges which must be canceled by adding D-branes to the model [69]. For $\Theta = \mathbb{1}$, the O-plane obviously extends along the non-compact directions and the directions X^6 and X^8, i.e. the real parts of Z^i. To find the location of the remaining O-planes we note that

$$\Omega\mathcal{R}\,\Theta : Z^i \quad = \quad \Theta^{-\frac{1}{2}}\,\Omega\mathcal{R}\,\Theta^{\frac{1}{2}} : Z^i\,, \tag{2.7}$$

where the powers of $\pm\frac{1}{2}$ indicate that the rotations are performed with plus/minus half the angle as compared to (2.2). Thus, a fixed plane under $\Omega\mathcal{R}\Theta$ is obtained by acting with $\Theta^{-\frac{1}{2}}$ on the set of points fixed under $\mathcal{R}$. Therefore (starting from the O7-plane at $Z^i = \bar{Z}^i$, $i = 1, 2$), one obtains a set of O7-planes intersecting at angles, whose values are given by half the order of the corresponding $\mathbb{Z}_N$ element. As an example, the location of the O7-planes in the compact directions is shown in figure 2.1 for the case of $\mathbb{Z}_4$. Since all these O7-planes have compact transverse directions and carry RR charges, one expects that for consistency one needs to include a certain amount of D7-branes cancelling exactly those charges. The most obvious arrangement of D7-branes, namely to place them parallel to the O7-planes, turns out to yield a consistent model, as we will show in the following.

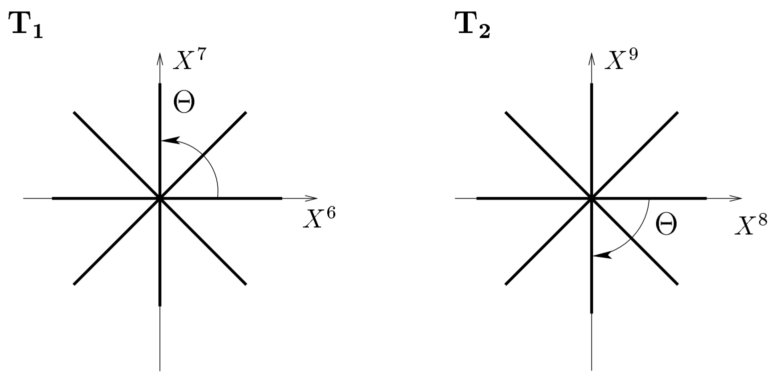

Figure 2.1: Location of O7-planes in the case of $\mathbb{Z}_4$. The intersection angle is half the angle of the corresponding rotation from the orbifold group.

But first we would like to clarify some aspects of this nice geometrical picture of D-branes intersecting at angles. Consider an open string starting and ending on the same D7-brane which is rotated by an angle φ with respect to X^6-axis on the torus T_1. The boundary conditions for this open string on both ends (i.e. at $\sigma = 0$ and $\sigma = \pi$) are given by mixed Neumann-Dirichlet conditions

$$\begin{aligned} \cos\varphi\,\partial_\sigma X^6 + \sin\varphi\,\partial_\sigma X^7 &= 0 \\ -\sin\varphi\,\partial_\tau X^6 + \cos\varphi\,\partial_\tau X^7 &= 0\,, \end{aligned} \tag{2.8}$$

or equivalently

$$\begin{aligned} \partial_\sigma X^6 + \tan\varphi\,\partial_\sigma X^7 &= 0 \\ \partial_\tau X^7 - \tan\varphi\,\partial_\tau X^6 &= 0\,. \end{aligned} \tag{2.9}$$

The second torus T_2 is treated similarly. Now, T-duality in the 7th and 9th direction takes the D7-branes into D9-branes and thus interchanges Neumann- and Dirichlet-boundary conditions in the 7th and 9th direction, i.e. (2.9) becomes

$$\begin{aligned} \partial_\sigma X^6 + \tan\varphi\,\partial_\tau X^7 &= 0 \\ \partial_\sigma X^7 - \tan\varphi\,\partial_\tau X^6 &= 0\,. \end{aligned} \tag{2.10}$$

With T_2 treated similarly, the boundary conditions (2.10) describe D9-branes with magnetic background flux $F = \tan\varphi$ [12, 22]. A special case is encountered if the D7-branes are aligned with the action of $\mathcal{R}$, i.e. if the D7-branes extend along 7th and the 9th direction. Performing T-duality in the 7th and 9th direction obviously transforms these D7-branes into D5-branes. By this means, the $\Omega\mathcal{R}$ orientifold in the case of $\mathbb{Z}_2$ is T-dual to an Ω orientifold with D9-branes and D5-branes which in turn is the D-brane content of the model discussed in [44].

Now we consider an open string stretching around an angle φ, e.g. an open string starting ($\sigma = 0$) on a D7-brane aligned with the X^6-axis and ending

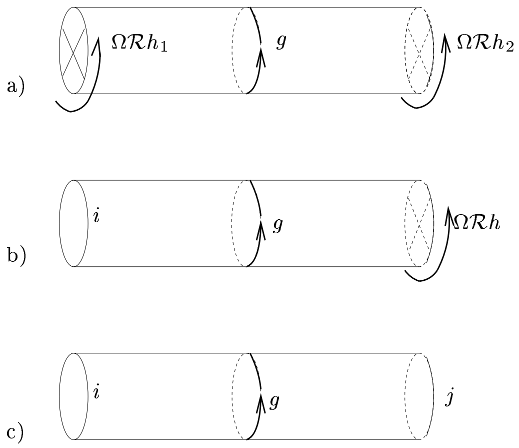

Figure 2.2: Tree channel diagrams for the exchange of closed strings between O-planes and D-branes: a) Klein bottle, b) Möbius strip, c) cylinder. Worldsheet time is horizontal.

($\sigma = \pi$) on the rotated D7-brane described above. I.e., for $\sigma = 0$ the open string obeys the boundary conditions

$$\partial_\sigma X^6 = 0\,, \quad \partial_\tau X^7 = 0\,, \tag{2.11}$$

whereas for $\sigma = \pi$ the boundary conditions are given by (2.8). The solutions to these boundary conditions are given by the mode expansions

$$\begin{aligned} X^6 &= \sum_{m\in\mathbb{Z}+\varphi/\pi} \frac{1}{m}\alpha_m e^{-im\tau}\cos(m\sigma) + \sum_{l\in\mathbb{Z}-\varphi/\pi} \frac{1}{l}\alpha_l e^{-il\tau}\cos(l\sigma) \\ X^7 &= \sum_{m\in\mathbb{Z}+\varphi/\pi} \frac{1}{m}\alpha_m e^{-im\tau}\sin(m\sigma) - \sum_{l\in\mathbb{Z}-\varphi/\pi} \frac{1}{l}\alpha_l e^{-il\tau}\sin(l\sigma)\,, \end{aligned} \tag{2.12}$$

which suggest to denote the open strings stretched between D-branes at angles as twisted open strings [20], in analogy to the closed string twisted sectors. In this sense, we use the terminology twisted open strings from now on.

In the next paragraphs we are going to review some of the technical aspects necessary for orientifold constructions. The main consistency requirement comes from RR charge conservation. The RR charges describe the size of the couplings of O-planes and D-branes to RR gauge fields. The numerical value of these couplings can be computed by extracting the RR exchange contribution to the forces acting between O-planes and D-branes [69]. The closed string exchange between two O-planes is described by the Klein bottle, between an O-plane and a D-brane by the Möbius strip and between two D-branes by the cylinder diagram, see figure 2.2. The infrared divergences contained in the contributions from RR closed strings to these diagrams have to cancel for the theory to be consistent. Technically, this translates into the tadpole cancellation conditions [44]. Note that, if some supersymmetry is left unbroken, the RR exchange is always cancelled by the corresponding NSNS exchange for each diagram. But since, as stated above, the RR exchange corresponds to some physical charge, it has to vanish by itself.

To calculate the contributions from the diagrams shown in figure 2.2 directly in the tree channel, one has to introduce the boundary state formalism [71, 42], what we will do later. For the moment, we will pursue another strategy. By worldsheet duality, i.e. the interchange of σ and τ on the worldsheet, each process in the tree channel is mapped to a process in the loop channel. In the following, we would like to shed some light on this transformation between the loop and the tree channel. Consider the Klein bottle diagram from figure 2.2 in the tree channel, i.e. the worldsheet time proceeds horizontally. One can obtain this diagram with the standard parameter range for closed strings

$$0 \leq \sigma < 2\pi\,, \quad 0 \leq \tau < 2\pi l\,, \tag{2.13}$$

if one starts with the two dimensional plane (τ, σ) and identifies

$$\begin{aligned}(\tau, \sigma) &\cong (\tau + 4\pi l, \sigma)\\ &\cong (-\tau, \sigma + \pi)\,,\end{aligned} \tag{2.14}$$

see figure 2.3. However, the prescription (2.14) is ambiguous and may yield the triangulated representation shown in figure 2.4, as well. Now, if one interchanges τ and σ in figure 2.4, one has to rescale each axis by a factor of $2t$ to obtain the standard parameter range

$$0 \leq \tau < 2\pi t \tag{2.15}$$

for the worldsheet time (now in the loop channel). But, by this rescaling, the parameter range for σ (in the loop channel) now reads

$$0 \leq \sigma < 8\pi l t\,. \tag{2.16}$$

Demanding the standard parameter range $0 \leq \sigma < 2\pi$, we obtain the relation

$$lt = \frac{1}{4} \tag{2.17}$$

in the case of the Klein bottle. Proceeding in a similar fashion, one obtains the relations

$$lt = \frac{1}{8} \tag{2.18}$$

for the Möbius strip and

$$lt = \frac{1}{2} \tag{2.19}$$

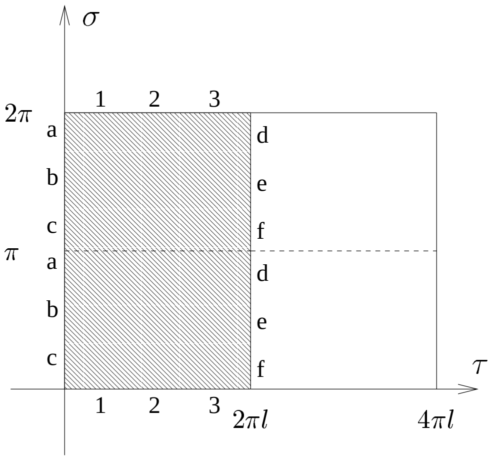

Figure 2.3: The shaded area is the triangulated version of the Klein bottle diagram in the tree channel with the standard parameter range (2.13). Under (2.14), e.g. the points with the same letters are identified and yield two crosscaps on the left and on the right hand side. The points with the same numbers are identified, too.

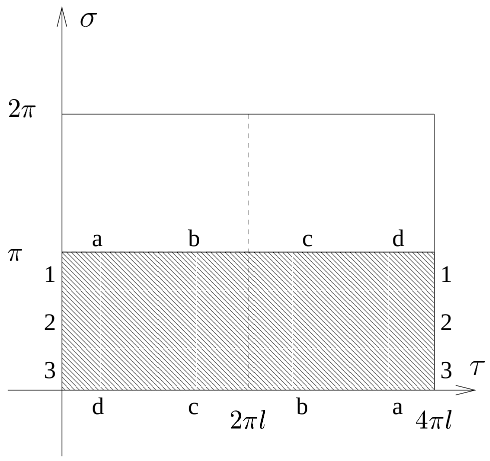

Figure 2.4: The shaded area is another triangulated version of the Klein bottle diagram in the tree channel, now with another parameter range. The points with the same letters are identified and correspond to an insertion of the worldsheet parity Ω, if one interchanges σ and τ. This leads to the loop channel interpretation. The points with the same numbers are identified, too.

for the cylinder, which is called annulus in the loop channel[1]. Note that the Möbius strip in the loop channel and the annulus are open string amplitudes, where we choose the standard parameter range $0 \leq \sigma < \pi$ for the open string, according to the literature.

Figure 2.2 contains some more information. Orbifold group elements are denoted by h or g. In the tree channel picture the crosscaps correspond to O-planes invariant under $\Omega\mathcal{R}h$. D-branes are assigned a letter i or j. The orbifold group element g denotes the twist sector of the closed strings propagating in the tree channel. (For further details see [44].) Consistency of the boundary conditions requires

$$(\Omega\mathcal{R}h_1)^2 = (\Omega\mathcal{R}h_2)^2 = g \tag{2.20}$$

in the Klein bottle diagram and

$$(\Omega\mathcal{R}h)^2 = g \tag{2.21}$$

in the Möbius strip. For the class of orientifolds discussed here (as a consequence of $\mathcal{R}\Theta = \Theta^{-1}\mathcal{R}$), the lhs of (2.20) and (2.21) yield the identity. Hence, in the tree channel only untwisted closed strings propagate in the Klein bottle and in the Möbius strip. Since these states must be invariant under the orbifold group, the tree channel amplitude must contain the insertion of the complete projector $\mathbf{P}$ (consider appendix B) on invariant states, which we will introduce in the following.

The actual calculation of the diagrams depicted in figure 2.2 will be done in the loop and in the tree channel, separately. The requirement to obtain the same results in these two approaches, i.e. worldsheet duality, leads to restrictions on the possible orbifold lattices from the Klein bottle and further conditions for the representation of the orientifold group on the Chan-Paton matrices from the Möbius strip.

In the loop channel, the expressions for the Klein bottle, annulus and Möbius strip amplitudes are

$$\mathcal{K} = \int_0^\infty \frac{dt}{t} \mathrm{Tr}_{\mathrm{closed}} \left(\frac{\Omega\mathcal{R}}{2} \mathbf{P} \left(\frac{1+(-1)^F}{2} \right) (-1)^{\mathbf{S}} e^{-2\pi t (H_L + H_R)} \right) \tag{2.22}$$

$$\mathcal{A} = \int_0^\infty \frac{dt}{t} \mathrm{Tr}_{\mathrm{open}} \left(\frac{1}{2} \mathbf{P} \left(\frac{1+(-1)^F}{2} \right) (-1)^{\mathbf{S}} e^{-2\pi t H} \right) \tag{2.23}$$

$$\mathcal{M} = \int_0^\infty \frac{dt}{t} \mathrm{Tr}_{\mathrm{open}} \left(\frac{\Omega\mathcal{R}}{2} \mathbf{P} \left(\frac{1+(-1)^F}{2} \right) (-1)^{\mathbf{S}} e^{-2\pi t H} \right) , \tag{2.24}$$

with the modular parameter t, the traces 'Tr' over the closed or open string states, respectively, the projector

$$\mathbf{P} = \frac{1}{N} \left(1 + \Theta + \cdots + \Theta^{N-1} \right) \tag{2.25}$$

[1]We will use the term 'annulus' for both the loop and the tree channel in the following.

on states invariant under the orbifold group $\mathbb{Z}_N$, the GSO projector (which we will comment on later), the spacetime fermion number $\mathbf{S}$ and the exponential time evolution operator containing the closed or open string Hamiltonians, respectively. In the case of the closed string, the Hamiltonian for the left movers is given by

$$\begin{aligned} H_L = \frac{\alpha'}{4} p_L^2 &+ \sum_{m_\mu > 0} \alpha^\mu_{-m_\mu} \alpha^\mu_{m_\mu} + \sum_{r_\mu > 0} r_\mu \psi^\mu_{-r_\mu} \psi^\mu_{r_\mu} \\ &+ \sum_{m_i > 0} \alpha^i_{-m_i} \alpha^{\bar{i}}_{m_i} + \sum_{l_i > 0} \alpha^{\bar{i}}_{-l_i} \alpha^i_{l_i} \\ &+ \sum_{r_i > 0} r_i \psi^i_{-r_i} \psi^{\bar{i}}_{r_i} + \sum_{s_i > 0} s_i \psi^{\bar{i}}_{-s_i} \psi^i_{s_i} + E_0 \,, \end{aligned} \tag{2.26}$$

where p_L is the left-moving momentum and E_0 is the zero point energy. The sums over the directions are implicit and we work in the light cone gauge. The modings of the bosonic and fermionic oscillators in the compact directions depend on the twist sector of the states where they act upon. The modings of all fermionic oscillators further are different for NS and R sector fermions. The eigenvalues of p_L and E_0 are dependent on these facts, too. H_R for the right movers is similar to (2.26). H for the open string also is similar to (2.26), but now the first term is given by $\alpha' p^2$ and the meaning of twisted sectors in the case of the closed string is replaced by open strings stretching between D-branes intersecting at angles, as explained above. Note that, as a further consequence of (2.7), $H_L + H_R$ and H are invariant under $\Omega\mathcal{R}$, whereas the action of Ω alone interchanges the twisted with the inverse twisted sectors. For further details, see appendix A.

In the following, we introduce some notation and definitions which we mainly borrow from [19]. The action of the orientifold group on closed string degenerate ground states[2] is specified by

$$\begin{aligned} \mathcal{R}: \quad & |s_1, s_2, s_3, s_4\rangle_{L,R} \longrightarrow \quad |s_1, s_2, -s_3, -s_4\rangle_{L,R} \\ \Theta: \quad & |s_1, s_2, s_3, s_4\rangle_{L,R} \longrightarrow \quad e^{2\pi i \vec{v}\cdot\vec{s}} \, |s_1, s_2, s_3, s_4\rangle_{L,R} \end{aligned} \tag{2.27}$$

Actually, the GSO projection operator in (2.22) is given by $\frac{1}{2}(1 + (-1)^{F_L})\frac{1}{2}(1 + (-1)^{F_R})$. But since worldsheet parity inversion Ω interchanges the left with the right moving sector, only states with $(-1)^{F_L} = (-1)^{F_R} \equiv (-1)^F$ contribute to the trace in (2.22). We project on the states with $(-1)^F = +1$. The definition

$$\begin{aligned} (-1)^{F_L} |s_1, s_2, s_3, s_4\rangle_L &= e^{\pi i (s_1 + s_2 - s_3 - s_4)} |s_1, s_2, s_3, s_4\rangle_L \\ (-1)^{F_R} |s_1, s_2, s_3, s_4\rangle_R &= e^{\pi i (s_1 + s_2 + s_3 + s_4)} |s_1, s_2, s_3, s_4\rangle_R \end{aligned} \tag{2.28}$$

is consistent with this choice and the orientifold symmetries and confirms that we are dealing with a compactification of Type IIB.

[2] All states are in light cone gauge. The first two entries in the state correspond to four non-compact directions, whereas the other two belong to the two complex compact directions.

To figure out which sectors of the 1-loop amplitudes (2.22), (2.24) and (2.23) correspond to the exchange of RR states in the tree channel, one has to consider the periodicities of the corresponding worldsheet fermions [71] and obtains:

$$\begin{array}{rl} \text{Klein bottle:} & \text{Closed string NSNS states with } \mathbf{P}\Omega\mathcal{R}\,(-)^F \text{ insertion} \\ \text{Möbius strip:} & \text{Open string R states with } -\mathbf{P}\Omega\mathcal{R} \text{ insertion} \\ \text{Annulus:} & \text{Open string NS states with } \mathbf{P}(-)^F \text{ insertion} \end{array} \qquad (2.29)$$

The minus sign in the case of the Möbius strip is generated by the spacetime fermion number.

2.2 The $\mathbb{Z}_2$ model

The torus lattices T_1 and T_2 have to respect the symmetries of the orientifold group, i.e. they have to be symmetric with respect to $\mathcal{R}$ and the orbifold group $\mathbb{Z}_2$. In figure 2.5, the two possible orientations, labelled by **A** and **B**, with respect to $\mathcal{R}$ are shown. In the case of $\mathbb{Z}_2$, one could choose more general lattices, namely with two basis vectors of different length for the **A** and at an arbitrary angle for the **B** lattice. But since the tadpole cancellation conditions and the massless spectra are the same, we restrict ourselves to the cases shown in figure 2.5. Thus, the possible models we may obtain, are of type **AA**, **AB** (equivalent to **BA**, therefore we will only mention **AB** from now on) and **BB**, as we will discuss in the following.

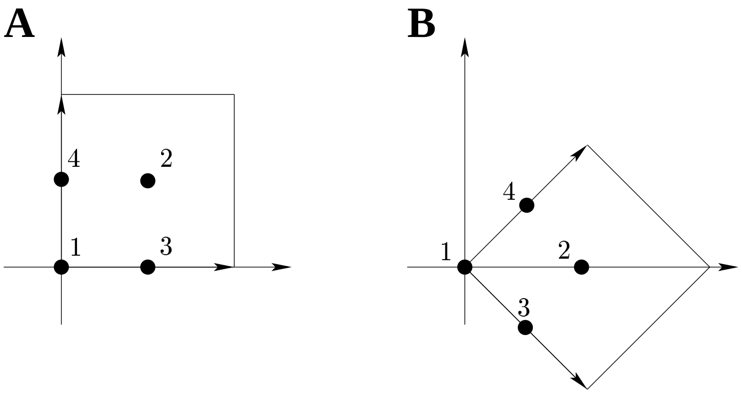

Figure 2.5: Lattices for $\mathbb{Z}_2$. Black circles denote the fixed points which are labelled by $1, \ldots, 4$.

2.2.1 The Klein bottle 1-loop amplitude

The Klein bottle 1-loop amplitude (2.22) for this model is given by

$$\mathcal{K} = c(1_{\mathrm{RR}} - 1_{\mathrm{NSNS}}) \int_0^\infty \frac{dt}{t^4} \mathrm{Tr}_{\mathrm{NSNS}} \left(\Omega\mathcal{R}\,(1+\Theta)\,(-1)^F e^{-2\pi t(H_L+H_R)} \right) , \quad (2.30)$$

where we already included some results from the previous section, especially (2.29). The factor $(1_{\rm RR} - 1_{\rm NSNS})$ is a consequence of supersymmetry, i.e. the RR exchange is cancelled by the NSNS exchange, from the tree channel point of view. We already performed the integration over the non-compact momenta, where the factor $c = V_6/(8\pi^2\alpha')^3$ stems from, with V_6 the regularized volume of momentum space.

We begin with evaluating the expression (2.30) by considering the compact momenta on one torus. The Kaluza-Klein (KK) and winding (W) states are generally given by

$$P = \frac{\sqrt{2}}{r}\left(m_1 \vec{e_1}^{\,*} + m_2 \vec{e_2}^{\,*}\right) \ , \tag{2.31}$$

$$W = \frac{r}{\sqrt{2}\alpha'}\left(n_1 \vec{e_1} + n_2 \vec{e_2}\right) \ , \tag{2.32}$$

where m_i and n_i are integers, $\vec{e_i}$ are the basis vectors of the corresponding torus with radius r and $\vec{e_i}^{\,*}$ are the basis vectors of the dual torus $(i = 1, 2)$. The $SU(2)^2$ lattices in figure 2.5 are spanned by

$$\vec{e_1}^{\,\mathbf{A}} = \begin{pmatrix} \sqrt{2} \\ 0 \end{pmatrix} , \qquad \vec{e_2}^{\,\mathbf{A}} = \begin{pmatrix} 0 \\ \sqrt{2} \end{pmatrix} , \tag{2.33}$$

$$\vec{e_1}^{\,\mathbf{B}} = \begin{pmatrix} 1 \\ -1 \end{pmatrix} , \qquad \vec{e_2}^{\,\mathbf{B}} = \begin{pmatrix} 1 \\ 1 \end{pmatrix} , \tag{2.34}$$

with the corresponding dual basis. In the loop channel, we have

$$\Omega P \Omega^{-1} = P \tag{2.35}$$

$$\Omega W \Omega^{-1} = -W \tag{2.36}$$

so that $\Omega\mathcal{R}$ invariant states have to fulfill

$$\mathcal{R} P \mathcal{R}^{-1} = P \tag{2.37}$$

$$\mathcal{R} W \mathcal{R}^{-1} = -W \, . \tag{2.38}$$

Thus we obtain the $\Omega\mathcal{R}$ invariant Kaluza-Klein and winding states

$$P^{\mathbf{A}} = \frac{m}{r}\begin{pmatrix} 1 \\ 0 \end{pmatrix} , \qquad W^{\mathbf{A}} = \frac{nr}{\alpha'}\begin{pmatrix} 0 \\ 1 \end{pmatrix} , \tag{2.39}$$

$$P^{\mathbf{B}} = \frac{\sqrt{2}m}{r}\begin{pmatrix} 1 \\ 0 \end{pmatrix} , \qquad W^{\mathbf{B}} = \frac{\sqrt{2}nr}{\alpha'}\begin{pmatrix} 0 \\ 1 \end{pmatrix} , \tag{2.40}$$

where m, n are integers. In the twisted sector, KK and W momenta vanish, thus we obtain no lattice contributions in the twisted sector. From

$$p_{L,R} = P \pm W \tag{2.41}$$

it follows that the lattice contributions for one torus are of the form

$$\mathcal{L}\left[a,b\right](t) \equiv \left(\sum_{m\in\mathbb{Z}} e^{-a\pi t m^2/\rho}\right)\left(\sum_{n\in\mathbb{Z}} e^{-b\pi t n^2 \rho}\right) , \tag{2.42}$$

where $\rho = r^2/\alpha'$. The notation is adopted from [20, 19]. Inserting (2.39) and (2.40), we obtain the contribution $\mathcal{L}_i^{\mathcal{K}} = \mathcal{L}[1,1](t)$ for an **A** type torus and $\mathcal{L}_i^{\mathcal{K}} = \mathcal{L}[2,2](t)$ for a **B** type torus T_i. In principle, the radii on the different tori can be different, but we choose them to be equal for simplicity. Note, that the KK and W momenta invariant under $\Omega\mathcal{R}\Theta$ are different from those invariant under $\Omega\mathcal{R}$, but their squares are the same, and thus lead to the same lattice contributions. This will turn out to be different in the cases of $\mathbb{Z}_4$ and $\mathbb{Z}_6$.

The oscillator contributions to (2.30) can easily be assembled using the results of the detailed calculations in appendix A as building blocks. We obtain

$$\mathcal{K} = 2c(1_{\rm RR} - 1_{\rm NSNS}) \int_0^\infty \frac{dt}{t^4} \frac{\vartheta\left[{0 \atop 1/2}\right]^2}{\eta^6} \left\{ \mathcal{L}_1^{\mathcal{K}} \mathcal{L}_2^{\mathcal{K}} \frac{\vartheta\left[{0 \atop 1/2}\right]^2}{\eta^6} + \chi_{\mathcal{K}} \frac{\vartheta\left[{1/2 \atop 1/2}\right]^2}{\vartheta\left[{0 \atop 1/2}\right]^2} \right\} , \tag{2.43}$$

where the argument of the theta and eta functions is $2t$. The factor of two arises because all terms in the trace are independent of the insertions from the orbifold group. For the lattice contributions, this may be different, as we will see in the other models, but for the oscillator contributions this is a general property due to the presence of $\Omega\mathcal{R}$, which implies a cancellation of the phases from the orbifold elements between the left and the right movers. The first term within the braces comes from the untwisted sector and the second term from the twisted sector. In the twisted sector, there are no lattice contributions. The factor $\chi_{\mathcal{K}}$ denotes the multiplicity of $\mathbb{Z}_2$ fixed points which are invariant under $\Omega\mathcal{R}$. For an **A** type torus, all four fixed points are invariant under $\Omega\mathcal{R}$, for a **B** type torus (see figure 2.5), the fixed points 1 and 2 are invariant, while 3 and 4 are interchanged under $\Omega\mathcal{R}$. Thus, we obtain

$$\chi_{\mathcal{K}} = \begin{cases} 16 & (\mathbf{AA}) \\ 8 & (\mathbf{AB}) \\ 4 & (\mathbf{BB}) \end{cases} \tag{2.44}$$

Note, that the second term within the braces in (2.43) vanishes anyway (we have an insertion of $(-1)^F$ in the trace and the twisted NS sector becomes degenerate in the compact directions), but formally the result looks like this.

2.2.2 The annulus 1-loop amplitude

The total Klein bottle 1-loop amplitude (2.43) vanishes by supersymmetry. However, the part that corresponds to the RR-exchange in the tree channel contains

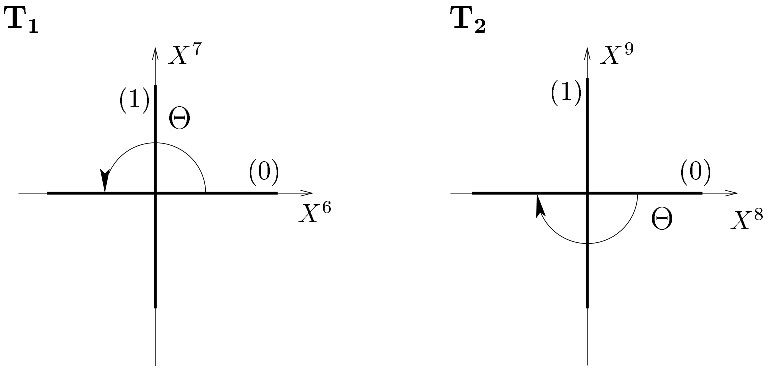

Figure 2.6: Location of D7-branes in the case of $\mathbb{Z}_2$. The intersection angle is half the angle of the corresponding rotation from the orbifold group. The different types of D-branes are labelled by (0) and (1).

an ultraviolet divergence. We will discuss the asymptotic behaviour in more detail later. This divergence, or tadpole, has to be cancelled by the introduction of D-branes to render the model consistent. As was found in [20, 19] and explained in section 2.1 for the orientifold models under consideration the most obvious possibility is to introduce D7-branes rotated by half the angles which are given by the elements of the orbifold group. In the case of $\mathbb{Z}_2$ this is particularly simple and the configuration of two different types of D7-branes is shown in figure 2.6. Let us introduce some general conventions at this point: We label the D7-branes which lie on the real axes (i.e. those which lie on top of the O7-planes invariant under $\Omega\mathcal{R}$) by (0) and the D7-branes which are obtained by a rotation of $\Theta^{-n/2}$ (i.e. those which lie on top of the O7-planes invariant under $\Omega\mathcal{R}\Theta^n$) by (n) with $0 \leq n < N$ for $\mathbb{Z}_N$. The mode expansions for an open string stretching from brane (0) to brane (n) are similar to those for a closed string in the sector twisted by Θ^{-n}. Thus, an open string stretching from brane (a) to brane $(a-n)$, $0 \leq a < N$, is said to belong to the n^{th} twisted sector. In the case of $\mathbb{Z}_2$, the sectors twisted by Θ^1 and Θ^{-1} are identical, of course.

The annulus amplitude (2.23) for this model is given by

$$\mathcal{A} = \frac{c}{8}(1_{\mathrm{RR}} - 1_{\mathrm{NSNS}}) \int_0^\infty \frac{dt}{t^4} \mathrm{Tr}_{\mathrm{NS}} \left((1+\Theta)\,(-1)^F e^{-2\pi t H} \right) , \tag{2.45}$$

where we already used (2.29) and integrated over the non-compact momenta.

We begin the evaluation of the annulus 1-loop amplitude (2.45) by considering the compact momenta. For the open string the compact momenta p are given by the distance of parallel D7-branes in the corresponding directions. Therefore we consider the location of the D-branes in the fundamental cells of the lattices $\mathbf{A}$ and $\mathbf{B}$, see figure 2.7. Thus we get $p^{\mathbf{A}} = P^{\mathbf{A}}$ for the directions 6 and 8 and $p^{\mathbf{A}} = W^{\mathbf{A}}$ for the directions 7 and 9 as well as $p^{\mathbf{B}} = \frac{1}{2}P^{\mathbf{B}}$ (6 and 8) and

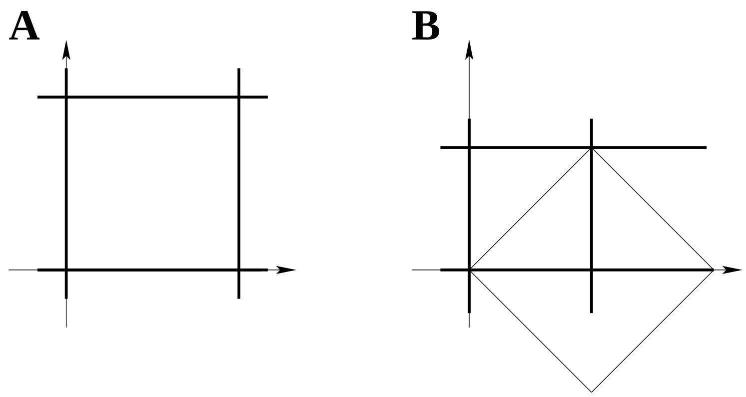

Figure 2.7: Location of D-branes in the fundamental cells for $\mathbb{Z}_2$

$p^{\mathbf{B}} = \frac{1}{2}W^{\mathbf{B}}$ (7 and 9), see equations (2.39) and (2.40). It follows, that the lattice contribution to the 1-loop amplitude for the annulus is given by $\mathcal{L}_i^{\mathcal{A}} = \mathcal{L}[2,2](t)$ for an **A** torus and by $\mathcal{L}_i^{\mathcal{A}} = \mathcal{L}[1,1](t)$ for a **B** torus. The compact momenta are nonzero again only for untwisted states, i.e. for open strings which do not stretch around an angle.

Implicit in expression (2.45) are the Chan-Paton factors, i.e. the description of the various endpoints of the open strings. We introduce the notation for $\mathbb{Z}_N$ in general. The action of an orbifold group element Θ^k, $0 \leq k < N$, on an open string state starting on brane (a) and ending on brane (b) is given by

$$\Theta^k : \quad |\psi, ij\rangle \lambda_{ji}^{(a,b)} \quad \longrightarrow \quad |\Theta^k \cdot \psi, ij\rangle \left(\gamma_k^{(b)} \lambda^{(a,b)} \gamma_k^{(a)-1} \right)_{ji} \tag{2.46}$$

This requires some explanation. $\lambda^{(a,b)}$ is the Chan-Paton matrix for an open string starting on brane (a) and ending on brane (b). It is an $M \times M$ matrix, where M is the number of D7-branes sitting on top of each other. $\gamma_k^{(a)}$ is the representation matrix of the orbifold group element Θ^k on brane (a) in the Chan-Paton basis. ψ denotes the vacuum together with some combination of oscillators. Thus, for a string stretching from brane (a) to brane $(a-n)$, i.e. a Θ^n twisted string, and for an insertion of Θ^k, we obtain a factor of

$$\mathrm{tr}\gamma_k^{(a-n)} \mathrm{tr}\gamma_k^{(a)-1} \tag{2.47}$$

in the corresponding term of the amplitude. 'tr' in small letters denotes the ordinary matrix trace. It turns out that we can perform all the calculations for strings starting on brane (0) and multiply the result with a factor of N to take into account the other D-branes at angles. We can always choose $\gamma_0^{(a)} = \mathbb{1}$ for all a, thus we obtain a factor of M^2 for an untwisted or twisted string with insertion $\mathbb{1}$ from the orbifold group. Furthermore (always starting on brane (0)), the only orbifold insertions that contribute to the annulus amplitude are $\mathbb{1}$ and $\Theta^{N/2}$

(N even), because the others do not leave the D-branes invariant. However, an orbifold insertion different from $\mathbb{I}$, by worldsheet duality leads to a twisted sector contribution to the tree channel cylinder amplitude which cannot be cancelled by the other diagrams, as was explained in section 2.1. Thus we obtain as a result the twisted sector tadpole cancellation condition

$$\mathrm{tr}\gamma^{(a)}_{N/2} = 0 \tag{2.48}$$

for all a. This result can explicitly be confirmed by calculating the tree channel cylinder amplitude directly in the boundary state approach, as we will do later. Nevertheless, we will use the result (2.48) from now on.

Putting all this together and again using the results from appendix A, we obtain the annulus 1-loop amplitude

$$\mathcal{A} = \frac{c}{4} M^2 (1_{\mathrm{RR}} - 1_{\mathrm{NSNS}}) \int_0^\infty \frac{dt}{t^4} \frac{\vartheta\left[{0 \atop 1/2}\right]^2}{\eta^6} \left\{ \mathcal{L}_1^{\mathcal{A}} \mathcal{L}_2^{\mathcal{A}} \frac{\vartheta\left[{0 \atop 1/2}\right]^2}{\eta^6} + \chi_{\mathcal{A}} \frac{\vartheta\left[{1/2 \atop 1/2}\right]^2}{\vartheta\left[{0 \atop 1/2}\right]^2} \right\}, \tag{2.49}$$

where the argument of the theta- and eta-functions is t. Since the twisted open strings are localized at the intersection points, we have to include the multiplicity 1 for an **A** type and 2 for a **B** type torus, see figure 2.7, i.e.

$$\chi_{\mathcal{A}} = \begin{cases} 1 & (\mathbf{AA}) \\ 2 & (\mathbf{AB}) \\ 4 & (\mathbf{BB}) \end{cases} \tag{2.50}$$

2.2.3 The Möbius strip 1-loop amplitude

Having introduced D-branes one also has to consider the tree channel diagram of closed strings being emitted from a D-brane and absorbed by an O-plane, or vice versa, i.e. the Möbius strip. In the open string picture this corresponds to a 1-loop diagram of open strings with an insertion of $\Omega\mathcal{R}$, which reads for this model

$$\mathcal{M} = -\frac{c}{8} (1_{\mathrm{RR}} - 1_{\mathrm{NSNS}}) \int_0^\infty \frac{dt}{t^4} \mathrm{Tr}_{\mathrm{R}} \left(\Omega\mathcal{R} \, (1+\Theta) \, e^{-2\pi t H} \right), \tag{2.51}$$

where we again used (2.29) and integrated over the non-compact momenta.

In the case of the Möbius strip, the compact momenta for a **B** type torus have to be doubled in the 7,9 directions because of the $\Omega\mathcal{R}$-projection[3], therefore one also gets $\mathcal{L}_i^{\mathcal{M}} = \mathcal{L}[2,2]$ for an **A** type torus but $\mathcal{L}_i^{\mathcal{M}} = \mathcal{L}[1,4]$ for a **B** type torus. Again, the lattice contributions only appear for untwisted strings.

[3] $\Omega\mathcal{R}$ projects out the D-branes which do not cross the imaginary axis in a lattice point

Which strings contribute to the Möbius strip 1-loop amplitude? We answer this question for $\mathbb{Z}_N$ in general. Let us denote a Θ^n twisted string starting on brane (a) by $(a, a-n)$ as explained in the previous section and consider the action of the insertion $\Omega\mathcal{R}\Theta^k$ thereupon:

$$\begin{aligned} (a, a-n) &\xrightarrow{\Theta^k} (a-2k, a-n-2k) \\ &\xrightarrow{\mathcal{R}} (-a+2k, -a+n+2k) \\ &\xrightarrow{\Omega} (-a+n+2k, -a+2k) \end{aligned} \tag{2.52}$$

Thus only terms with

$$n + 2k = 2a \bmod N \tag{2.53}$$

contribute to the Möbius strip amplitude. Again, we can do the calculations for $(a) = (0)$ and include a factor of N in the end. In the case of $\mathbb{Z}_2$, (2.52) simply means, that for $(a) = (0)$ only the untwisted sector contributes with both insertions $\mathbb{1}$ and Θ.

To obtain the Chan-Paton factors that appear in the Möbius strip 1-loop amplitude, we consider the action of the insertion $\Omega\mathcal{R}\Theta^k$ on an open string state

$$\Omega\mathcal{R}\Theta^k: \quad |\psi, ij\rangle\lambda^{(a,b)}_{ji} \quad \longrightarrow \quad |\Omega\mathcal{R}\Theta^k \cdot \psi, ij\rangle \left(\gamma^{(b)}_{\Omega\mathcal{R}k}\lambda^{(a,b)}\gamma^{(a)-1}_{\Omega\mathcal{R}k}\right)^T_{ji} \tag{2.54}$$

Thus, for an open string in the Θ^n twisted sector starting on the brane (a) with an insertion of $\Omega\mathcal{R}\Theta^k$ we find the Chan-Paton factor

$$\mathrm{tr}\left(\gamma^{(a-n)-T}_{\Omega\mathcal{R}k}\gamma^{(a)}_{\Omega\mathcal{R}k}\right) \tag{2.55}$$

in the Möbius strip amplitude. We introduce the abbreviation

$$C^n_k \equiv \mathrm{tr}\left(\gamma^{(-n)-T}_{\Omega\mathcal{R}k}\gamma^{(0)}_{\Omega\mathcal{R}k}\right) \tag{2.56}$$

for the Chan-Paton factors of Θ^n twisted open strings with an insertion of Θ^k starting on brane (0).

We obtain the Möbius strip amplitude

$$\mathcal{M} = -\frac{c}{4}(1_{\mathrm{RR}} - 1_{\mathrm{NSNS}}) \int_0^\infty \frac{dt}{t^4} \frac{\vartheta\left[{1/2 \atop 0}\right]^2}{\eta^6} \left\{ C^0_0 \mathcal{L}^{\mathcal{M}}_1 \mathcal{L}^{\mathcal{M}}_2 \frac{\vartheta\left[{1/2 \atop 0}\right]^2}{\eta^6} - 4C^0_1 \frac{\vartheta\left[{1/2 \atop 1/2}\right]^2}{\vartheta\left[{1/2 \atop 0}\right]^2} \right\}, \tag{2.57}$$

where the argument of the theta- and eta-functions is now $t+i/2$, consider again appendix A. The factor -4 in the last term arises from (A.32). Since only the untwisted sectors contribute, there appears no multiplicity from the intersection points.

2.2.4 Modular transformation to the tree channel

As we already explained in section 2.1, the modular parameter t in the loop channel is related to the modular parameter l in the tree channel by worldsheet duality. We obtained the relations

$$lt = \begin{cases} \frac{1}{4} & \text{(Klein bottle)} \\ \frac{1}{2} & \text{(annulus / cylinder)} \\ \frac{1}{8} & \text{(Möbius strip)} \end{cases} . \tag{2.58}$$

As shown above, the lattice contributions for one torus are of the general form

$$\mathcal{L}\left[a,b\right](t) \equiv \left(\sum_{m\in\mathbb{Z}} e^{-a\pi t m^2/\rho}\right)\left(\sum_{n\in\mathbb{Z}} e^{-b\pi t n^2\rho}\right) , \tag{2.59}$$

with $\rho = r^2/\alpha'$. To perform the transformation to the tree channel we use Poisson resummation

$$\sum_{n\in\mathbb{Z}} e^{-\pi n^2/t} = \sqrt{t}\sum_{n\in\mathbb{Z}} e^{-\pi n^2 t} \tag{2.60}$$

and obtain as a general expression for the lattice contributions in the tree channel

$$\tilde{\mathcal{L}}\left[\tilde{a},\tilde{b}\right](l) \equiv \left(\sum_{m\in\mathbb{Z}} e^{-\tilde{a}\pi l m^2\rho}\right)\left(\sum_{n\in\mathbb{Z}} e^{-\tilde{b}\pi l n^2/\rho}\right) . \tag{2.61}$$

(2.59) and (2.61) are related via

$$\mathcal{L}[a,b](t) = \frac{\kappa l}{\sqrt{ab}}\tilde{\mathcal{L}}\left[\frac{\kappa}{a},\frac{\kappa}{b}\right](l) , \tag{2.62}$$

with with $lt = 1/\kappa$, i.e. the coefficients from (2.58).

The modular transformation of the oscillator contributions can easily be performed with the help of the modular transformation properties

$$\begin{aligned} \vartheta\left[{\alpha \atop \beta}\right](1/t) &= \sqrt{t}e^{2\pi i\alpha\beta}\vartheta\left[{-\beta \atop \alpha}\right](t) , \\ \eta(1/t) &= \sqrt{t}\eta(t) . \end{aligned} \tag{2.63}$$

For the Möbius strip we need the additional identities

$$\frac{\vartheta\left[{\alpha+1/2 \atop \beta}\right]}{\vartheta\left[{\alpha+1/2 \atop \beta+1/2}\right]}(t+i/2) = e^{-\pi i\alpha}\frac{\vartheta\left[{(\alpha+1)/2 \atop \alpha/2+\beta}\right]\vartheta\left[{\alpha/2 \atop (\alpha+1)/2+\beta}\right]}{\vartheta\left[{(\alpha+1)/2 \atop (\alpha+1)/2+\beta}\right]\vartheta\left[{\alpha/2 \atop \alpha/2+\beta}\right]}(2t) \tag{2.64}$$

$$\frac{\vartheta\left[{1/2 \atop 0}\right]}{\eta^3}(t+i/2) = \frac{\vartheta\left[{1/2 \atop 0}\right]\vartheta\left[{0 \atop 1/2}\right]}{\eta^3\vartheta\left[{0 \atop 0}\right]}(2t) \tag{2.65}$$

Using these identities a second time, we obtain the modular transformations for the Möbius strip

$$\frac{\vartheta\left[{\alpha+1/2 \atop \beta}\right]}{\vartheta\left[{\alpha+1/2 \atop \beta+1/2}\right]}(t+i/2) = -ie^{-2\pi i(\alpha+\beta)}\frac{\vartheta\left[{-(\alpha+2\beta)+1/2 \atop \alpha+\beta}\right]}{\vartheta\left[{-(\alpha+2\beta)+1/2 \atop \alpha+\beta+1/2}\right]}(2l+i/2) \tag{2.66}$$

$$\frac{\vartheta\left[{1/2 \atop 0}\right]}{\eta^3}(t+i/2) = \frac{1}{4l}\frac{\vartheta\left[{1/2 \atop 0}\right]}{\eta^3}(2l+i/2) \tag{2.67}$$

Starting with the Klein bottle (i.e. $lt = 1/4$), we obtain for the modular transformation of the lattice contributions

$$\begin{aligned} \mathcal{L}[1,1](t) &= 4l\tilde{\mathcal{L}}[4,4](l) \\ \mathcal{L}[2,2](t) &= 2l\tilde{\mathcal{L}}[2,2](l)\,, \end{aligned} \tag{2.68}$$

in short

$$\mathcal{L}_i^{\mathcal{K}} = c_i^{\mathcal{K}} l \tilde{\mathcal{L}}_i^{\mathcal{K}} \tag{2.69}$$

with

$$c_i^{\mathcal{K}} = \begin{cases} 4 & (\mathbf{A}) \\ 2 & (\mathbf{B}) \end{cases} . \tag{2.70}$$

Transforming the oscillator contributions as well, we obtain the tree channel amplitude

$$\tilde{\mathcal{K}} = 8cc_1^{\mathcal{K}}c_2^{\mathcal{K}}(1_{\mathrm{RR}} - 1_{\mathrm{NSNS}})\int_0^\infty dl \frac{\vartheta\left[{1/2 \atop 0}\right]^2}{\eta^6}\left\{\tilde{\mathcal{L}}_1^{\mathcal{K}}\tilde{\mathcal{L}}_2^{\mathcal{K}}\frac{\vartheta\left[{1/2 \atop 0}\right]^2}{\eta^6} - 4\frac{\vartheta\left[{1/2 \atop 1/2}\right]^2}{\vartheta\left[{1/2 \atop 0}\right]^2}\right\}\,, \tag{2.71}$$

where the argument of the theta- and eta-functions is $2l$. Note, that $\chi_{\mathcal{K}}/(c_1^{\mathcal{K}}c_2^{\mathcal{K}}) = 1$ for any combination of the tori.

In the case of the annulus ($lt = 1/2$), the lattice contributions transform

$$\begin{aligned} \mathcal{L}[2,2](t) &= l\tilde{\mathcal{L}}[1,1](l) \\ \mathcal{L}[1,1](t) &= 2l\tilde{\mathcal{L}}[2,2](l)\,, \end{aligned} \tag{2.72}$$

in short

$$\mathcal{L}_i^{\mathcal{A}} = c_i^{\mathcal{A}} l \tilde{\mathcal{L}}_i^{\mathcal{A}} \tag{2.73}$$

with

$$c_i^{\mathcal{A}} = \begin{cases} 1 & (\mathbf{A}) \\ 2 & (\mathbf{B}) \end{cases} . \tag{2.74}$$

We obtain the tree channel amplitude for the cylinder

$$\tilde{\mathcal{A}} = \frac{c}{8} c_1^{\mathcal{A}} c_2^{\mathcal{A}} M^2 (1_{\mathrm{RR}} - 1_{\mathrm{NSNS}}) \int_0^\infty dl \frac{\vartheta\left[{1/2 \atop 0}\right]^2}{\eta^6} \left\{ \tilde{\mathcal{L}}_1^{\mathcal{A}} \tilde{\mathcal{L}}_2^{\mathcal{A}} \frac{\vartheta\left[{1/2 \atop 0}\right]^2}{\eta^6} - 4 \frac{\vartheta\left[{1/2 \atop 1/2}\right]^2}{\vartheta\left[{1/2 \atop 0}\right]^2} \right\}, \tag{2.75}$$

where the argument of the theta- and eta-functions is $2l$ and we find $\chi_{\mathcal{A}}/(c_1^{\mathcal{A}} c_2^{\mathcal{A}}) = 1$ again for any model.

For the Möbius strip ($lt = 1/8$), we find for the lattice contributions

$$\begin{aligned} \mathcal{L}[2,2](t) &= 4l\tilde{\mathcal{L}}[4,4](l) \\ \mathcal{L}[1,4](t) &= 4l\tilde{\mathcal{L}}[8,2](l)\,, \end{aligned} \tag{2.76}$$

thus $c_i^{\mathcal{M}} = 4$ for an **A** and a **B** type torus. The tree channel amplitude for the Möbius strip reads

$$\tilde{\mathcal{M}} = -8c(1_{\mathrm{RR}} - 1_{\mathrm{NSNS}}) \int_0^\infty dl \frac{\vartheta\left[{1/2 \atop 0}\right]^2}{\eta^6} \left\{ C_0^0 \tilde{\mathcal{L}}_1^{\mathcal{M}} \tilde{\mathcal{L}}_2^{\mathcal{M}} \frac{\vartheta\left[{1/2 \atop 0}\right]^2}{\eta^6} + 4C_1^0 \frac{\vartheta\left[{1/2 \atop 1/2}\right]^2}{\vartheta\left[{1/2 \atop 0}\right]^2} \right\}, \tag{2.77}$$

where the argument of the theta- and eta-functions now is $2l + i/2$.

2.2.5 Direct calculation of the tree channel amplitudes

One can calculate the tree channel amplitudes directly (up to a normalization) by constructing the crosscap and boundary states of the O-planes and D-branes, respectively, and calculating their overlaps. The technical details are given in appendix B. For further information, see [42] and [8]. But why should we calculate the tree channel amplitudes directly? In principle, we already have all the results we need. Firstly, in more complicated models it can be easier to calculate parts of the amplitudes by considering the corresponding overlaps of the crosscap and boundary states. Secondly, and more important, in this way it is possible to check worldsheet duality explicitly. As we will see later, this can lead to further consistency conditions for the models under consideration.

In the case of the Klein bottle, we obtain in this way

$$\tilde{\mathcal{K}} = 4\mathcal{N}_C^2 (1_{\mathrm{RR}} - 1_{\mathrm{NSNS}}) \int_0^\infty dl \frac{\vartheta\left[{1/2 \atop 0}\right]^2}{\eta^6} \left\{ \tilde{\mathcal{L}}_1^{\mathcal{K}} \tilde{\mathcal{L}}_2^{\mathcal{K}} \frac{\vartheta\left[{1/2 \atop 0}\right]^2}{\eta^6} - 4 \frac{\vartheta\left[{1/2 \atop 1/2}\right]^2}{\vartheta\left[{1/2 \atop 0}\right]^2} \right\}, \tag{2.78}$$

where one factor of 2 comes from the two different spin structures and another factor of two from $k = 0, 1$ in $|\Omega\mathcal{R}\Theta^k\rangle$ for $\mathbb{Z}_2$. The argument of the theta- and eta-functions is $2l$. Comparing this result with (2.71), we find the normalization of the crosscap states to be

$$\mathcal{N}_C = \sqrt{2cc_1^{\mathcal{K}} c_2^{\mathcal{K}}} \tag{2.79}$$

in the case of $\mathbb{Z}_2$. For general $\mathbb{Z}_N$, we easily find

$$\mathcal{N}_C = \sqrt{\frac{4cc_1^{\mathcal{K}}c_2^{\mathcal{K}}}{N}}. \tag{2.80}$$

The prescription for calculating the lattice contributions directly in the tree channel goes as follows: As shown in appendix B, the role of Kaluza Klein momenta and windings is interchanged compared to the loop channel, i.e. now the Kaluza Klein momenta exist perpendicular to the position of the crosscap state, while windings are parallel. The exact magnitude of the momenta can then be fixed following the logics of Poisson resummation.

From the boundary states, we obtain the annulus amplitude

$$\tilde{\mathcal{A}} = 4\mathcal{N}_B^2 M^2(1_{\mathrm{RR}} - 1_{\mathrm{NSNS}}) \int_0^\infty dl \frac{\vartheta\left[{1/2 \atop 0}\right]^2}{\eta^6} \left\{ \tilde{\mathcal{L}}_1^{\mathcal{A}} \tilde{\mathcal{L}}_2^{\mathcal{A}} \frac{\vartheta\left[{1/2 \atop 0}\right]^2}{\eta^6} - 4 \frac{\vartheta\left[{1/2 \atop 1/2}\right]^2}{\vartheta\left[{1/2 \atop 0}\right]^2} \right\}, \tag{2.81}$$

where we can read off the normalization of the boundary states by comparison with (2.75)

$$\mathcal{N}_B = \sqrt{\frac{cc_1^{\mathcal{A}}c_2^{\mathcal{A}}}{32}} \tag{2.82}$$

in the case of $\mathbb{Z}_2$, and for general $\mathbb{Z}_N$

$$\mathcal{N}_B = \sqrt{\frac{cc_1^{\mathcal{A}}c_2^{\mathcal{A}}}{16N}}. \tag{2.83}$$

The argument of the theta- and eta-functions is $2l$.

To obtain the Möbius strip amplitude, we just have to calculate the overlap between the crosscaps and the boundary states, consider again appendix B, which leads to

$$\tilde{\mathcal{M}} = \pm 8\mathcal{N}_C\mathcal{N}_B M(1_{\mathrm{RR}} - 1_{\mathrm{NSNS}}) \int_0^\infty dl \frac{\vartheta\left[{1/2 \atop 0}\right]^2}{\eta^6} \left\{ \tilde{\mathcal{L}}_1^{\mathcal{M}} \tilde{\mathcal{L}}_2^{\mathcal{M}} \frac{\vartheta\left[{1/2 \atop 0}\right]^2}{\eta^6} - 4 \frac{\vartheta\left[{1/2 \atop 1/2}\right]^2}{\vartheta\left[{1/2 \atop 0}\right]^2} \right\}, \tag{2.84}$$

where the argument of the theta- and eta-functions is $2l + i/2$. The additional factor of 2 with respect to (2.78) and (2.81) results from the 'h.c.' in (B.26). The overall sign is fixed by the tadpole cancellation conditions.

Note that in the case of $\mathbb{Z}_2$, the direct calculation of the amplitudes in the tree channel yields no new results or further constraints. This will turn out to be different in the cases of $\mathbb{Z}_{4,6}$. Anyway, we have learned how to construct crosscap and boundary states and have checked worldsheet duality explicitly.

2.2.6 Asymptotic behaviour and tadpole cancellation conditions

The infrared divergences of the RR exchange, the tadpoles, in (2.71), (2.75) and (2.77) can be extracted by taking the limit $l \longrightarrow \infty$ (i.e. the limit of a long hose) of the various functions in the integrands.

$$\begin{aligned} \tilde{\mathcal{L}}[\cdot,\cdot] &\longrightarrow 1 \\ \eta &\longrightarrow 1 \\ \vartheta\left[{\alpha \atop \beta}\right] &\longrightarrow \begin{cases} 2\cos(\pi\beta) & (\alpha = 1/2) \\ e^{2\pi i\alpha\beta} & (\alpha \neq 1/2) \end{cases} . \end{aligned} \tag{2.85}$$

In this manner we find the tadpole cancellation conditions

$$0 = \begin{cases} 32^2 \mp 2\cdot 32 C^0_{0,1} + M^2 & (\mathbf{AA}) \\ 16^2 \mp 2\cdot 16 C^0_{0,1} + M^2 & (\mathbf{AB}) \\ 8^2 \mp 2\cdot 8 C^0_{0,1} + M^2 & (\mathbf{BB}) \end{cases} , \tag{2.86}$$

or

$$\begin{aligned} M &= 32 \quad (\mathbf{AA}) \\ M &= 16 \quad (\mathbf{AB}) \\ M &= 8 \quad (\mathbf{BB}) \end{aligned} , \tag{2.87}$$

together with

$$C^0_0 = -C^0_1 = M\,. \tag{2.88}$$

These are the untwisted tadpole cancellation conditions. Since the representation matrices of the orientifold (and orbifold) group are unitary $M \times M$ matrices, (2.88) corresponds to

$$\begin{aligned} \gamma^{(0)}_{\Omega\mathcal{R}0}\gamma^{(0)-T}_{\Omega\mathcal{R}0} &= \mathbb{1}_M \\ \gamma^{(0)}_{\Omega\mathcal{R}1}\gamma^{(0)-T}_{\Omega\mathcal{R}1} &= -\mathbb{1}_M\,. \end{aligned} \tag{2.89}$$

For a string starting on brane (1), we have to include another insertion of Θ. In this case, this simply means that we have to interchange the signs in (2.89). Remember that we already found the twisted tadpole cancellation conditions (2.48), which read in the case of $\mathbb{Z}_2$

$$\mathrm{tr}\gamma^{(0)}_1 = \mathrm{tr}\gamma^{(1)}_1 = 0\,. \tag{2.90}$$

Performing T-duality in the 7th and 9th direction, the horizontal D7-branes transform into D9-branes, whereas the perpendicular ones transform into D5-branes. Thus, the D-brane content dictated by the tadpole cancellation conditions in the case of the **AA** model transforms into the D-brane content of [44] and reflects the fact that these models are T-dual to each other.

In the following, we will show how to find the various representation matrices of the orbifold and orientifold group elements. Taking into account (2.46) and Schur's lemma, we can choose the representation matrix of Θ^0 to be

$$\gamma_0^{(a)} = \mathbb{1}_M \,, \tag{2.91}$$

the $M \times M$ unit matrix. In addition to the tadpole cancellation conditions, our choice of γ-matrices has to fulfill several operator identities, e.g.

$$\Omega\mathcal{R}\Theta^k\Omega\mathcal{R}\Theta^l = \Theta^{l-k} \,. \tag{2.92}$$

If $\Omega\mathcal{R}\Theta^l$ takes the brane (a) into the brane (a'), this leads to the consistency condition

$$\gamma_{\Omega\mathcal{R}k}^{(a')-T}\gamma_{\Omega\mathcal{R}l}^{(a)} \simeq \gamma_{l-k}^{(a)} \,, \tag{2.93}$$

where '$\simeq$' means equal up to an irrelevant phase. Furthermore,

$$\left(\Theta^{N/2}\right)^2 = \mathbb{1} \tag{2.94}$$

implies

$$\left(\gamma_{N/2}^{(a)}\right)^2 \simeq \mathbb{1}_M \,. \tag{2.95}$$

In the case of $\mathbb{Z}_2$, the choice [44]

$$\begin{aligned} \gamma_{\Omega\mathcal{R}0}^{(0)} = \gamma_{\Omega\mathcal{R}1}^{(1)} &= \mathbb{1}_M \\ \gamma_1^{(0)} = \gamma_1^{(1)} = \gamma_{\Omega\mathcal{R}1}^{(0)} = \gamma_{\Omega\mathcal{R}0}^{(1)} &= I \,, \end{aligned} \tag{2.96}$$

with

$$I = \begin{pmatrix} 0 & i\mathbb{1}_{M/2} \\ -i\mathbb{1}_{M/2} & 0 \end{pmatrix} \tag{2.97}$$

turns out to satisfy all the constraints. Note, that I fulfills

$$I = I^{-1} = -I^T \,. \tag{2.98}$$

2.2.7 The massless spectrum

In this section we will calculate the massless spectrum of the $\Omega\mathcal{R} \times \mathbb{Z}_2$ orientifold and explicitly verify that we obtain the same massless spectrum as for the T-dual model of [44] in the case of **AA**. The massless spectrum is found by symmetrizing the massless states which satisfy the GSO projection with respect to $\Omega\mathcal{R}$ and Θ.

The closed string spectrum

We begin with the untwisted NSNS sector. In the following, we denote the tachyonic vacuum of this sector by $|0\rangle$. The states are given up to normalization. Ω exchanges left and right movers and is defined as

$$\Omega\alpha_r\Omega^{-1} = \tilde{\alpha}_r\,, \qquad \Omega\psi_r\Omega^{-1} = \tilde{\psi}_r\,, \qquad \Omega\tilde{\psi}_r\Omega^{-1} = -\psi_r\,, \tag{2.99}$$

for integer and half-integer r. The action of $\mathcal{R}$ and Θ is defined in (2.27). We have to symmetrize the states with respect to $\Omega\mathcal{R}$. From the non-compact dimensions we find

$$\left(\psi^{\mu}_{-1/2}\tilde{\psi}^{\nu}_{-1/2} + \psi^{\nu}_{-1/2}\tilde{\psi}^{\mu}_{-1/2}\right)|0\rangle\,, \tag{2.100}$$

which is the graviton of $\mathcal{N}=1$ SUGRA in $d=6$ plus one scalar. In addition, we have

$$\psi^{i}_{-1/2}\tilde{\psi}^{\bar{i}}_{-1/2}|0\rangle\,, \qquad \psi^{\bar{i}}_{-1/2}\tilde{\psi}^{i}_{-1/2}|0\rangle\,, \tag{2.101}$$

and

$$\left(\psi^{i}_{-1/2}\tilde{\psi}^{i}_{-1/2} + \psi^{\bar{i}}_{-1/2}\tilde{\psi}^{\bar{i}}_{-1/2}\right)|0\rangle\,, \tag{2.102}$$

as well as

$$\begin{aligned}
&\left(\psi^{1}_{-1/2}\tilde{\psi}^{2}_{-1/2} + \psi^{\bar{2}}_{-1/2}\tilde{\psi}^{\bar{1}}_{-1/2}\right)|0\rangle\,,\\
&\left(\psi^{2}_{-1/2}\tilde{\psi}^{1}_{-1/2} + \psi^{\bar{1}}_{-1/2}\tilde{\psi}^{\bar{2}}_{-1/2}\right)|0\rangle\,,\\
&\left(\psi^{1}_{-1/2}\tilde{\psi}^{\bar{2}}_{-1/2} + \psi^{2}_{-1/2}\tilde{\psi}^{\bar{1}}_{-1/2}\right)|0\rangle\,,\\
&\left(\psi^{\bar{1}}_{-1/2}\tilde{\psi}^{2}_{-1/2} + \psi^{\bar{2}}_{-1/2}\tilde{\psi}^{1}_{-1/2}\right)|0\rangle\,,
\end{aligned} \tag{2.103}$$

i.e. 10 additional scalars. Note, that the massless states displayed in (2.100), (2.101) and the first two lines of (2.103) are model independent and therefore appear in the other $\mathbb{Z}_N$ models as well.

Now we discuss the untwisted RR sector. In the following, e.g. $|++++\rangle_L$ stands for $|\frac{1}{2},\frac{1}{2},\frac{1}{2},\frac{1}{2}\rangle_L$. Again, we have to symmetrize with respect to $\Omega\mathcal{R}$, but now there arises an additional minus sign because of the anticommuting behaviour of the R ground states. Thus, from now on 'symmetrizing with respect to $\Omega\mathcal{R}$' means symmetrizing the NSNS and antisymmetrizing the RR sectors. We find the invariant states

$$\begin{aligned}
&|++++\rangle_L|++++\rangle_R - |++--\rangle_L|++--\rangle_R\,,\\
&|++++\rangle_L|--++\rangle_R - |----\rangle_L|++--\rangle_R\,,\\
&|++--\rangle_L|----\rangle_R - |--++\rangle_L|++++\rangle_R\,,\\
&|--++\rangle_L|--++\rangle_R - |----\rangle_L|----\rangle_R\,,\\
&|++++\rangle_L|----\rangle_R - |--++\rangle_L|++--\rangle_R\,,\\
&|++--\rangle_L|--++\rangle_R - |----\rangle_L|++++\rangle_R\,,
\end{aligned} \tag{2.104}$$

where the first two states together with a linear combination of the third and fourth state yield the anti-self-dual 2-form which, together with the graviton from the NSNS sector, constitutes the SUGRA multiplet (the fermionic content of course comes from the NSR and RNS sectors; we only discuss the bosonic content explicitly, since all the models are supersymmetric). The remaining states are three scalars. In addition, we find the invariant states

$$\begin{aligned}
&|+-+-\rangle_L|+-+-\rangle_R-|+--+\rangle_L|+--+\rangle_R\,,\\
&|+-+-\rangle_L|-++-\rangle_R-|-+-+\rangle_L|+--+\rangle_R\,,\\
&|-++-\rangle_L|+-+-\rangle_R-|+--+\rangle_L|-+-+\rangle_R\,,\\
&|-++-\rangle_L|-++-\rangle_R-|-+-+\rangle_L|-+-+\rangle_R\,,\\
&|+-+-\rangle_L|-+-+\rangle_R-|-++-\rangle_L|+--+\rangle_R\,,\\
&|+--+\rangle_L|-++-\rangle_R-|-+-+\rangle_L|+-+-\rangle_R\,,
\end{aligned} \tag{2.105}$$

where the first four states constitute one tensor multiplet and the remaining two scalars yield, together with the other scalars from above, 4 hypermultiplets of $\mathcal{N}=1$ SUSY in $d=6$. Note, that the states in (2.104) and the last two lines of (2.105) are model independent.

To summarize, in the untwisted closed string sector we find the $\mathcal{N}=1$, $d=6$ SUGRA multiplet, plus one tensor multiplet, plus 4 hypermultiplets. The fermionic content of these multiplets comes from the NSR and RNS sectors, of course.

In the Θ^n-twisted sectors the masses are given by

$$\frac{\alpha'}{4}m_{L,R}^2 = N_{L,R} + \frac{1}{2}q_{L,R}^2 + E_{vac} - \frac{1}{2}\,, \tag{2.106}$$

with the oscillator number $N_{L,R}$ and

$$q_{L,R} = \begin{cases} (0,0,\pm n\vec{v}) & \text{(NS)}\\ \left(\frac{1}{2},\frac{1}{2},\frac{1}{2}\pm n\vec{v}\right) & \text{(R)}\end{cases} \tag{2.107}$$

and

$$E_{vac} = \frac{1}{2}\sum_i |nv_i|(1-|nv_i|)\,. \tag{2.108}$$

In the following, we give a recipe of how to construct the massless twisted states. We denote the tachyonic untwisted NS groundstate for the left- (right-) movers by $|0,0,0,0\rangle_{L,R}$. It has the GSO projection $(-1)^{F_L,F_R}=-1$. We introduce the Θ twisted state $|0,0,\pm\frac{1}{2},\mp\frac{1}{2}\rangle_{L,R}$ with the same GSO projection. This state corresponds to the vector $q_{L,R}$ in (2.106). This state is already massless, but it has the wrong GSO projection. Therefore we have to apply fermionic oscillators. Since we are interested in the massless states, this oscillator should not change the mass and therefore has to be a zero mode, which we find in the compact directions. We define a complexified oscillator with nonpositive moding to raise the corresponding entry in the state by one and a complex conjugated oscillator with negative moding to lower the entry by one and vice versa. By this means, we find the massless states with correct GSO projection

$$\begin{aligned}
\psi_0^2|0,0,+\frac{1}{2},-\frac{1}{2}\rangle_L &= |0,0,+\frac{1}{2},+\frac{1}{2}\rangle_L \equiv |1\rangle_{\rm NS}\ ,\\
\psi_0^{\bar{1}}|0,0,+\frac{1}{2},-\frac{1}{2}\rangle_L &= |0,0,-\frac{1}{2},-\frac{1}{2}\rangle_L \equiv |2\rangle_{\rm NS}\ ,\\
\tilde{\psi}_0^{\bar{2}}|0,0,-\frac{1}{2},+\frac{1}{2}\rangle_R &= |0,0,-\frac{1}{2},-\frac{1}{2}\rangle_R \equiv |\tilde{1}\rangle_{\rm NS}\ ,\\
\psi_0^1|0,0,-\frac{1}{2},+\frac{1}{2}\rangle_R &= |0,0,+\frac{1}{2},+\frac{1}{2}\rangle_R \equiv |\tilde{2}\rangle_{\rm NS}\ .
\end{aligned} \tag{2.109}$$

Note that these states are degenerated in the compact directions. Therefore we can use (2.27) and easily see that each of them is invariant under Θ.

Furthermore, we have to consider the action of $\Omega\mathcal{R}$ on the fixed points (see figure 2.5). In the case of an **A** type torus, all four fixed points are invariant under $\Omega\mathcal{R}$. In the case of a **B** type torus, the fixed points 1 and 2 are invariant, whereas 3 and 4 get interchanged under $\Omega\mathcal{R}$. This means

AA : all 16 fixed points invariant
AB : 13-14, 23-24, 33-34, 43-44 form 4 pairs under $\Omega\mathcal{R}$,
the remaining 8 fixed points are invariant
BB : 13-14, 23-24, 31-41, 32-42, 33-44, 34-43 form 6 pairs under $\Omega\mathcal{R}$,
the remaining 4 fixed points are invariant

Tensorizing and symmetrizing the states (2.109), we obtain the Θ-twisted NSNS sector

$$\begin{aligned}
&|1\tilde{1}\rangle^\alpha_{\rm NSNS} + |1\tilde{1}\rangle^\beta_{\rm NSNS}\ ,\\
&|1\tilde{2}\rangle^\alpha_{\rm NSNS} + |2\tilde{1}\rangle^\beta_{\rm NSNS}\ ,\\
&|2\tilde{1}\rangle^\alpha_{\rm NSNS} + |1\tilde{2}\rangle^\beta_{\rm NSNS}\ ,\\
&|2\tilde{2}\rangle^\alpha_{\rm NSNS} + |2\tilde{2}\rangle^\beta_{\rm NSNS}\ ,
\end{aligned} \tag{2.110}$$

where α denotes some fixed point and β the resulting fixed point under the action of $\Omega\mathcal{R}$ upon it. This means, that a pair of fixed points under $\Omega\mathcal{R}$ contributes 4 scalars, whereas an invariant fixed point contributes 3 scalars. Thus we obtain 48 (40, 36) scalars in the Θ-twisted NSNS sector for the **AA** (**AB**, **BB**) model.

In the Θ-twisted RR sector, we proceed in a similar manner. We begin with the untwisted left-moving R ground state $|+\frac{1}{2},+\frac{1}{2},+\frac{1}{2},+\frac{1}{2}\rangle_L$. This state is massless and has the correct GSO projection. Corresponding to the vector q_L, we introduce the Θ twisted state $|+\frac{1}{2},+\frac{1}{2},+1,0\rangle_L$. This state has the correct GSO projection, but it is massive. Applying the oscillator $\psi^{\bar{1}}_{-1/2}$ yields $|+\frac{1}{2},+\frac{1}{2},0,0\rangle_L$, which is massless, but has the wrong GSO projection. Therefore we have to apply a zero mode in the non-compact directions and obtain the Θ twisted massless R states with the correct GSO projection

$$\begin{array}{ll} |+\tfrac{1}{2},-\tfrac{1}{2},0,0\rangle_L \equiv |1\rangle_{\rm R}\,, & |-\tfrac{1}{2},+\tfrac{1}{2},0,0\rangle_L \equiv |2\rangle_{\rm R}\,, \\ |+\tfrac{1}{2},-\tfrac{1}{2},0,0\rangle_R \equiv |\tilde{1}\rangle_{\rm R}\,, & |-\tfrac{1}{2},+\tfrac{1}{2},0,0\rangle_R \equiv |\tilde{2}\rangle_{\rm R}\,, \end{array} \tag{2.111}$$

where each state produces a minus sign under Θ, because one compact oscillator is implicit. Nevertheless, tensorizing always eliminates this minus sign and we find the invariant RR states

$$\begin{array}{l} |1\tilde{1}\rangle^{\alpha}_{\rm RR} - |1\tilde{1}\rangle^{\beta}_{\rm RR}\,, \\ |1\tilde{2}\rangle^{\alpha}_{\rm RR} - |2\tilde{1}\rangle^{\beta}_{\rm RR}\,, \\ |2\tilde{1}\rangle^{\alpha}_{\rm RR} - |1\tilde{2}\rangle^{\beta}_{\rm RR}\,, \\ |2\tilde{2}\rangle^{\alpha}_{\rm RR} - |2\tilde{2}\rangle^{\beta}_{\rm RR}\,. \end{array} \tag{2.112}$$

Thus a pair of fixed points under $\Omega\mathcal{R}$ contributes one tensor multiplet, whereas an invariant fixed point contributes 1 scalar. So we find 16 scalars (8 scalars + 4 tensors, 4 scalars + 6 tensors) in the Θ-twisted RR sector for the **AA** (**AB**, **BB**) model.

Altogether, we find the closed string spectrum of the $\mathbb{Z}_2$ model

twist sector	**AA**	**AB**	**BB**
untwisted	SUGRA + 1T + 4H		
Θ	16H	12H + 4T	10H + 6T

(2.113)

where 'H' stands for the hyper- and 'T' for the tensor multiplet.

The open string spectrum

In order to determine the open string spectrum we have to count the degrees of freedom of the Chan-Paton factors λ for the massless states. Remember, that we denote the state of an open string starting on brane (a) and ending on brane (b) by

$$|\psi, ij\rangle \lambda^{(a,b)}_{ji}\,, \tag{2.114}$$

where $1 \le i,j \le M$ and M is the number of D7-branes lying on top of each other, consider figure 2.6.

In the untwisted NS sector (i.e. strings which start and end on the same stack of D-branes) the massless states are given by $\psi^m_{-1/2}|0,ij\rangle\lambda^{(a,a)}_{ji}$ $(m = 0,\dots,9)$. The string (a,a) is invariant under $\Omega\mathcal{R}$ and $\Omega\mathcal{R}\Theta$. Applying these symmetries using equation (2.54), we obtain constraints on the Chan-Paton factors. In the non-compact directions $(\psi^\mu_{-1/2}|0,ij\rangle\lambda^{(a,a)}_{ji}$, $\mu = 0,\dots,5)$ they read

$$\lambda^{(a,a)} = -\left(\gamma^{(a)}_{\Omega\mathcal{R}0}\lambda^{(a,a)}\gamma^{(a)-1}_{\Omega\mathcal{R}0}\right)^T = -\left(\gamma^{(a)}_{\Omega\mathcal{R}1}\lambda^{(a,a)}\gamma^{(a)-1}_{\Omega\mathcal{R}1}\right)^T\,, \tag{2.115}$$

where the minus signs arise from the action of $\Omega\mathcal{R}$ on the massless state. Using the representation matrices (2.96) we found from the tadpole cancellation conditions and considering the string $(0,0)$, we obtain

$$\lambda^{(0,0)} = -\lambda^{(0,0)T} = -I\lambda^{(0,0)T}I\,. \tag{2.116}$$

Rewriting λ with $M/2 \times M/2$ block matrices yields

$$\lambda^{(0,0)} = \begin{pmatrix} \alpha & \beta \\ \gamma & \delta \end{pmatrix} = \begin{pmatrix} -\alpha^T & -\gamma^T \\ -\beta^T & -\delta^T \end{pmatrix} = \begin{pmatrix} -\delta^T & \beta^T \\ \gamma^T & -\alpha^T \end{pmatrix} \tag{2.117}$$

and thus

$$\lambda^{(0,0)} = \begin{pmatrix} A & S \\ -S & A \end{pmatrix}, \tag{2.118}$$

where A is an antisymmetric and S is a symmetric $M/2 \times M/2$ matrix. Therefore we are left with $(M/2)^2$ degrees of freedom for $\lambda^{(0,0)}$. Since $\psi^{\mu}_{-1/2}|0, ij\rangle\lambda^{(0,0)}_{ji}$ is a massless vector in spacetime, it has to be a gauge boson. This means that $(M/2)^2$ has to be the dimension of the adjoint representation and from this we learn that the gauge group which lives on the stack of (0) D-branes is $U(M/2)$. Since all this similarly applies to the $(1,1)$ strings, we find the gauge group for the $\mathbb{Z}_2$ model to be

$$U(M/2) \times U(M/2)\,. \tag{2.119}$$

Proceeding in the same way with $\psi^{i,\bar{i}}_{-1/2}|0, ij\rangle\lambda^{(a,a)}_{ji}$ in the compact dimensions, we obtain the constraints

$$\lambda^{(a,a)} = -\left(\gamma^{(a)}_{\Omega\mathcal{R}0}\lambda^{(a,a)}\gamma^{(a)-1}_{\Omega\mathcal{R}0}\right)^T = \left(\gamma^{(a)}_{\Omega\mathcal{R}1}\lambda^{(a,a)}\gamma^{(a)-1}_{\Omega\mathcal{R}1}\right)^T, \tag{2.120}$$

because Θ produces an additional minus sign. For the $(0,0)$ string, this gives

$$\lambda^{(0,0)} = -\lambda^{(0,0)T} = I\lambda^{(0,0)T}I\,. \tag{2.121}$$

In block matrices

$$\lambda^{(0,0)} = \begin{pmatrix} \alpha & \beta \\ \gamma & \delta \end{pmatrix} = \begin{pmatrix} -\alpha^T & -\gamma^T \\ -\beta^T & -\delta^T \end{pmatrix} = \begin{pmatrix} \delta^T & -\beta^T \\ -\gamma^T & \alpha^T \end{pmatrix} \tag{2.122}$$

From this we find

$$\lambda^{(0,0)} = \begin{pmatrix} A_1 & A_2 \\ A_2 & A_1 \end{pmatrix}, \tag{2.123}$$

where $A_{1,2}$ are antisymmetric $M/2 \times M/2$ matrices. This means that the compact scalars from the $(0,0)$ strings yield one hypermultiplet in the antisymmetric $(A,1) + (\bar{A},1)$, or equivalently two hypermultiplets in the $(A,1)$ of the gauge group $U(M/2) \times U(M/2)$. From the $(1,1)$ strings we find the same for the second factor of the gauge group.

It remains to determine the content of the twisted sector, i.e. of the $(0,1)$ strings. For these strings, $\Omega\mathcal{R}$ is no symmetry, it rather maps them to the $(1,0)$ strings which therefore do not have to be counted separately. Nevertheless, Θ is a symmetry in this sector, where the states are given by $|0,0,\pm\frac{1}{2},\pm\frac{1}{2};ij\rangle\lambda^{(0,1)}_{ji}$. Applying equation (2.46) and using the representation matrices (2.96), the Θ invariance leads to the constraint

$$\lambda^{(0,1)} = \pm I\lambda^{(0,1)}I\,, \tag{2.124}$$

where the sign is unphysical, because we only know that Θ^2 acts trivially on the state. In block matrices, this constraint reads

$$\lambda^{(0,1)} = \begin{pmatrix} \alpha & \beta \\ \gamma & \delta \end{pmatrix} = \pm \begin{pmatrix} \delta & -\gamma \\ -\beta & \alpha \end{pmatrix}, \tag{2.125}$$

i.e.

$$\lambda^{(0,1)} = \pm \begin{pmatrix} X_1 & X_2 \\ -X_2 & X_1 \end{pmatrix}, \tag{2.126}$$

where $X_{1,2}$ are some $M/2 \times M/2$ matrices and thus yield $2(M/2)^2$ degrees of freedom. Therefore we find the representation $(F,F)+(\bar{F},\bar{F})$ for the two scalars in this sector, or equivalently one hypermultiplet in the (F,F). Remember that the twisted open strings are localized at the intersection points of the D7-branes and therefore we have to include the multiplicities (2.50), i.e. 1 (2,4) for the **AA** (**AB**,**BB**) model. Note that all intersection points are invariant under the orientifold group in this model.

Altogether, we find the open string spectrum of the $\mathbb{Z}_2$ model

twist sector	**AA**	**AB**	**BB**	rep. of $[U(M/2)]^2$
untwisted		1V		$(ad,1)+(1,ad)$
		2H		$(A,1)+(1,A)$
Θ	1H	2H	4H	(F,F)

(2.127)

The spectrum of the **AA** model is the same as of the model discussed in [44], as expected because of T-duality. Moving some of the D-branes away from the O-planes in a way that respects the symmetry of the theory corresponds to higgsing the gauge group [44]. We will not discuss this issue in this thesis.

Since we are dealing with compactifications of type IIB theories, we have to check that the closed and open string massless spectrum satisfies the anomaly constraint [20]

$$n_H - n_V + 29n_T = 273\,, \tag{2.128}$$

which is the case, as one can easily check.

To summarize the results, in this section we have explicitely shown that the massless spectrum of the **AA** type $\Omega\mathcal{R}$ orientifold on $T^4/\mathbb{Z}_2$ with D7-branes perpendicular to each other is equal to the massless spectrum of [44]. Of course, this is a consequence of T-duality of these two models, where T-duality is applied in the 7th and 9th direction. Furthermore, we have explicitely calculated the **AB** and **BB** type models which were only briefly mentioned in [7]. In the T-dual picture, the tilting of the respective tori corresponds to switching on a discrete B-field of rank $r = 2$ for the **AB** and $r = 4$ for the **BB** model, consider [7] for further details.

Chapter 3

Four dimensional $\Omega\mathcal{R} \times \mathbb{Z}_N \times \mathbb{Z}_M$ orientifolds

In this chapter we construct supersymmetric $\Omega\mathcal{R} \times \mathbb{Z}_N \times \mathbb{Z}_M$ orientifolds of Type IIA in four dimensions with D6-branes at angles [41]. We find consistent models in the cases $\mathbb{Z}_2 \times \mathbb{Z}_2$, $\mathbb{Z}_3 \times \mathbb{Z}_3$, $\mathbb{Z}_4 \times \mathbb{Z}_2$ and $\mathbb{Z}_6 \times \mathbb{Z}_3$, again with various combinations of torus lattices. The six dimensional compact space is chosen to be a direct product of two-tori.

3.1 Setup of the four dimensional models

The modifications with respect to the six dimensional models are obvious and therefore can be treated very shortly. The non-compact coordinates are X^μ ($\mu = 0, \dots, 3$) and the compact coordinates are complexified

$$Z^1 = X^4 + iX^5\,, \quad Z^2 = X^6 + iX^7\,, \quad Z^3 = X^8 + iX^9\,, \tag{3.1}$$

i.e. a product of three two-tori $T_1 \times T_2 \times T_3$. The orbifold group is $\mathbb{Z}_N \times \mathbb{Z}_M$ with $N, M \in \{2, 3, 4, 6\}$. The action of an element (Θ_1, Θ_2) from the orbifold group is described by

$$\begin{array}{rccl} \Theta_1: & Z^i & \longrightarrow & e^{2\pi i v_i} Z^i \\ \Theta_2: & Z^i & \longrightarrow & e^{2\pi i w_i} Z^i\,, \end{array} \tag{3.2}$$

where $\vec{v} = \frac{1}{N}(1, -1, 0)$ and $\vec{w} = \frac{1}{M}(0, 1, -1)$. This preserves $\mathcal{N} = 1$ supersymmetry in four dimensions. Worldsheet parity Ω is combined with the reflection $\mathcal{R}$, which now acts in the 5th, 7th and 9th direction. The orientifold group acts on closed string degenerate ground states as

$$\begin{array}{rccl} \mathcal{R}: & |s_1, s_2, s_3, s_4\rangle & \longrightarrow & |s_1, -s_2, -s_3, -s_4\rangle \\ \Theta_1: & |s_1, s_2, s_3, s_4\rangle & \longrightarrow & e^{2\pi i \vec{v}\cdot\vec{s}}\, |s_1, s_2, s_3, s_4\rangle \\ \Theta_2: & |s_1, s_2, s_3, s_4\rangle & \longrightarrow & e^{2\pi i \vec{w}\cdot\vec{s}}\, |s_1, s_2, s_3, s_4\rangle \end{array} \tag{3.3}$$

Under GSO projection states with fermion numbers $(-1)^{F_L} = (-1)^{F_R} = 1$ are kept, where

$$
\begin{aligned}
(-1)^{F_L} \left|s_1, s_2, s_3, s_4\right\rangle_L &= -e^{\pi i(s_1 - s_2 - s_3 - s_4)} \left|s_1, s_2, s_3, s_4\right\rangle_L \\
(-1)^{F_R} \left|s_1, s_2, s_3, s_4\right\rangle_R &= -e^{\pi i(s_1 + s_2 + s_3 + s_4)} \left|s_1, s_2, s_3, s_4\right\rangle_R \, .
\end{aligned}
\tag{3.4}
$$

This is consistent with the orientifold symmetries and reflects the fact that we are now dealing with a compactification of Type IIA.

Before we go into the details, we want to figure out which models will lead to consistent solutions. Out of all possible combinations, the cases $\mathbb{Z}_4 \times \mathbb{Z}_3$ and $\mathbb{Z}_6 \times \mathbb{Z}_4$ are cristallographically forbidden, because the lattices of $\mathbb{Z}_4$ and $\mathbb{Z}_{3,6}$ are incompatible on the second torus. Of course, e.g. $\mathbb{Z}_4 \times \mathbb{Z}_3$ is equivalent to $\mathbb{Z}_3 \times \mathbb{Z}_4$. In the case of $\mathbb{Z}_3 \times \mathbb{Z}_2$, an insertion of Θ_1 interchanges **A** and **B** lattice contributions to the Klein bottle on the second torus only. Therefore no combination of **A** and **B** lattices exists which is symmetric under this interchange. This spoils worldsheet duality, as we have learned in the previous chapter. The same argument rules out the models $\mathbb{Z}_6 \times \mathbb{Z}_2$, $\mathbb{Z}_4 \times \mathbb{Z}_4$, and $\mathbb{Z}_6 \times \mathbb{Z}_6$. From the remaining models, $\mathbb{Z}_4 \times \mathbb{Z}_2$ and $\mathbb{Z}_6 \times \mathbb{Z}_3$ are constrained to the symmetric combination of tori for the same reason, such that we are left with

$$
\begin{aligned}
\mathbb{Z}_2 \times \mathbb{Z}_2 : &\quad \mathbf{AAA}, \mathbf{AAB}, \mathbf{ABB}, \mathbf{BBB} \\
\mathbb{Z}_3 \times \mathbb{Z}_3 : &\quad \mathbf{AAA}, \mathbf{AAB}, \mathbf{ABB}, \mathbf{BBB} \\
\mathbb{Z}_4 \times \mathbb{Z}_2 : &\quad \mathbf{ABA}, \mathbf{ABB} \\
\mathbb{Z}_6 \times \mathbb{Z}_3 : &\quad \mathbf{ABA}, \mathbf{ABB}
\end{aligned}
\tag{3.5}
$$

out of which the $\mathbb{Z}_2 \times \mathbb{Z}_2$ **AAA** is T-dual to the model discussed in [15]. The spectra of the T-duals of all four $\mathbb{Z}_2 \times \mathbb{Z}_2$ models are given in [61], which partly differ from our results. But since in this reference there are no detailed calculations, we can not make any further statements concerning this discrepancy.

Since we are familiar right now with the calculation of the amplitudes and since the expressions become rather lengthy in the case of $\mathbb{Z}_N \times \mathbb{Z}_M$, we introduce some abbreviations for the oscillator contributions of the $\Theta_1^{n_1}\Theta_2^{n_2}$ twisted sector with an insertion of $\Theta_1^{k_1}\Theta_2^{k_2}$ (in the cases of the Klein bottle and the Möbius strip, the insertions are accompanied by $\Omega\mathcal{R}$)

$$\mathcal{K}^{(n_1,k_1)(n_2,k_2)} = \frac{\vartheta\left[{0 \atop 1/2}\right]}{\eta^3} \prod_{n_1 v_i + n_2 w_i \notin \mathbb{Z}} \left(\frac{\vartheta\left[{n_1 v_i + n_2 w_i \atop 1/2}\right]}{\vartheta\left[{1/2 + n_1 v_i + n_2 w_i \atop 1/2}\right]} e^{\pi i \langle n_1 v_i + n_2 w_i \rangle} \right) \times \prod_{n_1 v_i + n_2 w_i \in \mathbb{Z}} \left(\frac{\vartheta\left[{0 \atop 1/2}\right]}{\eta^3} \right), \tag{3.6}$$

$$\mathcal{A}^{(n_1,k_1)(n_2,k_2)} = \frac{\vartheta\left[{0 \atop 1/2}\right]}{\eta^3} \prod_{(n_1 v_i + n_2 w_i, k_1 v_i + k_2 w_i) \notin \mathbb{Z}^2} \left(\frac{(-2i)^\delta \, \vartheta\left[{n_1 v_i + n_2 w_i \atop 1/2 + k_1 v_i + k_2 w_i}\right]}{\vartheta\left[{1/2 + n_1 v_i + n_2 w_i \atop 1/2 + k_1 v_i + k_2 w_i}\right]} e^{\pi i \langle n_1 v_i + n_2 w_i \rangle} \right) \times \prod_{(n_1 v_i + n_2 w_i, k_1 v_i + k_2 w_i) \in \mathbb{Z}^2} \left(\frac{\vartheta\left[{1/2 \atop 0}\right]}{\eta^3} \right), \tag{3.7}$$

$$\mathcal{M}^{(n_1,k_1)(n_2,k_2)} = \frac{\vartheta\left[{1/2 \atop 0}\right]}{\eta^3} \prod_{(n_1 v_i + n_2 w_i, k_1 v_i + k_2 w_i) \notin \mathbb{Z}^2} \left(\frac{(-2i)^\delta \, \vartheta\left[{1/2 + n_1 v_i + n_2 w_i \atop k_1 v_i + k_2 w_i}\right]}{\vartheta\left[{1/2 + n_1 v_i + n_2 w_i \atop 1/2 + k_1 v_i + k_2 w_i}\right]} e^{\pi i \langle n_1 v_i + n_2 w_i \rangle} \right) \times \prod_{(n_1 v_i + n_2 w_i, k_1 v_i + k_2 w_i) \in \mathbb{Z}^2} \left(\frac{\vartheta\left[{1/2 \atop 0}\right]}{\eta^3} \right), \tag{3.8}$$

consider again appendix A for the details. There appear phases which are always cancelled in the six dimensional models. The arguments in the theta and eta functions are $2t$ in the Klein bottle, $t + \frac{i}{2}$ in the Möbius strip, and t in the annulus. Furthermore, we used the notation [19],

$$\langle x \rangle \equiv x - [x] - \frac{1}{2}, \tag{3.9}$$

where the brackets on the rhs denote the integer part and

$$\delta = \begin{cases} 1 & \text{if} \quad (n_1 v_i + n_2 w_i, k_1 v_i + k_2 w_i) \in \mathbb{Z} \times (\mathbb{Z} + \frac{1}{2}) \\ 0 & \text{else.} \end{cases} \tag{3.10}$$

Since the Klein bottle 1-loop amplitude is independent of the insertions, we further abbreviate $\mathcal{K}^{(n_1,n_2)} = \mathcal{K}^{(n_1,k_1)(n_2,k_2)}$. In the case of the annulus, we have seen that, apart from the trivial insertion of $\mathbb{1}$, only insertions which square to the identity contribute (these insertions we will call $\mathbb{Z}_2$-like in the following), because the other insertions do not leave the D-branes invariant. But in the end, even the terms with the $\mathbb{Z}_2$-like insertions vanish due to the twisted tadpole cancellation conditions (2.48). Thus we get by with the terms $\mathcal{A}^{(n_1,0)(n_2,0)}$ which we abbreviate with $\mathcal{A}^{(n_1,n_2)}$ in the following.

In the tree channel amplitudes, we use the abbreviations

$$\tilde{\mathcal{K}}^{(n_1,n_2)} = \frac{\vartheta\left[{1/2 \atop 0}\right]}{\eta^3} \prod_{n_1 v_i + n_2 w_i \notin \mathbb{Z}} \left(\frac{\vartheta\left[{1/2 \atop n_1 v_i + n_2 w_i}\right]}{\vartheta\left[{1/2 \atop 1/2 + n_1 v_i + n_2 w_i}\right]} \right) \prod_{n_1 v_i + n_2 w_i \in \mathbb{Z}} \left(\frac{\vartheta\left[{1/2 \atop 0}\right]}{\eta^3} \right) , \tag{3.11}$$

$$\tilde{\mathcal{A}}^{(n_1,n_2)} = \frac{\vartheta\left[{1/2 \atop 0}\right]}{\eta^3} \prod_{n_1 v_i + n_2 w_i \notin \mathbb{Z}} \left(\frac{\vartheta\left[{1/2 \atop n_1 v_i + n_2 w_i}\right]}{\vartheta\left[{1/2 \atop 1/2 + n_1 v_i + n_2 w_i}\right]} \right) \prod_{n_1 v_i + n_2 w_i \in \mathbb{Z}} \left(\frac{\vartheta\left[{1/2 \atop 0}\right]}{\eta^3} \right) , \tag{3.12}$$

$$\tilde{\mathcal{M}}^{(n_1,n_2)} = \frac{\vartheta\left[{1/2 \atop 0}\right]}{\eta^3} \prod_{n_1 v_i + n_2 w_i \notin \mathbb{Z}} \left(\frac{\vartheta\left[{1/2 \atop n_1 v_i + n_2 w_i}\right]}{\vartheta\left[{1/2 \atop 1/2 + n_1 v_i + n_2 w_i}\right]} \right) \prod_{n_1 v_i + n_2 w_i \in \mathbb{Z}} \left(\frac{\vartheta\left[{1/2 \atop 0}\right]}{\eta^3} \right) , \tag{3.13}$$

where the arguments are $2l$ for $\tilde{\mathcal{K}}^{(n_1,n_2)}$ and $\tilde{\mathcal{A}}^{(n_1,n_2)}$ and $2l+i/2$ for $\tilde{\mathcal{M}}^{(n_1,n_2)}$. The arguments of the various functions in the amplitudes should be familiar by now and we will not explicitely mention them anymore in the following. Equipped with this, we can start calculating.

3.2 The $\mathbb{Z}_2 \times \mathbb{Z}_2$ model

3.2.1 Amplitudes and tadpole cancellation conditions

The Klein bottle 1-loop amplitude

The torus lattices are of course the same as in the six dimensional case, consider figure 2.5. Therefore, the lattice contributions are given by $\mathcal{L}_i^{\mathcal{K}} = \mathcal{L}[1,1]$ for an **A** type and $\mathcal{L}_i^{\mathcal{K}} = \mathcal{L}[2,2]$ for a **B** type torus. Thus, in the untwisted sector a lattice contribution of $\mathcal{L}_1^{\mathcal{K}}\mathcal{L}_2^{\mathcal{K}}\mathcal{L}_3^{\mathcal{K}}$ shows up, as usual. But now, e.g. in the Θ_1 twisted sector, the modes on the third torus T_3 are untwisted and therefore the corresponding term in the amplitude contains the lattice contribution $\mathcal{L}_3^{\mathcal{K}}$. In this sense, we use the terminology 'untwisted' and 'twisted tori' in the following. Furthermore, we do not have to worry about worldsheet duality, because the orbifold group leaves the lattice contributions invariant. We obtain the Klein bottle 1-loop amplitude

$$\begin{aligned}\mathcal{K} = c(1_{\mathrm{RR}} - 1_{\mathrm{NSNS}}) \int_0^\infty \frac{dt}{t^3} \times \\ \left\{ \mathcal{L}_1^{\mathcal{K}}\mathcal{L}_2^{\mathcal{K}}\mathcal{L}_3^{\mathcal{K}}\mathcal{K}^{(0,0)} + \chi_{\mathcal{K}}^{(1,0)}\mathcal{L}_3^{\mathcal{K}}\mathcal{K}^{(1,0)} + \chi_{\mathcal{K}}^{(0,1)}\mathcal{L}_1^{\mathcal{K}}\mathcal{K}^{(0,1)} + \chi_{\mathcal{K}}^{(1,1)}\mathcal{L}_2^{\mathcal{K}}\mathcal{K}^{(1,1)} \right\} ,\end{aligned} \tag{3.14}$$

where now $c = V_4/(8\pi^2\alpha')^2$, with V_4 the regularized volume of momentum space, since we are dealing with four non-compact dimensions. $\chi_{\mathcal{K}}^{(n_1,n_2)}$ denotes the various multiplicities of the $\Theta_1^{n_1}\Theta_2^{n_2}$ twisted fixed points invariant under $\Omega\mathcal{R}\Theta_1^{k_1}\Theta_2^{k_2}$

shown in the following table, consider also figure 2.5. There is obviously no k_1, k_2 dependence of the multiplicities in this model (this will turn out to be different if factors of $\mathbb{Z}_4$ or $\mathbb{Z}_6$ are involved).

	AAA	**AAB**	**ABB**	**BBB**
$\chi_{\mathcal{K}}^{(1,0)}$	16	16	8	4
$\chi_{\mathcal{K}}^{(0,1)}$	16	8	4	4
$\chi_{\mathcal{K}}^{(1,1)}$	16	8	8	4

(3.15)

The annulus 1-loop amplitude

The D6-branes are arranged as shown in figure 3.1, where the action of the orbifold group is visualized as well. In the $\mathbb{Z}_N \times \mathbb{Z}_M$ models, we label the D-branes by (a_1, a_2), such that an open string stretching from brane $(0,0)$ to brane (n_1, n_2) corresponds to the $\Theta_1^{-n_1}\Theta_2^{-n_2}$ twisted sector. Remember (see section 2.2.2), that

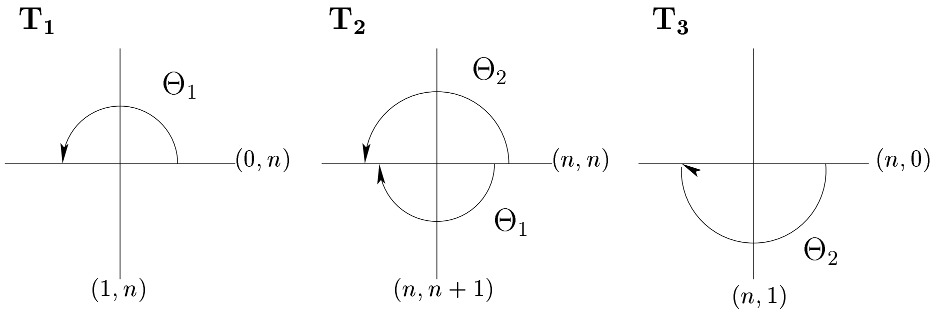

Figure 3.1: Arrangement of D-branes and action of the orbifold group for $\mathbb{Z}_2 \times \mathbb{Z}_2$. Inserting $n = 0, 1$ yields the four D-branes $(a_1, a_2) = (0,0), (1,0), (0,1), (1,1)$ mod $(2,2)$.

the lattice contributions are given by $\mathcal{L}_i^{\mathcal{A}} = \mathcal{L}[2,2]$ for an **A** type and $\mathcal{L}_i^{\mathcal{A}} = \mathcal{L}[1,1]$ for a **B** type torus. We obtain the annulus amplitude

$$\begin{aligned} \mathcal{A} = & \frac{c}{4} M^2 (1_{\text{RR}} - 1_{\text{NSNS}}) \int_0^\infty \frac{dt}{t^3} \times \\ & \left\{ \mathcal{L}_1^{\mathcal{A}} \mathcal{L}_2^{\mathcal{A}} \mathcal{L}_3^{\mathcal{A}} \mathcal{A}^{(0,0)} + \chi_{\mathcal{A}}^{(1,0)} \mathcal{L}_3^{\mathcal{A}} \mathcal{A}^{(1,0)} + \chi_{\mathcal{A}}^{(0,1)} \mathcal{L}_1^{\mathcal{A}} \mathcal{A}^{(0,1)} + \chi_{\mathcal{A}}^{(1,1)} \mathcal{L}_2^{\mathcal{A}} \mathcal{A}^{(1,1)} \right\} , \end{aligned} \tag{3.16}$$

where $\chi_{\mathcal{A}}^{(n_1,n_2)}$ are the multiplicities of the intersections of the $\Theta_1^{n_1}\Theta_2^{n_2}$ twisted strings with respect to brane $(0,0)$. Only the intersection points invariant under $\Theta_1^{k_1}\Theta_2^{k_2}$ are counted, which is always the case for the model under consideration, see figure 2.7. The various multiplicities are

	AAA	**AAB**	**ABB**	**BBB**
$\chi_{\mathcal{A}}^{(1,0)}$	1	1	2	4
$\chi_{\mathcal{A}}^{(0,1)}$	1	2	4	4
$\chi_{\mathcal{A}}^{(1,1)}$	1	2	2	4

(3.17)

In equation (3.16), M^2 again arises from the Chan-Paton factors (2.47) and describes the number M of D6-branes lying on top of each other (this M is not to be confused with the M from $\mathbb{Z}_N \times \mathbb{Z}_M$). Furthermore, we have already used the twisted sector tadpole cancellation conditions (2.48), which read in this case

$$\mathrm{tr}\gamma_{01}^{(a_1,a_2)} = \mathrm{tr}\gamma_{10}^{(a_1,a_2)} = \mathrm{tr}\gamma_{11}^{(a_1,a_2)} = 0\,, \tag{3.18}$$

where $\gamma_{k_1k_2}^{(a_1,a_2)}$ abbreviates $\gamma_{\Theta_1^{k_1}\Theta_2^{k_2}}^{(a_1,a_2)}$.

The Möbius strip 1-loop amplitude

To determine which strings contribute to the Möbius strip 1-loop amplitude, we easily generalize (2.52) to the case of $\mathbb{Z}_N \times \mathbb{Z}_M$. We denote a $\Theta_1^{n_1}\Theta_2^{n_2}$ twisted string starting on brane (a_1, a_2) by $(a_1, a_1-n_1|a_2, a_2-n_2)$ and consider the action of the insertion $\Omega\mathcal{R}\Theta_1^{k_1}\Theta_2^{k_2}$ thereupon:

$$\begin{aligned}
&(a_1, a_1 - n_1|a_2, a_2 - n_2)\\
&\quad\xrightarrow{\Theta^k} (a_1 - 2k_1, a_1 - n_1 - 2k_1|a_2 - 2k_2, a_2 - n_2 - 2k_2)\\
&\quad\xrightarrow{\mathcal{R}} (-a_1 + 2k_1, -a_1 + n_1 + 2k_1| - a_2 + 2k_2, -a_2 + n_2 + 2k_2)\\
&\quad\xrightarrow{\Omega} (-a_1 + n_1 + 2k_1, -a_1 + 2k_1| - a_2 + n_2 + 2k_2, -a_2 + 2k_2)
\end{aligned} \tag{3.19}$$

Thus only terms with

$$n_1 + 2k_1 = 2a_1 \bmod N \qquad \text{and} \qquad n_2 + 2k_2 = 2a_2 \bmod M \tag{3.20}$$

contribute. In the case of $\mathbb{Z}_2 \times \mathbb{Z}_2$ this simply means that, performing the calculation for the strings starting on stack $(0, 0)$ and including a factor of $NM = 4$ in the end, only untwisted strings with all possible insertions contribute. We obtain

$$\begin{aligned}
\mathcal{M} = &-\frac{c}{4}(1_{\mathrm{RR}} - 1_{\mathrm{NSNS}}) \int_0^\infty \frac{dt}{t^3}\times\\
&\big\{C_{00}^{00}\mathcal{L}_1^{\mathcal{M}}\mathcal{L}_2^{\mathcal{M}}\mathcal{L}_3^{\mathcal{M}}\mathcal{M}^{(0,0)(0,0)} + C_{10}^{00}\mathcal{L}_3^{\mathcal{M}}\mathcal{M}^{(0,1)(0,0)}\\
&+C_{01}^{00}\mathcal{L}_1^{\mathcal{M}}\mathcal{M}^{(0,0)(0,1)} + C_{11}^{00}\mathcal{L}_2^{\mathcal{M}}\mathcal{M}^{(0,1)(0,1)}\big\}\ ,
\end{aligned} \tag{3.21}$$

where we have included the lattice contributions $\mathcal{L}_i^{\mathcal{M}} = \mathcal{L}[2,2]$ ($\mathcal{L}_i^{\mathcal{M}} = \mathcal{L}[1,4]$) for an **A** (**B**) torus and the Chan-Paton factors

$$C_{k_1k_2}^{n_1n_2} \equiv \mathrm{tr}\left(\gamma_{\Omega\mathcal{R}k_1k_2}^{(-n_1,-n_2)-T}\gamma_{\Omega\mathcal{R}k_1k_2}^{(0,0)}\right) . \tag{3.22}$$

Since only the untwisted strings contribute, we do not have to include any additional multiplicities from intersections.

Tree channel amplitudes and tadpole cancellation

Modular transformation of the various amplitudes leads to

$$\begin{aligned}\tilde{\mathcal{K}} &= cc_1^{\mathcal{K}}c_2^{\mathcal{K}}c_3^{\mathcal{K}}(1_{\mathrm{RR}} - 1_{\mathrm{NSNS}})\int_0^\infty dl\times \\ &\quad \left\{\tilde{\mathcal{L}}_1^{\mathcal{K}}\tilde{\mathcal{L}}_2^{\mathcal{K}}\tilde{\mathcal{L}}_3^{\mathcal{K}}\tilde{\mathcal{K}}^{(0,0)} - 4\tilde{\mathcal{L}}_3^{\mathcal{K}}\tilde{\mathcal{K}}^{(1,0)} - 4\tilde{\mathcal{L}}_1^{\mathcal{K}}\tilde{\mathcal{K}}^{(0,1)} - 4\tilde{\mathcal{L}}_2^{\mathcal{K}}\tilde{\mathcal{K}}^{(1,1)}\right\} ,\end{aligned} \tag{3.23}$$

$$\begin{aligned}\tilde{\mathcal{A}} &= \frac{c}{16}cc_1^{\mathcal{A}}c_2^{\mathcal{A}}c_3^{\mathcal{A}}M^2(1_{\mathrm{RR}} - 1_{\mathrm{NSNS}})\int_0^\infty dl\times \\ &\quad \left\{\tilde{\mathcal{L}}_1^{\mathcal{A}}\tilde{\mathcal{L}}_2^{\mathcal{A}}\tilde{\mathcal{L}}_3^{\mathcal{A}}\tilde{\mathcal{A}}^{(0,0)} - 4\tilde{\mathcal{L}}_3^{\mathcal{A}}\tilde{\mathcal{A}}^{(1,0)} - 4\tilde{\mathcal{L}}_1^{\mathcal{A}}\tilde{\mathcal{A}}^{(0,1)} - 4\tilde{\mathcal{L}}_2^{\mathcal{A}}\tilde{\mathcal{A}}^{(1,1)}\right\} ,\end{aligned} \tag{3.24}$$

$$\begin{aligned}\tilde{\mathcal{M}} &= -4c(1_{\mathrm{RR}} - 1_{\mathrm{NSNS}})\int_0^\infty dl\times \\ &\quad \left\{C_{00}^{00}\tilde{\mathcal{L}}_1^{\mathcal{M}}\tilde{\mathcal{L}}_2^{\mathcal{M}}\tilde{\mathcal{L}}_3^{\mathcal{M}}\tilde{\mathcal{M}}^{(0,0)} + 4C_{10}^{00}\tilde{\mathcal{L}}_3^{\mathcal{M}}\tilde{\mathcal{M}}^{(1,0)} + 4C_{01}^{00}\tilde{\mathcal{L}}_1^{\mathcal{M}}\tilde{\mathcal{M}}^{(0,1)} + 4C_{11}^{00}\tilde{\mathcal{L}}_2^{\mathcal{M}}\tilde{\mathcal{M}}^{(1,1)}\right\} .\end{aligned} \tag{3.25}$$

From these amplitudes we find the tadpole cancellation conditions

$$\begin{aligned} M &= 32 \quad (\mathbf{AAA}) \\ M &= 16 \quad (\mathbf{AAB}) \\ M &= 8 \quad (\mathbf{ABB}) \\ M &= 4 \quad (\mathbf{BBB}) \end{aligned} \tag{3.26}$$

and

$$C_{00}^{00} = -C_{10}^{00} = -C_{01}^{00} = -C_{11}^{00} = M\,. \tag{3.27}$$

3.2.2 Representation matrices of the orientifold group

As we already have mentioned, the **AAA** model is T-dual to the model discussed in [15]. To be more specific, the $(0,0)$ D6-branes transform into D9-branes under T-duality in the 5th, 7th and 9th direction. The $(0,1)$, $(1,0)$ and $(1,1)$ D6-branes transform into three different types of D5-branes. Now, if we choose the representation matrices of the orientifold group similar to [15], this choice turns out to be consistent with the tadpole cancellation conditions (3.27) and (3.18) as well as the consistency conditions (2.92). The choice of matrices is, up to signs,

$$\begin{array}{|c|c|cccc|}\hline \multicolumn{2}{|c|}{\text{brane}} & \gamma_{\Omega\mathcal{R}00} & \gamma_{\Omega\mathcal{R}10} & \gamma_{\Omega\mathcal{R}01} & \gamma_{\Omega\mathcal{R}11} \\ \hline (0,0) & (0) & \mathbb{1}_M & M_1 & M_2 & M_3 \\ (1,0) & (1) & N_1 & D & M_1 & M_2 \\ (0,1) & (2) & N_1 & M_3 & D & M_2 \\ (1,1) & (3) & N_1 & M_2 & M_3 & D \\ \hline \end{array} \tag{3.28}$$

(where we introduced an alternative labelling of the D6-branes) with the $M \times M$ matrices

$$M_i = \left\{ \begin{pmatrix} 0 & \mathbb{1}_{M/2} \\ -\mathbb{1}_{M/2} & 0 \end{pmatrix}, \begin{pmatrix} -\epsilon & 0 \\ 0 & \epsilon \end{pmatrix}, \begin{pmatrix} 0 & \epsilon \\ \epsilon & 0 \end{pmatrix} \right\} \tag{3.29}$$

and

$$N_i = DM_i = \left\{ \begin{pmatrix} \epsilon & 0 \\ 0 & \epsilon \end{pmatrix}, \begin{pmatrix} 0 & \mathbb{1}_{M/2} \\ \mathbb{1}_{M/2} & 0 \end{pmatrix}, \begin{pmatrix} \mathbb{1}_{M/2} & 0 \\ 0 & -\mathbb{1}_{M/2} \end{pmatrix} \right\} \tag{3.30}$$

as well as

$$D = \begin{pmatrix} 0 & -\epsilon \\ \epsilon & 0 \end{pmatrix} \tag{3.31}$$

and the antisymmetric $M/2 \times M/2$ matrix

$$\epsilon = \begin{pmatrix} 0 & \mathbb{1}_{M/4} \\ -\mathbb{1}_{M/4} & 0 \end{pmatrix}. \tag{3.32}$$

These matrices fulfill several identities

$$\begin{aligned} M_i^{-1} &= M_i^T = -M_i \\ M_i M_j &= \epsilon_{ijk} M_k \\ N_1^{-1} &= N_1^T = -N_1 \\ N_{2,3}^{-1} &= N_{2,3}^T = N_{2,3} \\ D^{-1} &= D^T = D \end{aligned} \tag{3.33}$$

From (2.92) we obtain the representation matrices of the orbifold group

$$\begin{array}{|c|c|cccc|}\hline \multicolumn{2}{|c|}{\text{brane}} & \gamma_{00} & \gamma_{10} & \gamma_{01} & \gamma_{11} \\ \hline (0,0) & (0) & \mathbb{1}_M & M_1 & M_2 & M_3 \\ (1,0) & (1) & \mathbb{1}_M & M_1 & N_3 & N_2 \\ (0,1) & (2) & \mathbb{1}_M & N_2 & M_1 & N_3 \\ (1,1) & (3) & \mathbb{1}_M & N_3 & N_2 & M_1 \\ \hline \end{array} \tag{3.34}$$

3.2.3 The massless spectrum

The closed string spectrum

In the untwisted NSNS sector, we obtain from the non-compact dimensions

$$\left(\psi^{\mu}_{-1/2}\tilde{\psi}^{\nu}_{-1/2} + \psi^{\nu}_{-1/2}\tilde{\psi}^{\mu}_{-1/2}\right)|0\rangle\,, \tag{3.35}$$

which is the graviton plus the dilaton of $\mathcal{N}=1$ SUGRA in $d=4$. From the compact directions, we find model independently the six scalars

$$\psi^{i}_{-1/2}\tilde{\psi}^{\bar{i}}_{-1/2}|0\rangle\,, \qquad \psi^{\bar{i}}_{-1/2}\tilde{\psi}^{i}_{-1/2}|0\rangle\,, \tag{3.36}$$

and in addition the three scalars

$$\left(\psi^{i}_{-1/2}\tilde{\psi}^{i}_{-1/2} + \psi^{\bar{i}}_{-1/2}\tilde{\psi}^{\bar{i}}_{-1/2}\right)|0\rangle\,. \tag{3.37}$$

In the untwisted RR sector we find one model independent scalar

$$|++++\rangle_L|-+++\rangle_R - |----\rangle_L|+---\rangle_R\,. \tag{3.38}$$

This is the axion which completes the $\mathcal{N}=1$ $d=4$ SUGRA multiplet. Furthermore, we find the three scalars

$$\begin{aligned}
&|+--+\rangle_L|---+\rangle_R - |-++-\rangle_L|+++-\rangle_R\,,\\
&|++--\rangle_L|-+--\rangle_R - |--++\rangle_L|+-++\rangle_R\,,\\
&|+-+-\rangle_L|--+-\rangle_R - |-+-+\rangle_L|++-+\rangle_R\,.
\end{aligned} \tag{3.39}$$

To summarize, in the untwisted closed string sector we find the $\mathcal{N}=1$, $d=4$ SUGRA multiplet plus 6 chiral multiplets. In the following, we denote the chiral multiplet by 'C'.

Following the recipe we presented in the 6 dimensional models and taking into account the different features of the 4 dimensional model under consideration, we find that the Θ_1 twisted NSNS sector consists of the following massless states with correct GSO projection

$$\begin{aligned}
\psi^{2}_{0}|0,+\tfrac{1}{2},-\tfrac{1}{2},0\rangle_L &= |0,+\tfrac{1}{2},+\tfrac{1}{2},0\rangle_L \equiv |1\rangle_{\rm NS}\,,\\
\psi^{\bar{1}}_{0}|0,+\tfrac{1}{2},-\tfrac{1}{2},0\rangle_L &= |0,-\tfrac{1}{2},-\tfrac{1}{2},0\rangle_L \equiv |2\rangle_{\rm NS}\,,\\
\tilde{\psi}^{\bar{2}}_{0}|0,-\tfrac{1}{2},+\tfrac{1}{2},0\rangle_R &= |0,-\tfrac{1}{2},-\tfrac{1}{2},0\rangle_R \equiv |\tilde{1}\rangle_{\rm NS}\,,\\
\psi^{1}_{0}|0,-\tfrac{1}{2},+\tfrac{1}{2},0\rangle_R &= |0,+\tfrac{1}{2},+\tfrac{1}{2},0\rangle_R \equiv |\tilde{2}\rangle_{\rm NS}\,.
\end{aligned} \tag{3.40}$$

Note that, following (2.27), all these states produce a minus sign under Θ_1, which is always cancelled by tensorizing. But under Θ_2, the first and the fourth state produce a factor of i, whereas the other two states produce a factor of $-i$. Thus, only the combinations $|1\tilde{1}\rangle_{\rm NSNS}$ and $|2\tilde{2}\rangle_{\rm NSNS}$ are invariant under Θ_2 and symmetrizing with respect to $\Omega\mathcal{R}$ leaves us with

$$\begin{aligned} &|1\tilde{1}\rangle^{\alpha}_{\rm NSNS} + |1\tilde{1}\rangle^{\beta}_{\rm NSNS}\,, \\ &|2\tilde{2}\rangle^{\alpha}_{\rm NSNS} + |2\tilde{2}\rangle^{\beta}_{\rm NSNS} \end{aligned} \tag{3.41}$$

leading to one scalar for an invariant fixed point and two scalars for a pair under $\Omega\mathcal{R}$.

The Θ_1 twisted RR sector consists of the following states, which we find in a similar manner,

$$\begin{aligned} &|+\tfrac{1}{2},0,0,-\tfrac{1}{2}\rangle_L \equiv |1\rangle_{\rm R}\,, \quad |-\tfrac{1}{2},0,0,+\tfrac{1}{2}\rangle_L \equiv |2\rangle_{\rm R}\,, \\ &|+\tfrac{1}{2},0,0,+\tfrac{1}{2}\rangle_R \equiv |\tilde{1}\rangle_{\rm R}\,, \quad |-\tfrac{1}{2},0,0,-\tfrac{1}{2}\rangle_R \equiv |\tilde{2}\rangle_{\rm R}\,, \end{aligned} \tag{3.42}$$

where only the combinations $|1\tilde{1}\rangle_{\rm RR}$ and $|2\tilde{2}\rangle_{\rm RR}$ are invariant under Θ_2 in analogy to the NSNS sector. We find the invariant combinations

$$\begin{aligned} &|1\tilde{1}\rangle^{\alpha}_{\rm RR} - |1\tilde{1}\rangle^{\beta}_{\rm RR}\,, \\ &|2\tilde{2}\rangle^{\alpha}_{\rm RR} - |2\tilde{2}\rangle^{\beta}_{\rm RR}\,, \end{aligned} \tag{3.43}$$

which vanish for an invariant fixed point and contribute 1V for a pair under $\Omega\mathcal{R}$.

In the Θ_1 twisted sector, the tori $T_{1,2}$ are twisted, whereas the torus T_3 is untwisted, i.e. we have fixed points only on the first two tori

AA• : all 16 fixed points invariant
AB• : 13-14, 23-24, 33-34, 43-44 form 4 pairs under $\Omega\mathcal{R}$
the remaining 8 fixed points are invariant
BB• : 13-14, 23-24, 31-41, 32-42, 33-44, 34-43 form 6 pairs under $\Omega\mathcal{R}$,
the remaining 4 fixed points are invariant

where • denotes the untwisted third torus. In the Θ_2 twisted sector, the tori $T_{2,3}$ are twisted, whereas the torus T_3 is untwisted etc.

We find the closed string spectrum of the $\mathbb{Z}_2 \times \mathbb{Z}_2$ model

twist sector	**AAA**	**AAB**	**ABB**	**BBB**
untwisted	SUGRA + 6C			
Θ_1	16C	16C	12C + 4V	10C + 6V
Θ_2	16C	12C + 4V	10C + 6V	10C + 6V
$\Theta_1\Theta_2$	16C	12C + 4V	12C + 4V	10C + 6V

(3.44)

The open string spectrum

In this section, we use the alternative labelling of the D6-branes as shown in (3.28), i.e. the D-branes $(0,0)$, $(1,0)$, $(0,1)$ and $(1,1)$ are labelled by $(0),\dots,(3)$. The massless states $\psi^{\mu}_{-1/2}|0,ij\rangle\lambda^{(a,a)}_{ji}$, $\mu=0,\dots,3$ yield the gauge group. These states are all invariant under $\Omega\mathcal{R}$, $\Omega\mathcal{R}\Theta_1$, $\Omega\mathcal{R}\Theta_2$ and $\Omega\mathcal{R}\Theta_1\Theta_2$, where $\Omega\mathcal{R}\Theta_1\Theta_2$ is not independent. Equivalently, we can use the symmetries $\Omega\mathcal{R}$, Θ_1 and Θ_2 to obtain the full set of constraints

$$\lambda^{(a,a)} = -\left(\gamma^{(a)}_{\Omega\mathcal{R}00}\lambda^{(a,a)}\gamma^{(a)-1}_{\Omega\mathcal{R}00}\right)^T = \gamma^{(a)}_{10}\lambda^{(a,a)}\gamma^{(a)-1}_{10} = \gamma^{(a)}_{01}\lambda^{(a,a)}\gamma^{(a)-1}_{01}\,, \qquad (3.45)$$

where the minus sign again arises from the action of $\Omega\mathcal{R}$ on the vacuum. Using the matrices (3.28) and (3.34) we obtain for the $(0,0)$ strings

$$\lambda^{(0,0)} = -\lambda^{(0,0)T} = -M_1\lambda^{(0,0)}M_1 = -M_2\lambda^{(0,0)}M_2 \qquad (3.46)$$

$$\Rightarrow \qquad \lambda^{(0,0)} = \begin{pmatrix} A & S_1 & S_2 & S_3 \\ -S_1 & A & S_3 & -S_2 \\ -S_2 & -S_3 & A & S_1 \\ -S_3 & S_2 & -S_1 & A \end{pmatrix} \qquad (3.47)$$

with A an antisymmetric $M/4\times M/4$ and S_i symmetric $M/4\times M/4$ matrices. This leaves us with $\frac{1}{2}\frac{M}{2}(\frac{M}{2}+1)$ degrees of freedom and thus with $Sp(M/4)$ as the gauge group for the $(0,0)$ strings. For the other untwisted strings the results are similar and we obtain altogether

$$[Sp(M/4)]^4 \qquad (3.48)$$

as the gauge group for this model. In the compact directions the massless states are $\psi^{i,\bar{i}}_{-1/2}|0,ij\rangle\lambda^{(a,a)}_{ji}$ and the action of Θ_1 and Θ_2 produces additional minus signs, namely for the directions $1,\bar{1}$ (again for the $(0,0)$ strings)

$$\lambda^{(0,0)} = -\lambda^{(0,0)T} = M_1\lambda^{(0,0)}M_1 = -M_2\lambda^{(0,0)}M_2 \qquad (3.49)$$

$$\Rightarrow \qquad \lambda^{(0,0)} = \begin{pmatrix} A_1 & A_2 & S & A_3 \\ A_2 & -A_1 & -A_3 & S \\ -S & -A_3 & A_1 & A_2 \\ A_3 & S & A_2 & -A_1 \end{pmatrix}, \qquad (3.50)$$

for the directions $2,\bar{2}$

$$\lambda^{(0,0)} = -\lambda^{(0,0)T} = M_1\lambda^{(0,0)}M_1 = M_2\lambda^{(0,0)}M_2 \qquad (3.51)$$

$$\Rightarrow \qquad \lambda^{(0,0)} = \begin{pmatrix} A_3 & S & A_1 & A_2 \\ -S & A_3 & A_2 & -A_1 \\ A_1 & A_2 & -A_3 & -S \\ A_2 & -A_1 & S & -A_3 \end{pmatrix}, \qquad (3.52)$$

for the directions $3, \bar{3}$

$$\lambda^{(0,0)} = -\lambda^{(0,0)T} = -M_1\lambda^{(0,0)}M_1 = M_2\lambda^{(0,0)}M_2 \tag{3.53}$$

$$\Rightarrow \qquad \lambda^{(0,0)} = \begin{pmatrix} A_1 & A_2 & A_3 & S \\ A_2 & -A_1 & -S & A_3 \\ A_3 & S & -A_1 & -A_2 \\ -S & A_3 & -A_2 & A_1 \end{pmatrix} . \tag{3.54}$$

Each of these matrices leaves us with $\frac{1}{2}\frac{M}{2}(\frac{M}{2}-1)$ degrees of freedom and thus we find 3C in the antisymmetric $(A,1,1,1)+(1,A,1,1)+(1,1,A,1)+(1,1,1,A)$ of the gauge group.

The Θ_1 twisted sector (the $(0,1)$ and the $(2,3)$ strings) is invariant under Θ_1 and Θ_2. The constraints for the $(0,1)$ strings read

$$\lambda^{(0,1)} = x'\gamma_{10}^{(1)}\lambda^{(0,1)}\gamma_{10}^{(0)-1} = y'\gamma_{01}^{(1)}\lambda^{(0,1)}\gamma_{01}^{(0)-1} , \tag{3.55}$$

where the phases x' and y' are determined by consistency. Inserting the representations yields

$$\lambda^{(0,1)} = xM_1\lambda^{(0,1)}M_1 = yN_3\lambda^{(0,1)}M_2 \tag{3.56}$$

with $x = -x'$ and $y = -y'$. This is solved either by $\lambda^{(0,1)} \equiv 0$ (inconsistent) or for $x^2 = -y^2 = 1$ by $\alpha = -y\alpha\epsilon$, $\beta = y\beta\epsilon$, $\delta = -x\alpha$, $\gamma = x\beta$ which gives:

$$\lambda^{(0,1)} = \begin{pmatrix} m_1 & -ym_1 & m_3 & ym_3 \\ m_2 & -ym_2 & m_4 & ym_4 \\ xm_3 & xym_3 & -xm_1 & xym_1 \\ xm_4 & xym_4 & -xm_2 & xym_2 \end{pmatrix} \tag{3.57}$$

The m_i are arbitrary $\frac{M}{4}\times\frac{M}{4}$ matrices. This yields $(\frac{M}{2})^2$ degrees of freedom. The states in this sector are represented by the first two lines of (3.40). Therefore, the $(0,1)$ strings give 1C in the bifundamental $(F,F,1,1)$. Similarly, the $(2,3)$ strings give 1C in the bifundamental $(1,1,F,F)$. Analogously, we find 1C in the $(F,1,F,1)+(1,F,1,F)$ in the Θ_2 twisted sector and 1C in the $(F,1,1,F)+(1,F,F,1)$ in the $\Theta_1\Theta_2$ twisted sector. In addition, we have to include a factor of two for each **B** type lattice from the multiplicity of intersections, consider figure 2.7.

Altogether, we find the open string spectrum of the $\mathbb{Z}_2 \times \mathbb{Z}_2$ model

twist sector	**AAA**	**AAB**	**ABB**	**BBB**	rep. of $[Sp(M/4)]^4$
untwisted	1V				$(ad,1,1,1)+(1,ad,1,1)$ $+(1,1,ad,1)+(1,1,1,ad)$
	3C				$(A,1,1,1)+(1,A,1,1)$ $+(1,1,A,1)+(1,1,1,A)$
Θ_1	1C	1C	2C	4C	$(F,F,1,1)+(1,1,F,F)$
Θ_2	1C	2C	4C	4C	$(F,1,F,1)+(1,F,1,F)$
$\Theta_1\Theta_2$	1C	2C	2C	4C	$(F,1,1,F)+(1,F,F,1)$

(3.58)

The spectrum of the **AAA** model is the same as of the model discussed in [15], as expected because of T-duality. The **AAB**, **ABB** and **BBB** models are T-dual to the $\mathbb{Z}_2 \times \mathbb{Z}_2$ orientifolds with discrete B field of rank 2, 4 and 6, respectively, listed in [61]. We obtain different results for the twisted open string spectra, but because no explicit calculations are shown in [61], we can not make any further statements concerning this discrepancy. To our knowledge, orientifolds with discrete B field have been discussed first in [16].

3.3 The $\mathbb{Z}_3 \times \mathbb{Z}_3$ model

3.3.1 Amplitudes and tadpole cancellation conditions

The Klein bottle 1-loop amplitude

For the torus lattices, consider figure C.1. The lattice contributions are given by $\mathcal{L}_i^{\mathcal{K}} = \mathcal{L}[4,3]$ for an **A** type and $\mathcal{L}_i^{\mathcal{K}} = \mathcal{L}[4/3,1]$ for a **B** type torus. The Klein bottle 1-loop amplitude is given by

$$\begin{aligned}\mathcal{K} = c(1_{\mathrm{RR}} - 1_{\mathrm{NSNS}}) \int_0^\infty \frac{dt}{t^3} \times \\ \Big\{ \mathcal{L}_1^{\mathcal{K}} \mathcal{L}_2^{\mathcal{K}} \mathcal{L}_3^{\mathcal{K}} \mathcal{K}^{(0,0)} + \chi_{\mathcal{K}}^{(1,0)} \mathcal{L}_3^{\mathcal{K}} \mathcal{K}^{(1,0)} + \chi_{\mathcal{K}}^{(2,0)} \mathcal{L}_3^{\mathcal{K}} \mathcal{K}^{(2,0)} \\ + \chi_{\mathcal{K}}^{(0,1)} \mathcal{L}_1^{\mathcal{K}} \mathcal{K}^{(0,1)} + \chi_{\mathcal{K}}^{(1,1)} \mathcal{L}_2^{\mathcal{K}} \mathcal{K}^{(1,1)} + \chi_{\mathcal{K}}^{(2,1)} \mathcal{K}^{(2,1)} \\ + \chi_{\mathcal{K}}^{(0,2)} \mathcal{L}_1^{\mathcal{K}} \mathcal{K}^{(0,2)} + \chi_{\mathcal{K}}^{(1,2)} \mathcal{K}^{(1,2)} + \chi_{\mathcal{K}}^{(2,2)} \mathcal{L}_2^{\mathcal{K}} \mathcal{K}^{(2,2)} \Big\} .\end{aligned} \tag{3.59}$$

The multiplicities $\chi_{\mathcal{K}}^{(n_1,n_2)}$ of the $\Theta_1^{n_1}\Theta_2^{n_2}$ twisted fixed points invariant under $\Omega\mathcal{R}\Theta_1^{k_1}\Theta_2^{k_2}$ are shown in the following table (see figure C.1). As in the case of

$\mathbb{Z}_2 \times \mathbb{Z}_2$, there is obviously no k_1, k_2 dependence.

	AAA	**AAB**	**ABB**	**BBB**
$\chi_{\mathcal{K}}^{(1,0)} = \chi_{\mathcal{K}}^{(2,0)}$	1	1	3	9
$\chi_{\mathcal{K}}^{(0,1)} = \chi_{\mathcal{K}}^{(0,2)}$	1	3	9	9
$\chi_{\mathcal{K}}^{(1,1)} = \chi_{\mathcal{K}}^{(2,2)}$	1	3	3	9
$\chi_{\mathcal{K}}^{(1,2)} = \chi_{\mathcal{K}}^{(2,1)}$	1	3	9	27

(3.60)

The annulus 1-loop amplitude

For the arrangement of D6-branes we introduce, consider figure 3.2. The lattice

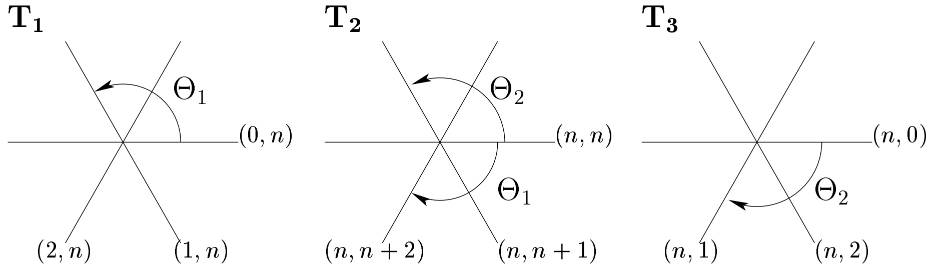

Figure 3.2: Arrangement of D-branes and action of the orbifold group for $\mathbb{Z}_3\times\mathbb{Z}_3$. Inserting $n = 0, 1, 2$ yields the nine D6-branes.

contributions are given by $\mathcal{L}_i^{\mathcal{A}} = \mathcal{L}[2, 3/2]$ for an **A** type and $\mathcal{L}_i^{\mathcal{A}} = \mathcal{L}[2/3, 1/2]$ for a **B** type torus. We obtain the annulus amplitude

$$\begin{aligned}\mathcal{A} = {}& \frac{c}{4} M^2 (1_{\mathrm{RR}} - 1_{\mathrm{NSNS}}) \int_0^\infty \frac{dt}{t^3} \times \\ & \Big\{ \mathcal{L}_1^{\mathcal{A}} \mathcal{L}_2^{\mathcal{A}} \mathcal{L}_3^{\mathcal{A}} \mathcal{A}^{(0,0)} + \chi_{\mathcal{A}}^{(1,0)} \mathcal{L}_3^{\mathcal{A}} \mathcal{A}^{(1,0)} + \chi_{\mathcal{A}}^{(2,0)} \mathcal{L}_3^{\mathcal{A}} \mathcal{A}^{(2,0)} \\ & + \chi_{\mathcal{A}}^{(0,1)} \mathcal{L}_1^{\mathcal{A}} \mathcal{A}^{(0,1)} + \chi_{\mathcal{A}}^{(1,1)} \mathcal{L}_2^{\mathcal{A}} \mathcal{A}^{(1,1)} + \chi_{\mathcal{A}}^{(2,1)} \mathcal{A}^{(2,1)} \\ & + \chi_{\mathcal{A}}^{(0,2)} \mathcal{L}_1^{\mathcal{A}} \mathcal{A}^{(0,2)} + \chi_{\mathcal{A}}^{(1,2)} \mathcal{A}^{(1,2)} + \chi_{\mathcal{A}}^{(2,2)} \mathcal{L}_2^{\mathcal{A}} \mathcal{A}^{(2,2)} \Big\} ,\end{aligned} \tag{3.61}$$

with $\chi_{\mathcal{A}}^{(n_1,n_2)}$ being the multiplicities of the intersections of the $\Theta_1^{n_1}\Theta_2^{n_2}$ twisted strings with respect to brane $(0,0)$. Again, all intersections are invariant under $\Theta_1^{k_1}\Theta_2^{k_2}$, consider figure C.3. This implies $\chi_{\mathcal{A}}^{(n_1,n_2)} = \chi_{\mathcal{K}}^{(n_1,n_2)}$. Since the orbifold group contains no $\mathbb{Z}_2$ type elements, no twisted sector tadpoles show up.

The Möbius strip 1-loop amplitude

From (2.53) we can read off that for a string starting on brane $(0,0)$ the $\Theta_1^{n_1}\Theta_2^{n_2}$ twisted strings with insertion of $\Omega\mathcal{R}\Theta_1^{n_1}\Theta_2^{n_2}$ for all n_1, n_2 contribute. With

$\mathcal{L}_i^{\mathcal{M}} = \mathcal{L}[2,2]$ ($\mathcal{L}_i^{\mathcal{M}} = \mathcal{L}[1,4]$) for an **A** (**B**) torus we find

$$\begin{aligned}\mathcal{M} = &-\frac{c}{4}(1_{\rm RR} - 1_{\rm NSNS})\int_0^\infty \frac{dt}{t^3}\times \\ &\Big\{C_{00}^{00}\mathcal{L}_1^{\mathcal{M}}\mathcal{L}_2^{\mathcal{M}}\mathcal{L}_3^{\mathcal{M}}\mathcal{M}^{(0,0)(0,0)} + C_{10}^{10}\chi_{\mathcal{M}}^{(1,0)}\mathcal{L}_3^{\mathcal{M}}\mathcal{M}^{(1,1)(0,0)} + C_{20}^{20}\chi_{\mathcal{M}}^{(2,0)}\mathcal{L}_3^{\mathcal{M}}\mathcal{M}^{(2,2)(0,0)} \\ &+C_{01}^{01}\chi_{\mathcal{M}}^{(0,1)}\mathcal{L}_1^{\mathcal{M}}\mathcal{M}^{(0,0)(1,1)} + C_{11}^{11}\chi_{\mathcal{M}}^{(1,1)}\mathcal{L}_2^{\mathcal{M}}\mathcal{M}^{(1,1)(1,1)} + C_{21}^{21}\chi_{\mathcal{M}}^{(2,1)}\mathcal{M}^{(2,2)(1,1)} \\ &+C_{02}^{02}\chi_{\mathcal{M}}^{(0,2)}\mathcal{L}_1^{\mathcal{M}}\mathcal{M}^{(0,0)(2,2)} + C_{12}^{12}\chi_{\mathcal{M}}^{(1,2)}\mathcal{M}^{(1,1)(2,2)} + C_{22}^{22}\chi_{\mathcal{M}}^{(2,2)}\mathcal{L}_2^{\mathcal{M}}\mathcal{M}^{(2,2)(2,2)}\Big\}\,,\end{aligned} \tag{3.62}$$

with the Chan-Paton factors $C_{k_1k_2}^{n_1n_2}$ and the multiplicities $\chi_{\mathcal{M}}^{(n_1,n_2)}$ which are the intersection numbers of the $\Theta_1^{n_1}\Theta_2^{n_2}$ twisted strings (with respect to brane $(0,0)$) which are invariant under $\Omega\mathcal{R}$. Since all these intersections are invariant under $\Omega\mathcal{R}$, consider figure C.3, we have $\chi_{\mathcal{M}}^{(n_1,n_2)} = \chi_{\mathcal{A}}^{(n_1,n_2)}$.

Tree channel amplitudes and tadpole cancellation

Modular transformation of the amplitudes yields (for the factors c_i, consider appendix C.1)

$$\begin{aligned}\tilde{\mathcal{K}} = &\, c c_1^{\mathcal{K}} c_2^{\mathcal{K}} c_3^{\mathcal{K}}(1_{\rm RR} - 1_{\rm NSNS})\int_0^\infty dl \times\Big\{\tilde{\mathcal{L}}_1^{\mathcal{K}}\tilde{\mathcal{L}}_2^{\mathcal{K}}\tilde{\mathcal{L}}_3^{\mathcal{K}}\tilde{\mathcal{K}}^{(0,0)} - 3\tilde{\mathcal{L}}_3^{\mathcal{K}}\tilde{\mathcal{K}}^{(1,0)} - 3\tilde{\mathcal{L}}_3^{\mathcal{K}}\tilde{\mathcal{K}}^{(2,0)} \\ &-3\tilde{\mathcal{L}}_1^{\mathcal{K}}\tilde{\mathcal{K}}^{(0,1)} - 3\tilde{\mathcal{L}}_2^{\mathcal{K}}\tilde{\mathcal{K}}^{(1,1)} - 3\sqrt{3}\tilde{\mathcal{K}}^{(2,1)} - 3\tilde{\mathcal{L}}_1^{\mathcal{K}}\tilde{\mathcal{K}}^{(0,2)} + 3\sqrt{3}\tilde{\mathcal{K}}^{(1,2)} - 3\tilde{\mathcal{L}}_2^{\mathcal{K}}\tilde{\mathcal{K}}^{(2,2)}\Big\}\,,\end{aligned} \tag{3.63}$$

$$\begin{aligned}\tilde{\mathcal{A}} = &\,\frac{c}{16}c_1^{\mathcal{A}}c_2^{\mathcal{A}}c_3^{\mathcal{A}}M^2(1_{\rm RR} - 1_{\rm NSNS})\int_0^\infty dl\times\Big\{\tilde{\mathcal{L}}_1^{\mathcal{A}}\tilde{\mathcal{L}}_2^{\mathcal{A}}\tilde{\mathcal{L}}_3^{\mathcal{A}}\tilde{\mathcal{A}}^{(0,0)} - 3\tilde{\mathcal{L}}_3^{\mathcal{A}}\tilde{\mathcal{A}}^{(1,0)} - 3\tilde{\mathcal{L}}_3^{\mathcal{A}}\tilde{\mathcal{A}}^{(2,0)} \\ &-3\tilde{\mathcal{L}}_1^{\mathcal{A}}\tilde{\mathcal{A}}^{(0,1)} - 3\tilde{\mathcal{L}}_2^{\mathcal{A}}\tilde{\mathcal{A}}^{(1,1)} - 3\sqrt{3}\tilde{\mathcal{A}}^{(2,1)} - 3\tilde{\mathcal{L}}_1^{\mathcal{A}}\tilde{\mathcal{A}}^{(0,2)} + 3\sqrt{3}\tilde{\mathcal{A}}^{(1,2)} - 3\tilde{\mathcal{L}}_2^{\mathcal{A}}\tilde{\mathcal{A}}^{(2,2)}\Big\}\,,\end{aligned} \tag{3.64}$$

$$\begin{aligned}\tilde{\mathcal{M}} = &-\frac{c}{16}c_1^{\mathcal{M}}c_2^{\mathcal{M}}c_3^{\mathcal{M}}(1_{\rm RR} - 1_{\rm NSNS})\int_0^\infty dl\times\Big\{C_{00}^{00}\tilde{\mathcal{L}}_1^{\mathcal{M}}\tilde{\mathcal{L}}_2^{\mathcal{M}}\tilde{\mathcal{L}}_3^{\mathcal{M}}\tilde{\mathcal{M}}^{(0,0)} \\ &-3C_{20}^{20}\tilde{\mathcal{L}}_3^{\mathcal{M}}\tilde{\mathcal{M}}^{(1,0)} - 3C_{10}^{10}\tilde{\mathcal{L}}_3^{\mathcal{M}}\tilde{\mathcal{M}}^{(2,0)} - 3C_{02}^{02}\tilde{\mathcal{L}}_1^{\mathcal{M}}\tilde{\mathcal{M}}^{(0,1)} - 3C_{22}^{22}\tilde{\mathcal{L}}_2^{\mathcal{M}}\tilde{\mathcal{M}}^{(1,1)} \\ &+3\sqrt{3}C_{12}^{12}\tilde{\mathcal{M}}^{(2,1)} - 3C_{01}^{01}\tilde{\mathcal{L}}_1^{\mathcal{M}}\tilde{\mathcal{M}}^{(0,2)} - 3\sqrt{3}C_{21}^{21}\tilde{\mathcal{M}}^{(1,2)} - 3C_{11}^{11}\tilde{\mathcal{L}}_2^{\mathcal{M}}\tilde{\mathcal{M}}^{(2,2)}\Big\}\end{aligned} \tag{3.65}$$

and the tadpole cancellation conditions

$$M = 4 \tag{3.66}$$

for each model and

$$C_{00}^{00} = C_{10}^{10} = C_{20}^{20} = C_{01}^{01} = C_{02}^{02} = C_{11}^{11} = C_{22}^{22} = -C_{12}^{12} = -C_{21}^{21} = M\,. \tag{3.67}$$

As stated above, there are no twisted sector tadpoles. We can easily satisfy these conditions by choosing all representation matrices to be the unit matrix, up to signs.

3.3.2 The massless spectrum

The closed string spectrum

The untwisted sector consists of the model independent states (3.35), (3.36) and (3.38), i.e. the SUGRA multiplet plus 3C.

The Θ_1 twisted NSNS sector is made up from the following massless states with correct GSO projection

$$\begin{aligned} \psi^2_{-1/6}|0,+\frac{1}{3},-\frac{1}{3},0\rangle_L &= |0,+\frac{1}{3},+\frac{2}{3},0\rangle_L \equiv |1\rangle_{\rm NS}\,, \\ \psi^{\bar 1}_{-1/6}|0,+\frac{1}{3},-\frac{1}{3},0\rangle_L &= |0,-\frac{2}{3},-\frac{1}{3},0\rangle_L \equiv |2\rangle_{\rm NS}\,, \\ \tilde\psi^{\bar 2}_{-1/6}|0,-\frac{1}{3},+\frac{1}{3},0\rangle_R &= |0,-\frac{1}{3},-\frac{2}{3},0\rangle_R \equiv |\tilde 1\rangle_{\rm NS}\,, \\ \psi^1_{-1/6}|0,-\frac{1}{3},+\frac{1}{3},0\rangle_R &= |0,+\frac{2}{3},+\frac{1}{3},0\rangle_R \equiv |\tilde 2\rangle_{\rm NS}\,. \end{aligned} \tag{3.68}$$

Now, the state in the first line produces a phase of $e^{2\pi i/3}$ and the state in the third line produces a phase of $e^{-2\pi i/3}$ under Θ_2, whereas the remaining two states are invariant. Therefore only the combinations $|1\tilde 1\rangle$ and $|2\tilde 2\rangle$ are invariant under the orbifold group. Symmetrizing with respect to $\Omega\mathcal{R}$ and including the action of the fixed points leads to the two invariant combinations

$$\begin{aligned} &|1\tilde 1\rangle^\alpha_{\rm NSNS} + |1\tilde 1\rangle^\beta_{\rm NSNS}\,, \\ &|2\tilde 2\rangle^\alpha_{\rm NSNS} + |2\tilde 2\rangle^\beta_{\rm NSNS} \end{aligned} \tag{3.69}$$

In the Θ_1 twisted RR sector we find the massless states with correct GSO projection

$$\begin{array}{ll} |+\frac{1}{2},-\frac{1}{6},+\frac{1}{6},-\frac{1}{2}\rangle_L \equiv |1\rangle_{\rm R}\,, & |-\frac{1}{2},-\frac{1}{6},+\frac{1}{6},+\frac{1}{2}\rangle_L \equiv |2\rangle_{\rm R}\,, \\ |+\frac{1}{2},+\frac{1}{6},-\frac{1}{6},+\frac{1}{2}\rangle_R \equiv |\tilde 1\rangle_{\rm R}\,, & |-\frac{1}{2},+\frac{1}{6},-\frac{1}{6},-\frac{1}{2}\rangle_R \equiv |\tilde 2\rangle_{\rm R}\,. \end{array} \tag{3.70}$$

Because of the degeneracy in the last entry, the states in the first and the last line produce a phase of $e^{\pi i/3}$ under Θ_2, whereas the other states produce a phase of $e^{-\pi i/3}$. Again, only the combinations $|1\tilde 1\rangle$ and $|2\tilde 2\rangle$ are invariant under the orbifold group. Symmetrizing leads to

$$\begin{aligned} &|1\tilde 1\rangle^\alpha_{\rm RR} - |1\tilde 1\rangle^\beta_{\rm RR}\,, \\ &|2\tilde 2\rangle^\alpha_{\rm RR} - |2\tilde 2\rangle^\beta_{\rm RR}\,. \end{aligned} \tag{3.71}$$

In the Θ_1 twisted sector, the tori $T_{1,2}$ are twisted, whereas the torus T_3 is untwisted, i.e. we have fixed points only on the first two tori

AA• :	11 is invariant; 12-13, 21-31, 23-32, 22-33 form 4 pairs under $\Omega\mathcal{R}$
AB• :	21-31, 22-32, 23-33 form 3 pairs under $\Omega\mathcal{R}$, the remaining 3 fixed points are invariant
BB• :	all 9 fixed points are invariant

Thus, each invariant fixed point contributes 1 scalar (from NSNS) and each pair under $\Omega\mathcal{R}$ 2 scalars (from NSNS) and 1V (from RR).

The Θ_1^2, Θ_2, Θ_2^2, $\Theta_1\Theta_2$ and $\Theta_1^2\Theta_2^2$ twisted sectors work out similarly, one just has to take care of the different distributions of twisted tori with respect to the lattice.

In the $\Theta_1^2\Theta_2$ twisted sector all three tori are twisted. In the NSNS sector, we find the massless state $|0,-\frac{1}{3},-\frac{1}{3},-\frac{1}{3}\rangle_L \equiv |1\rangle_{\rm NS}$ with correct GSO projection. In the right moving sector, we similarly find $|0,\frac{1}{3},\frac{1}{3},\frac{1}{3}\rangle_R \equiv |\tilde{1}\rangle_{\rm NS}$. The tensorized state is invariant under the orbifold group. The symmetrized state

$$|1\tilde{1}\rangle^{\alpha}_{\rm NSNS} + |1\tilde{1}\rangle^{\beta}_{\rm NSNS} \tag{3.72}$$

yields one scalar for an invariant fixed point as well as for a pair under $\Omega\mathcal{R}$. Similarly, from the RR sector we find the massless states $|-\frac{1}{2},+\frac{1}{6},+\frac{1}{6},+\frac{1}{6}\rangle_L \equiv |1\rangle_{\rm R}$ and $|-\frac{1}{2},-\frac{1}{6},-\frac{1}{6},-\frac{1}{6}\rangle_R \equiv |\tilde{1}\rangle_{\rm R}$ with correct GSO projection. The state

$$|1\tilde{1}\rangle^{\alpha}_{\rm RR} - |1\tilde{1}\rangle^{\beta}_{\rm R} \tag{3.73}$$

vanishes for an invariant fixed point and contributes $\frac{1}{2}$V for a pair under $\Omega\mathcal{R}$. The other half comes from the $\Theta_1\Theta_2^2$ twisted sector. Since all three tori are twisted, the fixed point structure is different

AAA :	111 is invariant; the remaining points form 13 pairs under $\Omega\mathcal{R}$
AAB :	111,112,113 are invariant; the remaining points form 12 pairs under $\Omega\mathcal{R}$
ABB :	111,112,113,121,122,123,131,132,133 are invariant; the remaining points form 9 pairs under $\Omega\mathcal{R}$
BBB :	all 27 fixed points are invariant

Altogether we obtain the closed string massless spectrum

twist sector	AAA	AAB	ABB	BBB
untwisted	SUGRA + 3C			
$\Theta_1 + \Theta_1^2$	10C+8V	10C+8V	12C + 6V	18C
$\Theta_2 + \Theta_2^2$	10C+8V	12C+6V	18C	18C
$\Theta_1\Theta_2 + \Theta_1^2\Theta_2^2$	10C+8V	12C+6V	12C + 6V	18C
$\Theta_1^2\Theta_2 + \Theta_1\Theta_2^2$	14C+13V	15C+12V	18C + 9V	27C

(3.74)

The open string spectrum

In this section, we relabel the different types of D-branes according to

$(0,0)$	$(1,0)$	$(2,0)$	$(0,1)$	$(0,2)$	$(1,1)$	$(2,2)$	$(2,1)$	$(1,2)$
(0)	(1)	(2)	(3)	(4)	(5)	(6)	(7)	(8)

(3.75)

In the untwisted sector, the only symmetry of the $(0,0)$ strings is $\Omega\mathcal{R}$, i.e.

$$\lambda^{(0,0)} = -\lambda^{(0,0)T} . \tag{3.76}$$

All the other untwisted strings are related to the $(0,0)$ strings by symmetries. This immediately leads to the gauge group

$$SO(4) \tag{3.77}$$

and from the compact directions we find 3C in the adjoint (or equivalently, the antisymmetric), i.e. the **6** of $SO(4)$.

The Θ_1 twisted sector consists of the $(0,2)$ strings, i.e. the strings which start on brane (0) and end on brane (2) in the alternative labelling. The states corresponding to these strings are given by the first two lines of (3.68). These strings are invariant under $\Omega\mathcal{R}\Theta_1^2$ and thus the constraint on the λ matrix reads

$$\lambda^{(0,2)} = -\left(\gamma^{(2)}_{\Omega\mathcal{R}20}\lambda^{(0,2)}\gamma^{(0)-1}_{\Omega\mathcal{R}20}\right)^T . \tag{3.78}$$

From the tadpole cancellation conditions (3.67) we know $C^{20}_{20} = M$, or

$$\gamma^{(2)-T}_{\Omega\mathcal{R}20}\gamma^{(0)}_{\Omega\mathcal{R}20} = \mathbb{1}_M . \tag{3.79}$$

Therefore we can rewrite (3.78)

$$\lambda^{(0,2)} = -\left(\gamma^{(0)T}_{\Omega\mathcal{R}20}\lambda^{(0,2)}\gamma^{(0)-1}_{\Omega\mathcal{R}20}\right)^T , \tag{3.80}$$

such that, whichever phase the unit matrices have, the phase cancels and we are left with

$$\lambda^{(0,2)} = -\lambda^{(0,2)T}\,, \tag{3.81}$$

which means 1C in the **6** of $SO(4)$. In addition, each twisted **B** type torus contributes a factor of three. The same applies for the Θ_1^2, Θ_2, Θ_2^2, $\Theta_1\Theta_2$ and $\Theta_1^2\Theta_2^2$ twisted sectors.

The $\Theta_1^2\Theta_2$ twisted sector consists of the $(0,8)$ strings. These strings are invariant under $\Omega\mathcal{R}\Theta_1\Theta_2^2$. The corresponding massless state consists of just one scalar, consider the discussion of the closed string $\Theta_1^2\Theta_2$ twisted sector. The constraint on the λ matrix reads

$$\lambda^{(0,8)} = -\left(\gamma^{(8)}_{\Omega\mathcal{R}12}\lambda^{(0,8)}\gamma^{(0)-1}_{\Omega\mathcal{R}12}\right)^T \tag{3.82}$$

and from the tadpole cancellation conditions (3.67) we know $C^{12}_{12} = M$, or

$$\gamma^{(8)-T}_{\Omega\mathcal{R}12}\gamma^{(0)}_{\Omega\mathcal{R}12} = -\mathbb{1}_M\,. \tag{3.83}$$

We can rewrite (3.82)

$$\lambda^{(0,8)} = \left(\gamma^{(0)T}_{\Omega\mathcal{R}12}\lambda^{(0,8)}\gamma^{(0)-1}_{\Omega\mathcal{R}12}\right)^T\,, \tag{3.84}$$

which leads to

$$\lambda^{(0,8)} = \lambda^{(0,8)T}\,, \tag{3.85}$$

i.e. $\frac{1}{2}$C in the symmetric **10** of $SO(4)$. The other half comes from the $\Theta_1\Theta_2^2$ twisted sector. Again, each twisted **B** type torus contributes a factor of three.

We obtain the open string spectrum

<table>
<tr><th>twist sector</th><th>AAA</th><th>AAB</th><th>ABB</th><th>BBB</th><th>rep. of $SO(4)$</th></tr>
<tr><td>untwisted</td><td colspan="4">1V</td><td>6</td></tr>
<tr><td></td><td colspan="4">3C</td><td>6</td></tr>
<tr><td>$\Theta_1 + \Theta_1^2$</td><td>2C</td><td>2C</td><td>6C</td><td>18C</td><td>6</td></tr>
<tr><td>$\Theta_2 + \Theta_2^2$</td><td>2C</td><td>6C</td><td>18C</td><td>18C</td><td>6</td></tr>
<tr><td>$\Theta_1\Theta_2 + \Theta_1^2\Theta_2^2$</td><td>2C</td><td>6C</td><td>6C</td><td>18C</td><td>6</td></tr>
<tr><td>$\Theta_1^2\Theta_2 + \Theta_1\Theta_2^2$</td><td>1C</td><td>3C</td><td>9C</td><td>27C</td><td>10</td></tr>
</table>

(3.86)

3.4 The $\mathbb{Z}_4 \times \mathbb{Z}_2$ model

The lattice is described by the shifts $\vec{v} = (1/4, -1/4, 0)$ for the $\mathbb{Z}_4$-factor and $\vec{w} = (0, 1/2, -1/2)$ for the $\mathbb{Z}_2$-factor of the orbifold-group, see figure C.4 for the first two tori $T_{1,2}$ and figure 2.5 for the third torus T_3. As explained in section 3.1, only the models **ABA** and **ABB** are in agreement with worldsheet duality.

3.4.1 Amplitudes and tadpole cancellation conditions

The Klein bottle 1-loop amplitude

The fixed point structure is slightly more complicated than in the case of $\mathbb{Z}_2 \times \mathbb{Z}_2$. Now, the $\Theta_1^{n_1}\Theta_2^{n_2}$ fixed points are not always invariant under $\Omega\mathcal{R}\Theta_1^{k_1}\Theta_2^{k_2}$. Consider e.g. the second torus T_2 twisted by Θ_2. In the **A** lattice, two of the four fixed points are interchanged under $\Omega\mathcal{R}\Theta_1^{k_1}\Theta_2^{k_2}$ for $k_1 = 0, 2$ and k_2 arbitrary. In the **B** lattice all four fixed points are invariant under these insertions, such that $\chi_{\mathcal{K}}^{(0,0)(1,k_2)} = \chi_{\mathcal{K}}^{(0,2)(1,k_2)} = 2(4)$ for an **A**(**B**) type T_2. The resulting multiplicities are shown in the following table

	ABA	ABB
$\chi_{\mathcal{K}}^{(0,k_1)(0,k_2)}$	1	1
$\chi_{\mathcal{K}}^{(2n_1+1,k_1)(0,k_2)}$	4	4
$\chi_{\mathcal{K}}^{(2,k_1)(0,k_2)}$	8	8
$\chi_{\mathcal{K}}^{(0,2k_1)(1,k_2)}$	8	4
$\chi_{\mathcal{K}}^{(0,2k_1+1)(1,k_2)}$	16	8
$\chi_{\mathcal{K}}^{(2n_1+1,k_1)(1,k_2)}$	16	8
$\chi_{\mathcal{K}}^{(2,2k_1)(1,k_2)}$	16	8
$\chi_{\mathcal{K}}^{(2,2k_1+1)(1,k_2)}$	8	4

(3.87)

In order to shorten the expressions, we write down the results for the **ABA** lattice in the following and comment on the differences in the case of **ABB**. The Klein bottle amplitude for the **ABA** model reads

$$\begin{aligned}\mathcal{K} = c(1_{\mathrm{RR}} - 1_{\mathrm{NSNS}}) \int_0^\infty \frac{dt}{t^3} \{&\mathcal{L}[1,1]^2\mathcal{L}[2,2]\mathcal{K}^{(0,0)} + 4\mathcal{L}[1,1]\mathcal{K}^{(1,0)} + 8\mathcal{L}[1,1]\mathcal{K}^{(2,0)} \\ &+4\mathcal{L}[1,1]\mathcal{K}^{(3,0)} + 8\mathcal{L}[1,1]\mathcal{K}^{(0,1)} + 16\mathcal{K}^{(1,1)} + 16\mathcal{L}[2,2]\mathcal{K}^{(2,1)} + 16\mathcal{K}^{(3,1)}\} \ .\end{aligned} \tag{3.88}$$

For the **ABB** model, one $\mathcal{L}[1,1]$ in every of the first four terms within the braces has to be exchanged for $\mathcal{L}[2,2]$ and the prefactors in the last four terms have to be divided by two. Note, that we used $\mathcal{K}^{(0,1)} = \mathcal{K}^{(2,1)}$ to write the amplitude in this simple form.

The annulus 1-loop amplitude

The D6-branes introduced to cancel the tadpoles from the Klein bottle are shown in figure 3.3. Since in the case of the annulus only terms without insertions contribute to the amplitude (the terms with $\mathbb{Z}_2$-like insertions again vanish due to the twisted tadpole cancellation conditions), we do not have to worry about

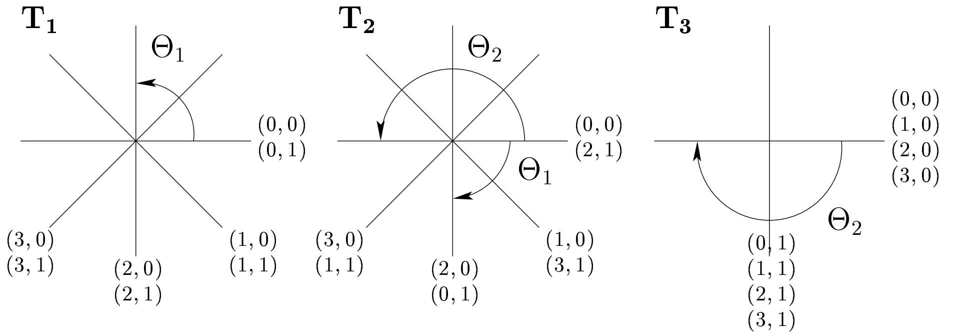

Figure 3.3: Arrangement of D-branes and action of the orbifold group for $\mathbb{Z}_4 \times \mathbb{Z}_2$.

the invariance of the intersection points. The multiplicities with respect to the $(0,0)$ brane are given by

	ABA	**ABB**
$\chi_{\mathcal{A}}^{(1,0)}$	1	1
$\chi_{\mathcal{A}}^{(2,0)}$	2	2
$\chi_{\mathcal{A}}^{(3,0)}$	1	2
$\chi_{\mathcal{A}}^{(0,1)}$	2	4
$\chi_{\mathcal{A}}^{(1,1)}$	1	2
$\chi_{\mathcal{A}}^{(2,1)}$	1	2
$\chi_{\mathcal{A}}^{(3,1)}$	1	2

(3.89)

We obtain the annulus amplitude for the **ABA** lattice

$$\begin{aligned}\mathcal{A} = \frac{c}{4} M^2 (1_{\mathrm{RR}} - 1_{\mathrm{NSNS}}) \frac{dt}{t^3} \{ & \mathcal{L}[1,1]\mathcal{L}[2,2]^2 \mathcal{A}^{(0,0)} + \mathcal{L}[2,2]\mathcal{A}^{(1,0)} + 2\mathcal{L}[2,2]\mathcal{A}^{(2,0)} \\ & + \mathcal{L}[2,2]\mathcal{A}^{(3,0)} + 2\mathcal{L}[2,2]\mathcal{A}^{(0,1)} + \mathcal{A}^{(1,1)} + \mathcal{L}[1,1]\mathcal{A}^{(2,1)} + \mathcal{A}^{(3,1)} \} \ .\end{aligned} \tag{3.90}$$

For the **ABB** model, one $\mathcal{L}[2,2]$ in every of the first four terms within the braces has to be exchanged for $\mathcal{L}[1,1]$ and the prefactors in the last four terms have to be multiplied by two.

The Möbius strip 1-loop amplitude

Performing the calculation for the strings starting on brane $(0,0)$ and including a factor of $NM = 8$ in the end, equation (2.53) tells us that the sectors $(n_1,k_1)(n_2,k_2) = (0,0)(0,0)$, $(0,0)(0,1)$, $(0,2)(0,0)$, $(0,2)(0,1)$, $(2,1)(0,0)$, $(2,1)(0,1)$, $(2,3)(0,0)$ and $(2,3)(0,1)$ contribute to the Möbius strip 1-loop amplitude, which reads for the **ABA** lattice

$$\begin{aligned}\mathcal{M} = -\frac{c}{4}(1_{\rm RR} - 1_{\rm NSNS}) \int_0^\infty \frac{dt}{t^3} \{ & C^{00}_{00}\mathcal{L}[1,4]\mathcal{L}[2,2]^2\mathcal{M}^{(0,0)(0,0)} + 2C^{20}_{10}\mathcal{L}[2,2]\mathcal{M}^{(2,1)(0,0)} \\ & + C^{00}_{20}\mathcal{L}[2,2]\mathcal{M}^{(0,2)(0,0)} + 2C^{20}_{30}\mathcal{L}[2,2]\mathcal{M}^{(2,3)(0,0)} + C^{00}_{01}\mathcal{L}[2,2]\mathcal{M}^{(0,0)(0,1)} \\ & + 2C^{20}_{11}\mathcal{M}^{(2,1)(0,1)} + C^{00}_{21}\mathcal{L}[1,4]\mathcal{M}^{(0,2)(0,1)} + 2C^{20}_{31}\mathcal{M}^{(2,3)(0,1)} \} \, .\end{aligned} \tag{3.91}$$

For the **ABB** model, one $\mathcal{L}[2,2]$ in every of the first four terms within the braces has to be exchanged for $\mathcal{L}[1,4]$. The multiplicities from the intersections are included and can be taken from (3.89), since the intersections are invariant under the insertions.

Tree channel amplitudes and tadpole cancellation

Modular transformation yields the tree channel amplitudes for the **ABA** model

$$\begin{aligned}\tilde{\mathcal{K}} = 32c(1_{\rm RR} - 1_{\rm NSNS}) \int_0^\infty dl \Big\{ & \tilde{\mathcal{L}}[4,4]^2\tilde{\mathcal{L}}[2,2]\tilde{\mathcal{K}}^{(0,0)} - 2\tilde{\mathcal{L}}[4,4]\tilde{\mathcal{K}}^{(1,0)} - 4\tilde{\mathcal{L}}[4,4]\tilde{\mathcal{K}}^{(2,0)} \\ & -2\tilde{\mathcal{L}}[4,4]\tilde{\mathcal{K}}^{(3,0)} - 4\tilde{\mathcal{L}}[4,4]\tilde{\mathcal{K}}^{(0,1)} + 4\tilde{\mathcal{K}}^{(1,1)} - 4\tilde{\mathcal{L}}[2,2]\tilde{\mathcal{K}}^{(2,1)} - 4\tilde{\mathcal{K}}^{(3,1)} \Big\} \, ,\end{aligned} \tag{3.92}$$

$$\begin{aligned}\tilde{\mathcal{A}} = \frac{c}{8}M^2(1_{\rm RR} - 1_{\rm NSNS}) \int_0^\infty dl \Big\{ & \tilde{\mathcal{L}}[2,2]\tilde{\mathcal{L}}[1,1]^2\tilde{\mathcal{A}}^{(0,0)} - 2\tilde{\mathcal{L}}[1,1]\tilde{\mathcal{A}}^{(1,0)} - 4\tilde{\mathcal{L}}[1,1]\tilde{\mathcal{A}}^{(2,0)} \\ & -2\tilde{\mathcal{L}}[1,1]\tilde{\mathcal{A}}^{(3,0)} - 4\tilde{\mathcal{L}}[1,1]\tilde{\mathcal{A}}^{(0,1)} + 4\tilde{\mathcal{A}}^{(1,1)} - 4\tilde{\mathcal{L}}[2,2]\tilde{\mathcal{A}}^{(2,1)} - 4\tilde{\mathcal{A}}^{(3,1)} \Big\} \, ,\end{aligned} \tag{3.93}$$

$$\begin{aligned}\tilde{\mathcal{M}} = -\frac{c}{4}(1_{\rm RR} - 1_{\rm NSNS}) \int_0^\infty dl \Big\{ & C^{00}_{00}\tilde{\mathcal{L}}[8,2]\tilde{\mathcal{L}}[4,4]^2\tilde{\mathcal{M}}^{(0,0)} - 2C^{20}_{30}\tilde{\mathcal{L}}[4,4]\tilde{\mathcal{M}}^{(1,0)} \\ & +4C^{00}_{20}\tilde{\mathcal{L}}[4,4]\tilde{\mathcal{M}}^{(2,0)} - 2C^{20}_{10}\tilde{\mathcal{L}}[4,4]\tilde{\mathcal{M}}^{(3,0)} + 4C^{00}_{01}\tilde{\mathcal{L}}[4,4]\tilde{\mathcal{M}}^{(0,1)} \\ & +4C^{20}_{31}\tilde{\mathcal{M}}^{(1,1)} + 4C^{00}_{21}\tilde{\mathcal{L}}[8,2]\tilde{\mathcal{M}}^{(2,1)} + 4C^{20}_{11}\tilde{\mathcal{M}}^{(3,1)} \Big\} \, .\end{aligned} \tag{3.94}$$

For the **ABB** lattice, besides of obvious exchanges of some lattice contributions, $\tilde{\mathcal{K}}$ has to be multiplied by $1/2$ and $\tilde{\mathcal{A}}$ by 2.

We find the tadpole cancellation conditions

$$\begin{aligned} M &= 16 \quad (\mathbf{ABA}) \\ M &= 8 \quad\; (\mathbf{ABB}) \end{aligned} \tag{3.95}$$

and

$$C^{00}_{00} = C^{20}_{10} = -C^{00}_{20} = C^{20}_{30} = -C^{00}_{01} = -C^{20}_{11} = -C^{00}_{21} = C^{20}_{31} = M \, , \tag{3.96}$$

together with the twisted sector tadpole cancellation conditions

$$\mathrm{tr}\gamma_{01}^{(a_1,a_2)} = \mathrm{tr}\gamma_{20}^{(a_1,a_2)} = \mathrm{tr}\gamma_{21}^{(a_1,a_2)} = 0\,. \tag{3.97}$$

3.4.2 Representation matrices of the orientifold group

A set of matrices, which satisfies the tadpole cancellation conditions together with the consistency conditions (2.92) is found to be

brane		$\gamma_{\Omega\mathcal{R}00}$	$\gamma_{\Omega\mathcal{R}10}$	$\gamma_{\Omega\mathcal{R}20}$	$\gamma_{\Omega\mathcal{R}30}$	$\gamma_{\Omega\mathcal{R}01}$	$\gamma_{\Omega\mathcal{R}11}$	$\gamma_{\Omega\mathcal{R}21}$	$\gamma_{\Omega\mathcal{R}31}$
$(0,0)$	(0)	$\mathbb{I}_M$	$+A$	M_1	$+B$	M_2	$+C$	M_3	$+E$
$(1,0)$	(1)	$+B$	$\mathbb{I}_M$	$+A$	M_1	$+E$	M_2	$+C$	M_3
$(2,0)$	(2)	N_1	$+A^T$	D	$+B^T$	M_2	$-C^T$	M_3	$+E^T$
$(3,0)$	(3)	$+B^T$	N_1	$+A^T$	D	$+E^T$	M_2	$-C^T$	M_3
$(0,1)$	(4)	N_1	$+F$	M_3	$+G$	D	$+H$	M_2	$+K$
$(1,1)$	(5)	$+G$	N_1	$+F$	M_3	$+K$	D	$+H$	M_2
$(2,1)$	(6)	N_1	$-F^T$	M_2	$+G^T$	M_3	$+H^T$	D	$+K^T$
$(3,1)$	(7)	$+G^T$	N_1	$-F^T$	M_2	$+K^T$	M_3	$+H^T$	D

(3.98)

where all relevant signs are listed explicitly, while the others are irrelevant. We used the matrices M_i, N_i, D from the $\mathbb{Z}_2 \times \mathbb{Z}_2$ model and have to introduce another set of matrices, namely

$$\begin{aligned} A &= \begin{pmatrix} a & b \\ -b & a \end{pmatrix}, & B &= \begin{pmatrix} -b & a \\ -a & -b \end{pmatrix}, \\ C &= i\begin{pmatrix} a & b \\ b & -a \end{pmatrix}, & E &= i\begin{pmatrix} b & -a \\ -a & -b \end{pmatrix}, \end{aligned} \tag{3.99}$$

where

$$a = \frac{1}{2}\begin{pmatrix} \mathbb{I}_{M/4} & i\mathbb{I}_{M/4} \\ -i\mathbb{I}_{M/4} & \mathbb{I}_{M/4} \end{pmatrix}, \qquad b = \frac{1}{2}\begin{pmatrix} -i\mathbb{I}_{M/4} & -\mathbb{I}_{M/4} \\ \mathbb{I}_{M/4} & -i\mathbb{I}_{M/4} \end{pmatrix} = -ia^T\,. \tag{3.100}$$

These matrices satisfy $A^{-1} = A$, $B^{-1} = -B$ and

$$C^{-1} = i\begin{pmatrix} -a & b \\ b & a \end{pmatrix}, \qquad E^{-1} = i\begin{pmatrix} b & a \\ a & -b \end{pmatrix} \tag{3.101}$$

as well as $C^T = iE$. Furthermore we need the set of matrices

$$\begin{aligned} F &= \frac{1}{\sqrt{2}}\begin{pmatrix} \mathbb{I} & \mathbb{I} \\ i & -i \end{pmatrix}, & G &= \frac{1}{\sqrt{2}}\begin{pmatrix} \mathbb{I} & \mathbb{I} \\ -i & i \end{pmatrix}, \\ H &= \frac{1}{\sqrt{2}}\begin{pmatrix} i & -i \\ \mathbb{I} & \mathbb{I} \end{pmatrix}, & K &= \frac{1}{\sqrt{2}}\begin{pmatrix} i & -i \\ -\mathbb{I} & -\mathbb{I} \end{pmatrix}, \end{aligned} \tag{3.102}$$

which satisfy $F^{-T} = G$ and $H^{-T} = -K$. From the identities (2.92), we obtain the representation matrices of the orbifold group

brane		γ_{00}	γ_{10}	γ_{20}	γ_{30}	γ_{01}	γ_{11}	γ_{21}	γ_{31}
$(0,0)$	$\mathbb{1}_M$	(0)	B^{-T}	M_1	A^{-T}	M_2	E^{-T}	M_3	C^{-T}
$(1,0)$	$\mathbb{1}_M$	(1)	B^{-T}	M_1	A^{-T}	M_2	E^{-T}	M_3	C^{-T}
$(2,0)$	$\mathbb{1}_M$	(2)	A^T	M_1	B^T	N_3	C^T	N_2	E^T
$(3,0)$	$\mathbb{1}_M$	(3)	A^T	M_1	B^T	N_3	C^T	N_2	E^T
$(0,1)$	$\mathbb{1}_M$	(4)	$G^{-T}N_1$	N_2	$F^{-T}N_1$	M_1	$K^{-T}N_1$	N_3	$H^{-T}N_1$
$(1,1)$	$\mathbb{1}_M$	(5)	$G^{-T}N_1$	N_2	$F^{-T}N_1$	M_1	$K^{-T}N_1$	N_3	$H^{-T}N_1$
$(2,1)$	$\mathbb{1}_M$	(6)	N_1F^T	N_3	N_1G^T	N_2	N_1H^T	M_1	N_1K^T
$(3,1)$	$\mathbb{1}_M$	(7)	N_1F^T	N_3	N_1G^T	N_2	N_1H^T	M_1	N_1K^T

(3.103)

up to an irrelevant phase. Again we introduce an alternative labelling of the D-branes.

3.4.3 The massless spectrum

The closed string spectrum

In addition to the model independent SUGRA plus 3C we find one scalar in the NSNS sector

$$\left(\psi^{3}_{-1/2}\tilde{\psi}^{3}_{-1/2} + \psi^{\bar{3}}_{-1/2}\tilde{\psi}^{\bar{3}}_{-1/2}\right)|0\rangle \tag{3.104}$$

and one more scalar in the RR sector

$$|+--+\rangle_L|---+\rangle_R - |-++-\rangle_L|+++-\rangle_R\,, \tag{3.105}$$

altogether 1 SUGRA plus 4C in the untwisted sector.

The Θ_1 twisted NSNS sector consists of the massless states with correct GSO projection

$$\begin{aligned}
\psi^{2}_{-1/4}|0,+\frac{1}{4},-\frac{1}{4},0\rangle_L &= |0,+\frac{1}{4},+\frac{3}{4},0\rangle_L \equiv |1\rangle_{\mathrm{NS}}\,,\\
\psi^{\bar{1}}_{-1/4}|0,+\frac{1}{4},-\frac{1}{4},0\rangle_L &= |0,-\frac{3}{4},-\frac{1}{4},0\rangle_L \equiv |2\rangle_{\mathrm{NS}}\,,\\
\tilde{\psi}^{\bar{2}}_{-1/4}|0,-\frac{1}{4},+\frac{1}{4},0\rangle_R &= |0,-\frac{1}{4},-\frac{3}{4},0\rangle_R \equiv |\tilde{1}\rangle_{\mathrm{NS}}\,,\\
\psi^{1}_{-1/4}|0,-\frac{1}{4},+\frac{1}{4},0\rangle_R &= |0,+\frac{3}{4},+\frac{1}{4},0\rangle_R \equiv |\tilde{2}\rangle_{\mathrm{NS}}\,.
\end{aligned} \tag{3.106}$$

The first and the third state produce a minus sign under Θ_2, whereas the other two states are invariant. Thus we are left with the symmetrized combinations

$$\begin{aligned}
&|1\tilde{1}\rangle^{\alpha}_{\mathrm{NSNS}} + |1\tilde{1}\rangle^{\beta}_{\mathrm{NSNS}}\,,\\
&|2\tilde{2}\rangle^{\alpha}_{\mathrm{NSNS}} + |2\tilde{2}\rangle^{\beta}_{\mathrm{NSNS}}\,.
\end{aligned} \tag{3.107}$$

Similarly, in the Θ_1 twisted RR sector we find the massless combinations

$$\begin{aligned} &|1\tilde{1}\rangle^{\alpha}_{\mathrm{RR}} - |1\tilde{1}\rangle^{\beta}_{\mathrm{RR}}\,, \\ &|2\tilde{2}\rangle^{\alpha}_{\mathrm{RR}} - |2\tilde{2}\rangle^{\beta}_{\mathrm{RR}}\,. \end{aligned} \tag{3.108}$$

In the Θ_1 twisted sector, the tori $T_{1,2}$ are twisted, whereas the torus T_3 is untwisted, i.e. we have fixed points only on the first two tori, which are of type **AB** in both models. The fixed points of the Θ_1 twisted sector are given by the points 11, 12, 21 and 22 which are all invariant under the elements of the orientifold and the orbifold group. Thus each fixed point contributes two scalars, i.e. altogether 4C in the Θ_1 twisted sector. The same amount is found in the Θ_1^3 twisted sector.

The Θ_1^2 twisted sector is similar to the Θ_1 twisted sector in the $\mathbb{Z}_2\times\mathbb{Z}_2$ model, but the fixed point structure is slightly different, consider figure C.4. Again, only the tori $T_{1,2}$ are twisted, which are of type **AB** in both models. The fixed points 11, 12, 21 and 22 are invariant; the fixed points 13-14 and 23-24 form pairs under $\Omega\mathcal{R}$ and Θ_1; the fixed points 31-41 and 32-42 form pairs under Θ_1; the fixed points 33-34-43-44 form a quartet under $\Omega\mathcal{R}$ and Θ_1. The invariant fixed points, the pairs under $\Omega\mathcal{R}$ and Θ_1 and the pairs under Θ_1 each contribute two scalars, whereas the quartet contributes two scalars and 1V. Altogether we find 9C plus 1V in the Θ_1^2 twisted sector.

In the Θ_2 twisted sector, the states are obtained similar to the Θ_1^2 twisted sector, but again we have to take into account the different fixed point structure. Now, only the tori $T_{2,3}$ are twisted, which are of type **BA** or **BB**.

•**BA** :	31-41, 32-42, 33-43, 34-44 form 4 pairs under $\Omega\mathcal{R}$ and Θ_1, the remaining 8 fixed points are invariant
•**BB** :	31-41, 32-42 form 2 pairs under $\Omega\mathcal{R}$ and Θ_1, 13-14, 23-24 form 2 pairs under $\Omega\mathcal{R}$, 33-34-43-44 a quartet under $\Omega\mathcal{R}$ and Θ_1 and the remaining 4 fixed points are invariant

The invariant fixed points and the pairs under $\Omega\mathcal{R}$ and Θ each contribute two scalars and the pairs under $\Omega\mathcal{R}$ and the quartet contributes two scalars and 1V.

In the $\Theta_1^2\Theta_2$ twisted sector, the states are again similar to the Θ_1^2 twisted sector, but now the tori $T_{1,3}$ are twisted, which are of type **AA** or **AB**.

A • A :	31-41, 32-42, 33-43, 34-44 form 4 pairs under Θ_1, the remaining 8 fixed points are invariant
A • B :	31-41, 32-42 form 2 pairs under Θ_1, 13-14, 23-24 form 2 pairs under $\Omega\mathcal{R}$, 33-34-43-44 a quartet under $\Omega\mathcal{R}$ and Θ_1 and the remaining 4 fixed points are invariant

The invariant fixed points and the pairs under Θ_1 each contribute two scalars and the pairs under $\Omega\mathcal{R}$ and the quartet contribute two scalars and 1V.

In the $\Theta_1\Theta_2$ twisted sector, all three tori are twisted and we find, in analogy to the $\Theta_1^2\Theta_2$ twisted sector of the $\mathbb{Z}_3 \times \mathbb{Z}_3$ model, only one invariant state in the NSNS and one in the RR sector. The fixed point structure is

ABA : all 16 fixed points are invariant
ABB : 113-114, 123-124, 213-214, 223-224 form
4 pairs under $\Omega\mathcal{R}$,
and the remaining 8 fixed points are invariant

Each invariant fixed point contributes 1 scalar and each pair under $\Omega\mathcal{R}$ 1 scalar and $\frac{1}{2}$V. The same amount is found in the $\Theta_1^3\Theta_2$ twisted sector.

Collecting the results yields the closed string massless spectrum

twist sector	**ABA**	**ABB**
untwisted	SUGRA + 4C	
$\Theta_1 + \Theta_1^3$	8C	8C
Θ_1^2	9C+1V	9C+1V
Θ_2	12C	9C+3V
$\Theta_1^2\Theta_2$	12C	9C+3V
$\Theta_1\Theta_2 + \Theta_1^3\Theta_2$	16C	12C+4V

(3.109)

The open string spectrum

In this section, we use the alternative labelling of the D6-branes shown in (3.98). The massless states $\psi^{\mu}_{-1/2}|0, ij\rangle\lambda^{(a,a)}_{ji}$, $\mu = 0, \ldots, 3$ yield the gauge group. In contrast to the $\mathbb{Z}_2 \times \mathbb{Z}_2$ model, not all (a, a) strings are independent, because $(0, 0)$ gets mapped to $(2, 2)$, $(1, 1)$ to $(3, 3)$, $(4, 4)$ to $(6, 6)$ and $(5, 5)$ to $(7, 7)$ by symmetries of the theory. We begin our discussion with the $(0, 0)$. These strings are invariant under $\Omega\mathcal{R}$, Θ_1^2 and Θ_2, which leads to the constraints

$$\lambda^{(0,0)} = -\left(\gamma^{(0)}_{\Omega\mathcal{R}00}\lambda^{(0,0)}\gamma^{(0)-1}_{\Omega\mathcal{R}00}\right)^T = \gamma^{(0)}_{20}\lambda^{(0,0)}\gamma^{(0)-1}_{20} = \gamma^{(0)}_{01}\lambda^{(0,0)}\gamma^{(0)-1}_{01}\,. \tag{3.110}$$

Using the matrices (3.98) and (3.103) we obtain

$$\lambda^{(0,0)} = -\lambda^{(0,0)T} = -M_1\lambda^{(0,0)}M_1 = -M_2\lambda^{(0,0)}M_2 \tag{3.111}$$

$$\Rightarrow \qquad \lambda^{(0,0)} = \begin{pmatrix} A & S_1 & S_2 & S_3 \\ -S_1 & A & S_3 & -S_2 \\ -S_2 & -S_3 & A & S_1 \\ -S_3 & S_2 & -S_1 & A \end{pmatrix} \tag{3.112}$$

with A an antisymmetric $M/4 \times M/4$ and S_i symmetric $M/4 \times M/4$ matrices. As in the case of $\mathbb{Z}_2 \times \mathbb{Z}_2$, this yields $Sp(M/4)$ as the gauge group for the $(0, 0)$

strings. Similarly, we obtain factors of $Sp(M/4)$ from the $(2,2)$, $(4,4)$ and $(6,6)$ strings, i.e. again

$$[Sp(M/4)]^4 \tag{3.113}$$

as the gauge group for this model. In the compact directions these strings give rise to 3C in the antisymmetric $(A,1,1,1)+(1,A,1,1)+(1,1,A,1)+(1,1,1,A)$, in complete analogy to the $\mathbb{Z}_2\times\mathbb{Z}_2$ model. Since Θ_1 maps the $(0,0)$ to the $(2,2)$ strings, we have the additional identities

$$\lambda^{(2,2)} = x\gamma_{10}^{(0)}\lambda^{(0,0)}\gamma_{10}^{(0)-1} \tag{3.114}$$

as a consistency check (with $x=1$ in the directions $0,\ldots,3$, $x=i$ on T_1, $x=-i$ on T_2 and $x=1$ on T_3 from the different oscillators). Using (3.103), one verifies that the consistency condition is fulfilled. The same applies for the remaining strings. Consistency checks like this one can be performed for any strings mapped onto each other by symmetries of the theory. In the case of $\mathbb{Z}_4\times\mathbb{Z}_2$ however, these checks helped us to establish the complicated structure of the representation matrices of the orientifold and orbifold group.

The Θ_1 twisted sector (the $(0,3)$ and the $(4,7)$ strings; the other Θ_1 twisted are related by symmetries) is invariant under Θ_1^2 and Θ_2. The constraints for the $(0,3)$ strings read

$$\lambda^{(0,3)} = x'\gamma_{20}^{(3)}\lambda^{(0,3)}\gamma_{20}^{(0)-1} = y'\gamma_{01}^{(3)}\lambda^{(0,3)}\gamma_{01}^{(0)-1}\,, \tag{3.115}$$

where the phases x' and y' are determined by consistency. Inserting the representations yields

$$\lambda^{(0,3)} = xM_1\lambda^{(0,3)}M_1 = yN_3\lambda^{(0,3)}M_2 \tag{3.116}$$

with $x=-x'$ and $y=-y'$. This is again equivalent to the Θ_1 twisted sector in the $\mathbb{Z}_2\times\mathbb{Z}_2$ model and thus is solved by the matrix (3.57). Since there are two massless ground states in this sector, the $(0,3)$ strings yield 1C in the bifundamental $(F,F,1,1)$. The $(4,7)$ strings similarly lead to 1C in the bifundamental $(1,1,F,F)$. There is no extra multiplicity from intersections, consider figure 2.7. The same amount is found in the Θ_1^3 twisted sector.

In addition to Θ_1^2 and Θ_2, the Θ_1^2 twisted sector (the $(0,2)$, $(1,3)$, $(4,6)$ and $(5,7)$ strings) is invariant under $\Omega\mathcal{R}\Theta_1$. This leads to the additional constraint, e.g. for the $(0,2)$ strings

$$\lambda^{(0,2)} = -A^{-T}\lambda^{(0,2)}A \tag{3.117}$$

which leads to 1C in the antisymmetric $(A,1,1,1)$. The multiplicity from the intersections is 2 in both models, thus we find 2C in the $(A,1,1,1)+(1,A,1,1)+(1,1,A,1)+(1,1,1,A)$ in the Θ_1^2 twisted sector.

The invariances of the remaining twisted sectors are again given by Θ_1^2 and Θ_2. The corresponding λ matrices are always related to (3.57) and easily calculated. For the Θ_2 twisted sector (the $(0,4)$ and $(1,5)$ strings) this leads to 2C

(4C) in the $(F,1,F,1)+(1,F,1,F)$ in the **ABA** (**ABB**), because the multiplicity from the intersections is 2 (4). Similarly, for the $\Theta_1^2\Theta_2$ twisted sector one finds 1C (2C) in the $(F,1,F,1)+(1,F,1,F)$. The $\Theta_1\Theta_2$ twisted sector contains only one massless ground state. One finds $\frac{1}{2}$C (1C) in the $(F,1,1,F)+(1,F,F,1)$ and the same amount in the $\Theta_1^3\Theta_2$ twisted sector.

Altogether, the open string spectrum reads

twist sector	**ABA**	**ABB**	rep. of $[Sp(M/4)]^4$
untwisted	1V		$(ad,1,1,1)+(1,ad,1,1)$
			$+(1,1,ad,1)+(1,1,1,ad)$
	3C		$(A,1,1,1)+(1,A,1,1)$
			$+(1,1,A,1)+(1,1,1,A)$
$\Theta_1+\Theta_1^3$	2C	2C	$(F,F,1,1)+(1,1,F,F)$
Θ_1^2	2C	2C	$(A,1,1,1)+(1,A,1,1)$
			$+(1,1,A,1)+(1,1,1,A)$
Θ_2	2C	4C	$(F,1,F,1)+(1,F,1,F)$
$\Theta_1^2\Theta_2$	1C	2C	$(F,1,F,1)+(1,F,1,F)$
$\Theta_1\Theta_2+\Theta_1^3\Theta_2$	1C	2C	$(F,1,1,F)+(1,F,F,1)$

(3.118)

3.5 The $\mathbb{Z}_6\times\mathbb{Z}_3$ model

The lattice is described by the shifts $\vec{v}=(1/6,-1/6,0)$ for the $\mathbb{Z}_6$-factor and $\vec{w}=(0,1/3,-1/3)$ for the $\mathbb{Z}_3$-factor of the orbifold-group. The torus lattices are the same as in the case of $\mathbb{Z}_3\times\mathbb{Z}_3$. For the fixed point structure on the first two tori, consider figure C.7, for the fixed point structure on the third torus, consider figure C.1. Similar to the $\mathbb{Z}_4\times\mathbb{Z}_2$, only the models **ABA** and **ABB** are consistent with worldsheet duality.

3.5.1 Amplitudes and tadpole cancellation conditions

The Klein bottle 1-loop amplitude

Again, the $\Theta_1^{n_1}\Theta_2^{n_2}$ fixed points are not invariant under $\Omega\mathcal{R}\Theta_1^{k_1}\Theta_2^{k_2}$ in general. In the following table, the multiplicities $\chi_{\mathcal{K}}^{(n_1,k_1)(n_2,k_2)}$ of the $\Theta_1^{n_1}\Theta_2^{n_2}$ fixed points invariant under $\Omega\mathcal{R}\Theta_1^{k_1}\Theta_2^{k_2}$ are shown.

	ABA	ABB
$\chi_{\mathcal{K}}^{(0,k_1)(0,k_2)} = \chi_{\mathcal{K}}^{(1,k_1)(0,k_2)} = \chi_{\mathcal{K}}^{(5,k_1)(0,k_2)}$	1	1
$\chi_{\mathcal{K}}^{(2,k_1)(0,k_2)} = \chi_{\mathcal{K}}^{(4,k_1)(0,k_2)}$	3	3
$\chi_{\mathcal{K}}^{(3,k_1)(0,k_2)}$	4	4
$\chi_{\mathcal{K}}^{(0,2k_1+1)(1,k_2)} = \chi_{\mathcal{K}}^{(0,2k_1+1)(2,k_2)} = \chi_{\mathcal{K}}^{(1,k_1)(1,k_2)}$ $= \chi_{\mathcal{K}}^{(5,k_1)(2,k_2)} = \chi_{\mathcal{K}}^{(2,2k_1)(1,k_2)} = \chi_{\mathcal{K}}^{(4,2k_1)(2,k_2)}$	1	3
$\chi_{\mathcal{K}}^{(0,2k_1)(1,k_2)} = \chi_{\mathcal{K}}^{(0,2k_1)(2,k_2)} = \chi_{\mathcal{K}}^{(2,k_1)(2,k_2)}$ $= \chi_{\mathcal{K}}^{(4,k_1)(1,k_2)} = \chi_{\mathcal{K}}^{(2,2k_1+1)(1,k_2)} = \chi_{\mathcal{K}}^{(4,2k_1+1)(2,k_2)}$	3	9
$\chi_{\mathcal{K}}^{(3,k_1)(1,k_2)} = \chi_{\mathcal{K}}^{(3,k_1)(2,k_2)} = \chi_{\mathcal{K}}^{(1,k_1)(2,k_2)}$ $= \chi_{\mathcal{K}}^{(5,k_1)(1,k_2)}$	2	6

(3.119)

Because of all these different $\chi_{\mathcal{K}}$, the general expression for the Klein bottle amplitude becomes very lengthy. Therefore we write down the amplitude for the **ABA** lattice and comment on the differences in the **ABB** model.

$$\begin{aligned}
\mathcal{K} = c(1_{\mathrm{RR}} - 1_{\mathrm{NSNS}}) \int_0^\infty \frac{dt}{t^3} \big\{ & \mathcal{L}[4,3]^2 \mathcal{L}[4/3,1] \mathcal{K}^{(0,0)} \\
& + \mathcal{L}[4,3] \left(\mathcal{K}^{(1,0)} + 3\mathcal{K}^{(2,0)} + 4\mathcal{K}^{(3,0)} + 3\mathcal{K}^{(4,0)} + \mathcal{K}^{(5,0)} \right) \\
& + \frac{1}{2} \left(3\mathcal{L}[4,3] + \mathcal{L}[4/3,1] \right) \left(\mathcal{K}^{(2,1)} + \mathcal{K}^{(4,1)} + \mathcal{K}^{(0,1)} + \mathcal{K}^{(0,2)} \right) \\
& + \mathcal{K}^{(1,1)} + 2\mathcal{K}^{(3,1)} + 3\mathcal{K}^{(4,1)} + 2\mathcal{K}^{(5,1)} + 2\mathcal{K}^{(1,2)} + 3\mathcal{K}^{(2,2)} + 2\mathcal{K}^{(3,2)} + \mathcal{K}^{(5,2)} \big\} ,
\end{aligned} \tag{3.120}$$

For the **ABB** model, one has to replace one $\mathcal{L}[4,3]$ in each term in the first two lines by $\mathcal{L}[4/3,1]$ and to multiply each term in the last two lines with a factor of three.

The annulus 1-loop amplitude

The D6-branes introduced to cancel the tadpoles from the Klein bottle are shown in figure 3.4. The multiplicities of the $\Theta^{n_1}\Theta^{n_2}$ twisted strings with respect to

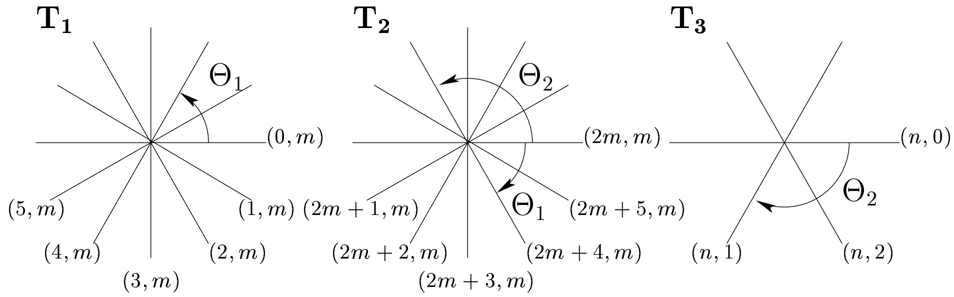

Figure 3.4: Arrangement of D-branes and action of the orbifold group for $\mathbb{Z}_6 \times \mathbb{Z}_3$. $m = 0, 1, 2$ and $n = 0, \ldots, 5$ label the D-branes.

the $(0,0)$ brane are given by (consider the figures C.3 and C.9)

	ABA	**ABB**
$\chi_{\mathcal{A}}^{(1,0)} = \chi_{\mathcal{A}}^{(5,0)}$	1	1
$\chi_{\mathcal{A}}^{(2,0)} = \chi_{\mathcal{A}}^{(4,0)}$	3	3
$\chi_{\mathcal{A}}^{(3,0)}$	4	4
$\chi_{\mathcal{A}}^{(0,1)} = \chi_{\mathcal{A}}^{(4,1)} = \chi_{\mathcal{A}}^{(0,2)} = \chi_{\mathcal{A}}^{(2,2)}$	3	9
$\chi_{\mathcal{A}}^{(1,1)} = \chi_{\mathcal{A}}^{(2,1)} = \chi_{\mathcal{A}}^{(4,2)} = \chi_{\mathcal{A}}^{(5,2)}$	1	3
$\chi_{\mathcal{A}}^{(3,1)} = \chi_{\mathcal{A}}^{(5,1)} = \chi_{\mathcal{A}}^{(1,2)} = \chi_{\mathcal{A}}^{(3,2)}$	1	3

(3.121)

We obtain the annulus amplitude for the **ABA** lattice

$$\begin{aligned}
\mathcal{A} = \frac{c}{4} M^2 (1_{\mathrm{RR}} - 1_{\mathrm{NSNS}}) \frac{dt}{t^3} \{ & \mathcal{L}[2,3/2]^2 \mathcal{L}[2/3,1/2] \mathcal{A}^{(0,0)} \\
& + \mathcal{L}[2,3/2] \left(\mathcal{A}^{(1,0)} + 3\mathcal{A}^{(2,0)} + 4\mathcal{A}^{(3,0)} + 3\mathcal{A}^{(4,0)} + \mathcal{A}^{(5,0)} \right) \\
& + 3\mathcal{L}[2,3/2]\mathcal{A}^{(0,1)} + 3\mathcal{L}[2,3/2]\mathcal{A}^{(0,2)} + \mathcal{A}^{(1,1)} + \mathcal{L}[2/3,1/2]\mathcal{A}^{(2,1)} \\
& + 2\mathcal{A}^{(3,1)} + 3\mathcal{A}^{(4,1)} + 2\mathcal{A}^{(5,1)} + 2\mathcal{A}^{(1,2)} + 3\mathcal{A}^{(2,2)} + 2\mathcal{A}^{(3,2)} \\
& + \mathcal{L}[2/3,1/2]\mathcal{A}^{(4,2)} + \mathcal{A}^{(5,2)} \} \; .
\end{aligned} \tag{3.122}$$

For the **ABB** model, one has to exchange one $\mathcal{L}[2,3/2]$ in each term in the first two lines for $\mathcal{L}[2/3,1/2]$ and to multiply each term in the last three lines with a factor of three.

The Möbius strip 1-loop amplitude

From equation (2.53) we find, that for strings starting on brane $(0,0)$, the sectors $(n_1,k_1)(n_2,k_2) = (2n,2n)(m,m)$, $(0,3)(m,m)$, $(4,1)(m,m)$ and $(2,5)(m,m)$ contribute. In this model, one can not directly use the intersection multiplicities from the annulus, since now some of the intersection points are not invariant under the insertions which are present in the case of the Möbius strip, consider figure C.9.

$$(3.123)$$

	ABA	ABB
$\chi_{\mathcal{M}}^{(0,3)(0,0)} = \chi_{\mathcal{M}}^{(2,5)(0,0)} = \chi_{\mathcal{M}}^{(4,1)(0,0)}$	1	1
$\chi_{\mathcal{M}}^{(2,2)(0,0)} = \chi_{\mathcal{M}}^{(4,4)(0,0)}$	3	3
$\chi_{\mathcal{M}}^{(0,0)(1,1)} = \chi_{\mathcal{M}}^{(0,0)(2,2} = \chi_{\mathcal{M}}^{(2,2)(2,2)} = \chi_{\mathcal{M}}^{(4,4)(1,1)}$	3	9
$\chi_{\mathcal{M}}^{(0,3)(1,1)} = \chi_{\mathcal{M}}^{(0,3)(2,2)} = \chi_{\mathcal{M}}^{(2,2)(1,1)} = \chi_{\mathcal{M}}^{(2,5)(1,1)}$ $= \chi_{\mathcal{M}}^{(2,5)(2,2)} = \chi_{\mathcal{M}}^{(4,1)(1,1)} = \chi_{\mathcal{M}}^{(4,1)(2,2)} = \chi_{\mathcal{M}}^{(4,4)(2,2)}$	1	3

For the **ABA** lattice, we find the Möbius strip 1-loop amplitude

$$\begin{aligned}
\mathcal{M} = -\frac{c}{4}(1_{\mathrm{RR}} - 1_{\mathrm{NSNS}})\frac{dt}{t^3}\,\{&C_{00}^{00}\mathcal{L}[2,6]^2\mathcal{L}[2/3,2]\mathcal{M}^{(0,0)(0,0)} + \mathcal{L}[2,6]\left(C_{50}^{20}\mathcal{M}^{(2,5)(0,0)}\right.\\
&\left.+3C_{40}^{40}\mathcal{M}^{(4,4)(0,0)} + C_{30}^{00}\mathcal{M}^{(0,3)(0,0)} + 3C_{20}^{20}\mathcal{M}^{(2,2)(0,0)} + C_{10}^{40}\mathcal{M}^{(4,1)(0,0)}\right)\\
&+3C_{02}^{02}\mathcal{L}[2,6]\mathcal{M}^{(0,0)(2,2)} + 3C_{01}^{01}\mathcal{L}[2,6]\mathcal{M}^{(0,0)(1,1)} + C_{52}^{22}\mathcal{M}^{(2,5)(2,2)}\\
&+C_{42}^{42}\mathcal{L}[2/3,2]\mathcal{M}^{(4,4)(2,2)} + C_{32}^{02}\mathcal{M}^{(0,3)(2,2)} + 3C_{22}^{22}\mathcal{M}^{(2,2)(2,2)} + C_{12}^{42}\mathcal{M}^{(4,1)(2,2)}\\
&+C_{51}^{21}\mathcal{M}^{(2,5)(1,1)} + 3C_{41}^{41}\mathcal{M}^{(4,4)(1,1)} + C_{31}^{01}\mathcal{M}^{(0,3)(1,1)} + C_{21}^{21}\mathcal{L}[2/3,2]\mathcal{M}^{(2,2)(1,1)}\\
&+C_{11}^{41}\mathcal{M}^{(4,1)(1,1)}\}\ .
\end{aligned} \tag{3.124}$$

For the **ABB** model, one has to exchange one $\mathcal{L}[2,6]$ in each term in the first two lines for $\mathcal{L}[2/3,2]$ and to multiply each term in the last four lines with a factor of three.

Tree channel amplitudes and tadpole cancellation

Modular transformation yields the tree channel amplitudes for the **ABA** model

$$\begin{aligned}
\tilde{\mathcal{K}} = \frac{4c}{\sqrt{3}}(1_{\mathrm{RR}} - 1_{\mathrm{NSNS}})\int_0^\infty dl\,\Big\{&\tilde{\mathcal{L}}[1,4/3]^2\tilde{\mathcal{L}}[3,4]\tilde{\mathcal{K}}^{(0,0)}\\
&-\tilde{\mathcal{L}}[1,4/3]\left(\tilde{\mathcal{K}}^{(1,0)} + 3\tilde{\mathcal{K}}^{(2,0)} + 4\tilde{\mathcal{K}}^{(3,0)} + 3\tilde{\mathcal{K}}^{(4,0)} + \tilde{\mathcal{K}}^{(5,0)}\right)\\
&-3\tilde{\mathcal{L}}[1,4/3]\tilde{\mathcal{K}}^{(0,1)} - 3\tilde{\mathcal{L}}[1,4/3]\tilde{\mathcal{K}}^{(0,2)} + \sqrt{3}\tilde{\mathcal{K}}^{(1,1)} - 3\tilde{\mathcal{L}}[3,4]\tilde{\mathcal{K}}^{(2,1)}\\
&-2\sqrt{3}\tilde{\mathcal{K}}^{(3,1)} - 3\sqrt{3}\tilde{\mathcal{K}}^{(4,1)} - 2\sqrt{3}\tilde{\mathcal{K}}^{(5,1)} + 2\sqrt{3}\tilde{\mathcal{K}}^{(1,2)} + 3\sqrt{3}\tilde{\mathcal{K}}^{(2,2)} + 2\sqrt{3}\tilde{\mathcal{K}}^{(3,2)}\\
&-3\tilde{\mathcal{L}}[3,4]\tilde{\mathcal{K}}^{(4,2)} - \sqrt{3}\tilde{\mathcal{K}}^{(5,2)}\Big\}\ ,
\end{aligned} \tag{3.125}$$

where we used $\tilde{\mathcal{K}}^{(0,1)} = \tilde{\mathcal{K}}^{(0,2)} = \tilde{\mathcal{K}}^{(2,1)} = \tilde{\mathcal{K}}^{(4,2)}$ to write the amplitude in the expected form of the complete projector. Note, that the placement of the lattice contributions in the corresponding terms is not unique, but this ambiguity does not affect the tadpole cancellation conditions and can be chosen in such a way that the formal expressions coincide with the other amplitudes. For the **ABB** model, one has to multiply $\tilde{\mathcal{K}}$ by a factor of three and exchange one $\tilde{\mathcal{L}}[1,4/3]$ in each term of the first two lines for $\tilde{\mathcal{L}}[3,4]$.

$$\begin{aligned}\tilde{\mathcal{A}} = \frac{c}{2\sqrt{3}} M^2 (1_{\mathrm{RR}} - 1_{\mathrm{NSNS}}) \int_0^\infty dl \, \Big\{ & \tilde{\mathcal{L}}[1,4/3]^2 \tilde{\mathcal{L}}[3,4] \tilde{\mathcal{A}}^{(0,0)} \\ & - \tilde{\mathcal{L}}[1,4/3] \left(\tilde{\mathcal{A}}^{(1,0)} + 3\tilde{\mathcal{A}}^{(2,0)} + 4\tilde{\mathcal{A}}^{(3,0)} + 3\tilde{\mathcal{A}}^{(4,0)} + \tilde{\mathcal{A}}^{(5,0)} \right) \\ & - 3\tilde{\mathcal{L}}[1,4/3]\tilde{\mathcal{A}}^{(0,1)} - 3\tilde{\mathcal{L}}[1,4/3]\tilde{\mathcal{A}}^{(0,2)} + \sqrt{3}\tilde{\mathcal{A}}^{(1,1)} - 3\tilde{\mathcal{L}}[3,4]\tilde{\mathcal{A}}^{(2,1)} \\ & - 2\sqrt{3}\tilde{\mathcal{A}}^{(3,1)} - 3\sqrt{3}\tilde{\mathcal{A}}^{(4,1)} - 2\sqrt{3}\tilde{\mathcal{A}}^{(5,1)} + 2\sqrt{3}\tilde{\mathcal{A}}^{(1,2)} + 3\sqrt{3}\tilde{\mathcal{A}}^{(2,2)} + 2\sqrt{3}\tilde{\mathcal{A}}^{(3,2)} \\ & - 3\tilde{\mathcal{L}}[3,4]\tilde{\mathcal{A}}^{(4,2)} - \sqrt{3}\tilde{\mathcal{A}}^{(5,2)} \Big\} \end{aligned} \tag{3.126}$$

For the **ABB** model, one has to multiply $\tilde{\mathcal{A}}$ by a factor of three and exchange one $\tilde{\mathcal{L}}[1,4/3]$ in each term of the first two lines for $\tilde{\mathcal{L}}[3,4]$.

$$\begin{aligned}\tilde{\mathcal{M}} = -\frac{4c}{\sqrt{3}} (1_{\mathrm{RR}} - 1_{\mathrm{NSNS}}) \int_0^\infty dl \, \Big\{ & C^{00}_{00} \tilde{\mathcal{L}}[4,4/3]^2 \tilde{\mathcal{L}}[12,4] \tilde{\mathcal{M}}^{(0,0)} \\ & - \tilde{\mathcal{L}}[4,4/3] \left(C^{20}_{50}\tilde{\mathcal{M}}^{(1,0)} + 3C^{40}_{40}\tilde{\mathcal{M}}^{(2,0)} - 4C^{00}_{30}\tilde{\mathcal{M}}^{(3,0)} + 3C^{20}_{20}\tilde{\mathcal{M}}^{(4,0)} + C^{40}_{10}\tilde{\mathcal{M}}^{(5,0)} \right) \\ & - 3C^{02}_{02}\tilde{\mathcal{L}}[4,4/3]\tilde{\mathcal{M}}^{(0,1)} - 3C^{01}_{01}\tilde{\mathcal{L}}[4,4/3]\tilde{\mathcal{M}}^{(0,2)} + \sqrt{3}C^{22}_{52}\tilde{\mathcal{M}}^{(1,1)} \\ & - 3C^{42}_{42}\tilde{\mathcal{L}}[12,4]\tilde{\mathcal{M}}^{(2,1)} + 2\sqrt{3}C^{02}_{32}\tilde{\mathcal{M}}^{(3,1)} + 3\sqrt{3}C^{22}_{22}\tilde{\mathcal{M}}^{(4,1)} + 2\sqrt{3}C^{42}_{12}\tilde{\mathcal{M}}^{(5,1)} \\ & + 2\sqrt{3}C^{21}_{51}\tilde{\mathcal{M}}^{(1,2)} - 3\sqrt{3}C^{41}_{41}\tilde{\mathcal{M}}^{(2,2)} + 2\sqrt{3}C^{01}_{31}\tilde{\mathcal{M}}^{(3,2)} - 3C^{21}_{21}\tilde{\mathcal{L}}[12,4]\tilde{\mathcal{M}}^{(4,2)} \\ & - \sqrt{3}C^{41}_{11}\tilde{\mathcal{M}}^{(5,2)} \Big\} \end{aligned} \tag{3.127}$$

For the **ABB** model, one has to multiply $\tilde{\mathcal{M}}$ by a factor of three and exchange one $\tilde{\mathcal{L}}[4,4/3]$ in each term of the first two lines for $\tilde{\mathcal{L}}[12,4]$.

This leads to the tadpole cancellation conditions

$$M = 4 \tag{3.128}$$

for both models and

$$\begin{aligned} & C^{00}_{00} = C^{20}_{50} = C^{40}_{40} = -C^{00}_{30} = C^{40}_{10} = C^{02}_{02} = C^{01}_{01} = C^{22}_{52} = C^{42}_{42} \\ & = -C^{02}_{32} = -C^{22}_{22} = -C^{42}_{12} = C^{21}_{51} = -C^{41}_{41} = C^{01}_{31} = C^{21}_{21} = C^{41}_{11} = M\,. \end{aligned} \tag{3.129}$$

and the twisted sector tadpole cancellation conditions

$$\mathrm{tr}\gamma^{(a_1,a_2)}_{30} = 0\,. \tag{3.130}$$

To satisfy these conditions, we get by with the unit matrix and the matrix I from (2.97). If we introduce $(a) = (0), \ldots, (17)$ as the alternative labelling of the 18 different stacks of D6-branes shown in figure 3.4, we can assign

$$\gamma^{(2a)}_{\Omega\mathcal{R}2k_1,k_2} = \mathbb{1}_4 \quad \text{and} \quad \gamma^{(2a+1)}_{\Omega\mathcal{R}2k_1+1,k_2} = I\,, \tag{3.131}$$

up to signs, to satisfy the tadpole cancellation conditions. Note, that all of these signs can be fixed by consistency, e.g. by consistent truncation to the $T^6/\mathbb{Z}_6$, $T^6/\mathbb{Z}_3$, $T^4/\mathbb{Z}_6$ and $T^4/\mathbb{Z}_3$ substructures.

3.5.2 The massless spectrum

The closed string spectrum

The untwisted sector consists of the model independent SUGRA plus 3C.

In the sectors twisted by $\Theta_1^{n_1}$, $\Theta_2^{n_2}$, $\Theta_1^2\Theta_2$ and $\Theta_1^4\Theta_2^2$ we always find the two $\Omega\mathcal{R}$ invariant massless combinations of the form (3.41) in the NSNS sector and of the form (3.43) in the RR sector, respectively. In the sectors twisted by $\Theta_1^{1,3,5}\Theta_2^{1,2}$, $\Theta_1^4\Theta_2$ and $\Theta_1^2\Theta_2^2$ we always find only one invariant massless combination of the form (3.72) in the NSNS sector and of the form (3.73) in the RR sector.

Now we discuss the fixed point structure in the various twisted sectors. We start with the Θ_1 twisted sector, which is equivalent to the Θ_1^5 twisted sector. The torus T_3 is untwisted. There is only one fixed point, namely 11.

In the Θ_1^2 (Θ_1^4) twisted sector, T_3 is untwisted

AB• : 11 is invariant,
12-13, 21-31 form 2 pairs under Θ_1,
22-23-32-33 a quartet under $\Omega\mathcal{R}$ and Θ_1

In the Θ_1^3 twisted sector, T_3 is untwisted

AB• : 11 is invariant,
14-15-16, 41-51-61, 44-55-66 form 3 triplets under Θ_1,
45-56-64-54-65-46 are connected under $\Omega\mathcal{R}$ and Θ_1

In the Θ_2 (Θ_2^2) twisted sector, T_1 is untwisted

•BA : 11 is invariant,
12-13 form a pair under $\Omega\mathcal{R}$, 21-31 a pair under Θ_1,
22-23-32-33 a quartet under $\Omega\mathcal{R}$ and Θ_1

•BB : 11, 12, 13 are invariant,
21-31, 22-32, 23-33 form 3 pairs under Θ_1

In the $\Theta_1^2\Theta_2$ ($\Theta_1^4\Theta_2^2$) twisted sector, T_2 is untwisted

A • A : 11 is invariant,
12-13 form a pair under $\Omega\mathcal{R}$, 21-31 a pair under Θ_1,
22-23-32-33 a quartet under $\Omega\mathcal{R}$ and Θ_1

A • B : 11, 12, 13 are invariant,
21-31, 22-32, 23-33 form 3 pairs under Θ_1

In the remaining sectors, all three tori are twisted. We begin with the $\Theta_1\Theta_2$ ($\Theta_1^5\Theta_2^2$) twisted sector

ABA : 111 is invariant,
112-113 form a pair under $\Omega\mathcal{R}$
ABB : 111, 112, 113 are invariant

The $\Theta_1^3\Theta_2$ ($\Theta_1^3\Theta_2^2$) twisted sector:

ABA : 111 is invariant,
112-113 form a pair under $\Omega\mathcal{R}$,
411-511-611 form a triplet under Θ_1,
412-512-612-413-513-613 are connected under $\Omega\mathcal{R}$ and Θ_1
ABB : 111, 112, 113 are invariant,
411-511-611, 412-512-612, 413-513-613 form 3 triplets under Θ_1

The $\Theta_1^4\Theta_2$ ($\Theta_1^2\Theta_2^2$) twisted sector:

ABA : 111 is invariant,
112-113 form a pair under $\Omega\mathcal{R}$,
121-131, 211-311 two pairs under Θ_1,
the remaining points 5 quartets under $\Omega\mathcal{R}$ and Θ_1
ABB : 111, 112, 113 are invariant
121-131, 122-132, 123-133, 211-311, 212-312, 213-313
form 5 pairs under Θ_1,
the remaining points 3 quartets under $\Omega\mathcal{R}$ and Θ_1

The $\Theta_1^5\Theta_2$ ($\Theta_1\Theta_2^2$) twisted sector:

ABA : 111 is invariant,
112-113 form a pair under $\Omega\mathcal{R}$,
141-151-161 form a triplet under Θ_1,
142-152-162-143-153-163 are connected under $\Omega\mathcal{R}$ and Θ_1
ABB : 111, 112, 113 are invariant,
141-151-161, 142-152-162, 143-153-163 form 3 triplets under Θ_1

The pairs under $\Omega\mathcal{R}$, the quartets and the six connected points each contribute $1(\frac{1}{2})$C plus $1(\frac{1}{2})$V, the other points, pairs, etc. each contribute $1(\frac{1}{2})$C, if there are 2(1) massless ground states.

We obtain the closed string spectrum

twist-sector	**ABA**	**ABB**
untwisted	SUGRA + 3C	
$\theta_1 + \theta_1^5$	2C	2C
$\theta_1^2 + \theta_1^4$	8C + 2V	8C + 2V
θ_1^3	5C + 1V	5C + 1V
$\theta_2 + \theta_2^2$	8C + 4V	12C
$\theta_1\theta_2 + \theta_1^5\theta_2^2$	2C + 1V	3C
$\theta_1^2\theta_2 + \theta_1^4\theta_2^2$	8C + 4V	12C
$\theta_1^3\theta_2 + \theta_1^3\theta_2^2$	4C + 2V	6C
$\theta_1^4\theta_2 + \theta_1^2\theta_2^2$	9C + 6V	12C + 3V
$\theta_1^5\theta_2 + \theta_1\theta_2^2$	4C + 2V	6C

(3.132)

The open string spectrum

In the untwisted NS sector, out of the 18 possibilities, only the $(0,0)$ and $(1,1)$ strings are independent. The others can be reached by symmetries of the theory. The $(0,0)$ strings are symmetric under $\Omega\mathcal{R}$ and $\Omega\mathcal{R}\Theta_1^3$, which leads to the constraints (consider section 2.2.7)

$$\lambda^{(0,0)} = -\lambda^{(0,0)T} = -I\lambda^{(0,0)T}I \tag{3.133}$$

in the non-compact directions, i.e. $U(M/2) = U(2)$ as one factor of the gauge group, which is rather small. Together with the $(1,1)$ strings, we obtain the gauge group

$$[U(2)]^2 \tag{3.134}$$

for this model. In the compact directions $1, \bar{1}, 2, \bar{2}$, Θ_1^3 produces an additional minus sign and the constraints read

$$\lambda^{(0,0)} = -\lambda^{(0,0)T} = I\lambda^{(0,0)T}I\,, \tag{3.135}$$

which gives two times the antisymmetric representation. Since the antisymmetric representation of unitary groups is complex, this means $(A,1) + (\bar{A},1)$, which we abbreviate by $(A,1) + h.c.$ in the following. However, the antisymmetric representation of $U(2)$ is one dimensional. Therefore we denote $(\mathbf{1}_A, \mathbf{1})$, since the two $\mathbf{1}$'s have different $U(1)$ charges. Together with the $(1,1)$ strings, these two complex compact directions give 2C in the $(\mathbf{1}_A, \mathbf{1}) + (\mathbf{1}, \mathbf{1}_A) + h.c.$ In the compact directions $3, \bar{3}$, Θ_1^3 produces no minus sign and we obtain 1C in the adjoint $(\mathbf{4}, \mathbf{1}) + (\mathbf{1}, \mathbf{4})$.

The Θ_1 twisted sector is invariant under Θ_1^3, i.e.

$$\lambda^{(0,5)} = \pm I \lambda^{(0,5)} I \,, \tag{3.136}$$

which gives 2 times the bifundamental. Since we have two massless ground states in this sector, we find 1C in $(F, F) + h.c.$ which is $(\mathbf{2}, \mathbf{2}) + h.c.$ for $[U(2)]^2$. The same content is found in the Θ_1^5 twisted sector.

In the Θ_1^2 twisted sector we have to be more careful. These strings are located at the intersection points 11, 12 and 13 of the twisted tori $T_{1,2}$. The $(0,4)$ strings located at the intersection point 11 are invariant under $\Omega\mathcal{R}\Theta_1$ and $\Omega\mathcal{R}\Theta_1^4$ (or equivalently $\Omega\mathcal{R}\Theta_1$ and Θ_1^3) whereas the intersection points 12 and 13 are interchanged under $\Omega\mathcal{R}\Theta_1$ such that these strings are symmetric under $\Omega\mathcal{R}\Theta_1^4$ only. For the strings on 11 this leads to (3.135), where the additional minus sign comes from the relative insertion of Θ_1^3, and since we have two massless ground states in this sector, we find 1C in the antisymmetric $(\mathbf{1}_A, \mathbf{1}) + (\mathbf{1}, \mathbf{1}_A) + h.c$, together with the $(1,5)$ strings. The $(0,4)$ strings on the intersection points 12 and 13 are constrained by

$$\lambda^{(0,4)} = -\lambda^{(0,4)T} \,, \tag{3.137}$$

which gives another 1C in the $(\mathbf{1}_A, \mathbf{1}) + (\mathbf{1}, \mathbf{1}_A) + h.c$ plus 1C in the adjoint $(\mathbf{4}, \mathbf{1}) + (\mathbf{1}, \mathbf{4})$ together with the $(1,5)$ strings (consider appendix C.3 for the λ matrices). The same amount is found in the Θ_1^4 twisted sector.

The Θ_1^3 twisted sector is invariant under Θ_1^3 and thus works out similar to the Θ_1 twisted sector. In addition, we have to include a multiplicity of 2 from the T_2, which is of type **B**, i.e. 2C in $(\mathbf{2}, \mathbf{2}) + h.c.$.

In the Θ_2 twisted sector, further peculiarities show up. The Θ_2 twisted sector consists of the $(0,12)$ and $(1,13)$ strings. The tori $T_{2,3}$ are twisted, which are, in the case of the **ABA** model, of type **BA**. We will discuss this case first. The $(0,12)$ strings are located at the intersection points 11, 21 and 31 on the tori $T_{2,3}$. The $(0,12)$ strings on the point 11 are invariant under $\Omega\mathcal{R}\Theta_2^2$ and $\Omega\mathcal{R}\Theta_1^3\Theta_2^2$, whereas the points 21 and 31 are interchanged under $\Omega\mathcal{R}\Theta_1^3\Theta_2^2$, such that the strings on these points are invariant under $\Omega\mathcal{R}\Theta_2^2$ only. The $(1,13)$ are located at the intersection point 11 only, so that we find the constraints for the strings $(0,12)$ and $(1,13)$ on intersection point 11 to be of the form (3.133), where another minus sign shows up because of the tadpole cancellation conditions. This gives 1C in the adjoint $(\mathbf{4}, \mathbf{1}) + (\mathbf{1}, \mathbf{4})$. The constraints for the strings $(0,12)$ on the intersection points 21 and 31 are of the form (3.137) and thus lead to 1C in the adjoint $(\mathbf{4}, \mathbf{1})$ and 1C in the antisymmetric $(\mathbf{1}_A, \mathbf{1}) + h.c.$ The Θ_2^2 twisted sector contributes the same amount. In the case of the **ABB** model, we have to include a multiplicity of 3 from the additional intersection points on the third torus.

The remaining twisted sectors work out similarly and we find the open string spectrum

twist-sector	**ABA**	**ABB**	rep of $U(2)\times U(2)$
untwisted	1V		$(\mathbf{4},\mathbf{1})+(\mathbf{1},\mathbf{4})$
	1C		$(\mathbf{4},\mathbf{1})+(\mathbf{1},\mathbf{4})$
	2C		$(\mathbf{1}_A,\mathbf{1})+(\mathbf{1},\mathbf{1}_A)+h.c.$
$\Theta_1+\Theta_1^5$	2C		$(\mathbf{2},\mathbf{2})+h.c.$
$\Theta_1^2+\Theta_1^4$	2C		$(\mathbf{4},\mathbf{1})+(\mathbf{1},\mathbf{4})$
	4C		$(\mathbf{1}_A,\mathbf{1})+(\mathbf{1},\mathbf{1}_A)+h.c.$
Θ_1^3	2C		$(\mathbf{2},\mathbf{2})+h.c.$
$\Theta_2+\Theta_2^2$	2C	6C	$(\mathbf{4},\mathbf{1})+(\mathbf{1},\mathbf{4})$
	2C	6C	$(\mathbf{1}_A,\mathbf{1})+h.c.$
	2C	6C	$(\mathbf{4},\mathbf{1})$
$\Theta_1\Theta_2+\Theta_1^5\Theta_2^2$	1C	3C	$(\mathbf{2},\mathbf{2})+h.c.$
$\Theta_1^2\Theta_2+\Theta_1^4\Theta_2^2$	1C	3C	$(\mathbf{1}_A,\mathbf{1})+(\mathbf{1},\mathbf{1}_A)+h.c.$
	2C	6C	$(\mathbf{1},\mathbf{1}_A)+h.c.$
	2C	6C	$(\mathbf{1},\mathbf{4})$
$\Theta_1^3\Theta_2+\Theta_1^3\Theta_2^2$	2C	6C	$(\mathbf{2},\mathbf{2})+h.c.$
$\Theta_1^4\Theta_2+\Theta_1^2\Theta_2^2$	2C	6C	$(\mathbf{4},\mathbf{1})+(\mathbf{1},\mathbf{4})$
	1C	3C	$(\mathbf{3},\mathbf{1})+(\mathbf{1},\mathbf{3})+h.c.$
$\Theta_1^5\Theta_2+\Theta_1\Theta_2^2$	2C	6C	$(\mathbf{2},\mathbf{2})+h.c.$

(3.138)

Chapter 4

Summary and Conclusions

In this work we show the explicit construction and detailed calculation of $\mathcal{N}=1$ supersymmetric six dimensional $\Omega\mathcal{R}\times\mathbb{Z}_N$ orientifolds of type IIB [20, 7] as well as four dimensional $\Omega\mathcal{R}\times\mathbb{Z}_N\times\mathbb{Z}_M$ orientifolds of type IIA [41]. In contrast to 'ordinary' Ω orientifolds, the additional complex conjugation $\mathcal{R}$ leads to O7-planes in the six dimensional models and O6-planes in the four dimensional models intersecting at angles in the compact directions, which are chosen to be direct products of two-tori. As a consequence of the relation

$$\Omega\mathcal{R}\Theta=\Theta^{-1/2}\Omega\mathcal{R}\Theta^{1/2}\,,$$

these angles are given by half the rotation angles of the corresponding orbifold elements. To cancel the tadpoles arising from the Klein bottle amplitude, D7-branes (D6-branes) have to be added. In this thesis, we perform the analysis for D-branes lying on top of the corresponding O-planes. By this means, D-branes intersecting at angles are naturally introduced. Besides the fact that gauge theories are known to live on the worldvolumes of D-branes, chiral fermions charged under the bifundamental representation of the respective gauge groups are expected to be localized at the intersection points. This opens up new possibilities to obtain phenomenologically interesting compactifications of string theory. It is also possible to break supersymmetry completely with D-branes intersecting at angles, see the introduction and the references given therein for further details.

The inclusion of $\mathcal{R}$ also has an impact on the orbifold lattices in the compact directions, i.e. each two-torus can either be of type **A** or type **B**. Exchanging an **A** for a **B** torus corresponds to switching on a discrete B field in the T-dual picture, see [7] for details. We calculate the Klein bottle, annulus and Möbius strip 1-loop amplitudes, perform the modular transformation to the tree channel and extract the tadpole cancellation conditions which determine the number of D-branes and impose constraints on the matrix representations of the elements of the orientifold and the orbifold group. Furthermore, we show how to calculate the amplitudes directly in the tree channel using the boundary state formalism in order to check worldsheet duality. For the models under consideration, worldsheet duality simply means that in the tree channel the twisted sectors do not contribute. For the six dimensional models, this leaves the possibilities

$$\begin{array}{ll} \mathbb{Z}_{2,3}: & \mathbf{AA},\ \mathbf{AB},\ \mathbf{BB}\,, \\ \mathbb{Z}_{4,6}: & \mathbf{AB}\,, \end{array}$$

where **AB** is equivalent to **BA**. The $\mathbb{Z}_{3,4,6}$ models, which are T-dual to asymmetric orientifolds, are discussed in [20, 7] and we reproduce their results. The case of $\mathbb{Z}_2$, however, is only briefly mentioned in these references and we perform a detailed calculation. The $\mathbb{Z}_2$ **AA** model is an explicit example of a model T-dual to the one presented in [44], where T-duality is applied in the 7th and the 9th direction. Indeed, we obtain the same massless spectrum. Since dualities are an important and powerful concept in the recent developments in string theory, we hope to shed some light on this aspect with this example. As already mentioned above, the $\mathbb{Z}_2$ **AB** and **BB** models are T-dual to Ω orientifolds with discrete B field.

For the four dimensional models, we find the following solutions consistent with worldsheet duality [41]:

$$\begin{array}{ll} \mathbb{Z}_2 \times \mathbb{Z}_2\,,\ \ \mathbb{Z}_3 \times \mathbb{Z}_3: & \mathbf{AAA},\ \mathbf{AAB},\ \mathbf{ABB},\ \mathbf{BBB}\,, \\ \mathbb{Z}_4 \times \mathbb{Z}_2\,,\ \ \mathbb{Z}_6 \times \mathbb{Z}_3: & \mathbf{ABA},\ \mathbf{ABB}\,. \end{array}$$

In the cases of $\mathbb{Z}_2 \times \mathbb{Z}_2$ and $\mathbb{Z}_3 \times \mathbb{Z}_3$, **AAB** (**ABB**) is equivalent to **ABA**, **BAA** (**BAB**, **BBA**). In the remaining models, **ABA** (**ABB**) is equivalent to **BAA** (**BAB**). In analogy to the six dimensional models, some types of lattices for the $\mathbb{Z}_4 \times \mathbb{Z}_2$ and $\mathbb{Z}_6 \times \mathbb{Z}_3$ models are ruled out. But now, worldsheet duality has somewhat more dramatic consequences: The models $\mathbb{Z}_3 \times \mathbb{Z}_2$, $\mathbb{Z}_6 \times \mathbb{Z}_2$, $\mathbb{Z}_4 \times \mathbb{Z}_4$ and $\mathbb{Z}_6 \times \mathbb{Z}_6$ are not allowed at all[1]. The $\mathbb{Z}_2 \times \mathbb{Z}_2$ **AAA** model is T-dual to the model presented in [15], where T-duality now is applied in the 5th, 7th and 9th direction. We verify the equivalence of the massless spectra. This is another example of an explicit construction T-dual to a previously known model. The remaining cases of $\mathbb{Z}_2 \times \mathbb{Z}_2$ are again T-dual to Ω orientifolds with discrete B field and the models with larger orbifold groups are T-dual to asymmetric orientifolds. It would be interesting to study these orientifolds directly in the T-dual picture to investigate the role of the discrete B fields, the D-brane content of asymmetric orientifolds and the connection to noncommutative geometry in analogy to [21], where this analysis has been performed for some of the six dimensional models. To summarize the formal aspects of our work, we have

[1] The cases $\mathbb{Z}_4 \times \mathbb{Z}_3$ and $\mathbb{Z}_6 \times \mathbb{Z}_4$ are obviously forbidden, because the second torus T_2 can not be chosen to be invariant under both factors of these orbifold groups.

constructed new supersymmetric orientifold compactifications of type II string theory, we have provided explicit examples T-dual to models presented in the literature and we have investigated worldsheet duality as an additional constraint using the boundary state formalism.

Now we turn to the phenomenological implications of this work. As already mentioned, our main motivation to consider these models was the fact that chiral fermions are expected to be localized at the intersection points of the D-branes. However, it turns out that the spectra of all the four dimensional models are non-chiral. Furthermore, the gauge groups are quite restricted, i.e. $SO(4)$ for $\mathbb{Z}_3 \times \mathbb{Z}_3$, $[U(2)]^2$ for $\mathbb{Z}_6 \times \mathbb{Z}_3$ and $[Sp(M/4)]^4$ for the remaining models[2]. Nevertheless, our models are not that far away from a phenomenological utility as it seems at first sight. Both, the non-chirality of the spectra and the restricted gauge groups are a consequence of the symmetric positioning of the D6-branes on top of the orientifold planes. In [29], our $\mathbb{Z}_2 \times \mathbb{Z}_2$ model is generalized in exactly that respect, namely the D6-branes are chosen to intersect at almost arbitrary angles. 'Almost' means, that the D6-branes are not aligned with the O6-planes anymore, but the intersection angles are chosen in such a way that $\mathcal{N} = 1$ supersymmetry in four dimensions is preserved. This slight generalization of our $\mathbb{Z}_2 \times \mathbb{Z}_2$ model leads to the first D-brane construction of a chiral three-family $\mathcal{N} = 1$ supersymmetric solution with the SM gauge group as part of the gauge structure. It would be interesting to perform the same generalization for the other orbifold product groups. Another interesting possibility would be to consider our four dimensional models with D6-branes intersecting at angles, such that supersymmetry is completely broken. By this means, one could obtain further non-supersymmetric compactifications of type IIA string theory close to the SM, analyze the regions where tachyons develop and investigate the link between tachyon condensation and spontaneous symmetry breaking, as already mentioned in the introduction.

[2]Where M is the number of D6-branes on top of each other.

Appendix A

Computation of 1-loop diagrams

In this appendix we will give some details of the computation of the diagrams shown in figure 2.2 in the loop channel. The computation of the lattice contributions in the loop channel was already explained in section 2.2.

In the following we show the details of how to calculate the oscillator contributions to the 1-loop amplitudes (2.22), (2.24) and (2.23). To begin, we redisplay the Hamiltonian for the left movers

$$
\begin{aligned}
H_L = \frac{\alpha'}{4}p_L^2 &+ \sum_{m_\mu>0} \alpha^\mu_{-m_\mu}\alpha^\mu_{m_\mu} + \sum_{r_\mu>0} r_\mu \psi^\mu_{-r_\mu}\psi^\mu_{r_\mu} \\
&+ \sum_{m_i>0} \alpha^i_{-m_i}\alpha^{\bar{i}}_{m_i} + \sum_{l_i>0} \alpha^{\bar{i}}_{-l_i}\alpha^i_{l_i} \\
&+ \sum_{r_i>0} r_i \psi^i_{-r_i}\psi^{\bar{i}}_{r_i} + \sum_{s_i>0} s_i \psi^{\bar{i}}_{-s_i}\psi^i_{s_i} + E_0\,,
\end{aligned}
\tag{A.1}
$$

The oscillators in the compact directions are complexified, e.g.

$$
\alpha^{1,\bar{1}} = \frac{1}{\sqrt{2}}\left(\alpha^6 \pm i\alpha^7\right) \tag{A.2}
$$

and similar for the fermionic oscillators. The modings for the n^{th} twisted sector are given by

$$
\begin{aligned}
m_\mu &\in \mathbb{Z} \\
m_i &\in \mathbb{Z} + nv_i \\
l_i &\in \mathbb{Z} - nv_i \\
r_\mu &\in \mathbb{Z}\ (+1/2) \quad \text{R (NS)} \\
r_i &\in \mathbb{Z} + nv_i\ (+1/2) \quad \text{R (NS)} \\
s_i &\in \mathbb{Z} - nv_i\ (+1/2) \quad \text{R (NS)}
\end{aligned}
\tag{A.3}
$$

The zero-point energy contributions to the traces are

$$
E_0^i = -\frac{1}{12} + \frac{1}{2}\nu_i(1-\nu_i) \tag{A.4}
$$

for a complex boson in the n^{th} twisted sector where

$$\nu_i = nv_i \bmod \mathbb{Z} \qquad 0 \leqslant \nu_i < 1 \tag{A.5}$$

and

$$E_0^{\mathrm{NS,R},i} = -\frac{1}{24} + \frac{1}{2}(\frac{1}{2} - \nu_i)^2 \tag{A.6}$$

for a complex fermion in the n^{th} twisted sector where

$$\nu_i = nv_i \bmod \mathbb{Z} \qquad 0 \leqslant \nu_i < 1 \qquad (\mathrm{R}) \tag{A.7}$$

$$\nu_i = \frac{1}{2} \pm nv_i \bmod \mathbb{Z} \qquad 0 \leqslant \nu_i < 1 \qquad (\mathrm{NS}) \tag{A.8}$$

Note, that the zero-point energy contributions for the n^{th} and the $(N-n)^{th}$ twisted sector are identical.

The oscillator contributions can be expressed in terms of Jacobi theta functions and the Dedekind eta function,

$$\vartheta\Big[{\alpha \atop \beta}\Big](t) = \sum_{m\in\mathbb{Z}} q^{\frac{(m+\alpha)^2}{2}} e^{2\pi i(m+\alpha)\beta}, \tag{A.9}$$

$$\eta(t) = q^{\frac{1}{24}} \prod_{m=1}^{\infty} (1-q^m) \,, \tag{A.10}$$

with $q = e^{-2\pi t}$. Useful identities are

$$\vartheta\Big[{\alpha \atop \beta+1}\Big](t) = e^{2\pi i\alpha}\vartheta\Big[{\alpha \atop \beta}\Big](t) \tag{A.11}$$

$$\vartheta\Big[{\alpha+1 \atop \beta}\Big](t) = \vartheta\Big[{\alpha \atop \beta}\Big](t)\,. \tag{A.12}$$

We will mainly use the product representation

$$\frac{\vartheta\big[{\alpha \atop \beta}\big]}{\eta}(t) = e^{2\pi i\alpha\beta} q^{\frac{\alpha^2}{2}-\frac{1}{24}} \prod_{m=1}^{\infty} \left[1 + q^{m-\frac{1}{2}+\alpha} e^{2\pi i\beta}\right] \left[1 + q^{m-\frac{1}{2}-\alpha} e^{-2\pi i\beta}\right] . \tag{A.13}$$

The first factor on the rhs of equation (A.13) can be interpreted as the charge of the corresponding ground state with respect to the insertion and the exponent of the second factor as the vacuum energy.

As one can read off from the Hamiltonian (A.1), the 1-loop amplitudes factorize in lattice contributions (which we do not consider in this section), in bosonic and fermionic contributions and in contributions from the different dimensions. Therefore, we calculate the various twist sectors and insertions for one complex compact dimension i. The results for two (real) non-compact dimensions are just the same (of course, in the non-compact dimensions there are no twisted sectors and no insertions from the orbifold group).

In the following sections, we will calculate the oscillator contributions to $\mathrm{Tr}\big(\mathcal{O}q^H\big)$, where $\mathcal{O}$ is some insertion from the GSO projector or from the orbifold group and H can be H or H_L or H_R. Thus, terms like this directly appear in the annulus amplitude. For the Klein bottle, the additional insertion of $\Omega\mathcal{R}$ implies that H_L and H_R yield the same contributions such that one, in principle, only has to replace t by $2t$ in the following results. For the Möbius strip, the additional insertion of $\Omega\mathcal{R}$ implies that one has to replace t by $t+i/2$, as follows from (A.18).

Before we calculate the various traces, we collect some basics about the states over which we take the trace. We consider one complex compact dimension, as the results for the non-compact dimensions can easily be read off from that. We discuss the open string case and the left movers in the closed string case simultaneously. For the right movers, everything is similar. In the bosonic case, the oscillator algebra is given by

$$\begin{aligned} \left[\alpha^i_m, \alpha^i_l\right] &= \left[\alpha^{\bar{i}}_m, \alpha^{\bar{i}}_l\right] = 0 \\ \left[\alpha^i_m, \alpha^{\bar{i}}_l\right] &= \left[\alpha^{\bar{i}}_m, \alpha^i_l\right] = m\delta_{m,-l} \end{aligned} \tag{A.14}$$

We define the ON basis

$$\begin{aligned} |0,m,N\rangle &\equiv \frac{1}{\sqrt{N!m^N}} \left(\alpha^i_{-m}\right)^N |0\rangle \\ \langle 0,m,N| &\equiv \frac{1}{\sqrt{N!m^N}} \langle 0| \left(\alpha^{\bar{i}}_m\right)^N \end{aligned} \tag{A.15}$$

where N is the occupation number. Therefore

$$\langle 0,m,N| \left(\alpha^i_{-m}\alpha^{\bar{i}}_m\right)^k |0,m,N\rangle = (mN)^k \langle 0|0\rangle = (mN)^k \tag{A.16}$$

and

$$\langle 0,m,N| q^{\alpha^i_{-m}\alpha^{\bar{i}}_m} |0,m,N\rangle = q^{mN}\langle 0|0\rangle = q^{mN} \tag{A.17}$$

as one can check by expanding the exponential. Further, the insertions act as

$$\begin{aligned} \Omega\mathcal{R}|0,m,N\rangle &= \begin{cases} \overline{\widetilde{|0,m,N\rangle}} & \text{closed} \\ \left(-e^{\pi i m}\right)^N |0,m,N\rangle & \text{open} \end{cases} \\ \Theta|0,m,N\rangle &= \left(e^{2\pi i v_i}\right)^N |0,m,N\rangle \end{aligned} \tag{A.18}$$

where the bar and the tilde indicate that the state is built from the complex conjugated right movers acting on the vacuum. Remember, that $\Omega\mathcal{R}$ preserves the twist sector. The fermionic oscillator algebra is given by

$$\begin{aligned} \left\{\psi^i_r, \psi^i_s\right\} &= \left\{\psi^{\bar{i}}_r, \psi^{\bar{i}}_s\right\} = 0 \\ \left\{\psi^i_r, \psi^{\bar{i}}_s\right\} &= \left\{\psi^{\bar{i}}_r, \psi^i_s\right\} = \delta_{r,-s} \end{aligned} \tag{A.19}$$

The other results are similar to the bosonic case, except for the occupation number N, which is restricted to 0 or 1 for the fermions, due to Pauli's principle. In the following list of useful results, we abbreviate $\mathrm{Tr}\big(\mathcal{O}q^H\big)$ with Tr.

Bosonic contributions, $\mathcal{O} = \mathbb{1}$

$$\mathrm{Tr} = q^{E_0^i}\left[\prod_{m_i>0}^{\infty}\sum_{N_{m_i}=0}^{\infty} q^{m_i N_{m_i}}\right]\left[\prod_{l_i>0}^{\infty}\sum_{N_{l_i}=0}^{\infty} q^{l_i N_{l_i}}\right] \tag{A.20}$$

- untwisted sector:

$$\mathrm{Tr} = q^{-\frac{1}{12}}\prod_{m=1}^{\infty}\left(1-q^m\right)^{-2} = \eta^{-2}(t) \tag{A.21}$$

- n^{th} twisted sector with $0 < nv_i < 1$:

$$\begin{aligned}\mathrm{Tr} &= q^{-\frac{1}{2}nv_i(nv_i-1)-\frac{1}{12}}\prod_{m=1}^{\infty}\left[\left(1-q^{m-1+nv_i}\right)\left(1-q^{m-nv_i}\right)\right]^{-1}\\ &= e^{\pi i(nv_i-\frac{1}{2})}\left(\frac{\vartheta\left[\begin{smallmatrix}1/2+nv_i\\1/2\end{smallmatrix}\right]}{\eta}(t)\right)^{-1}\end{aligned} \tag{A.22}$$

Fermionic contributions, R sector, $\mathcal{O} = \mathbb{1}$

$$\mathrm{Tr} = q^{E_0^{\mathrm{R},i}}\left[\prod_{r_i>0}^{\infty}\sum_{N_{r_i}=0,1} q^{r_i N_{r_i}}\right]\left[\prod_{s_i>0}^{\infty}\sum_{N_{s_i}=0,1} q^{s_i N_{s_i}}\right] \tag{A.23}$$

- untwisted sector: there are zero modes, which contribute a factor of two

$$\mathrm{Tr} = 2q^{\frac{1}{12}}\left(\prod_{m=1}^{\infty}\left(1+q^m\right)\right)^2 = \frac{\vartheta\left[\begin{smallmatrix}1/2\\0\end{smallmatrix}\right]}{\eta}(t) \tag{A.24}$$

- n^{th} twisted sector with $0 < nv_i < 1$:

$$\begin{aligned}\mathrm{Tr} &= q^{\frac{1}{2}nv_i(nv_i-1)+\frac{1}{12}}\prod_{m=1}^{\infty}\left[\left(1+q^{m-1+nv_i}\right)\left(1+q^{m-nv_i}\right)\right]\\ &= \frac{\vartheta\left[\begin{smallmatrix}1/2+nv_i\\0\end{smallmatrix}\right]}{\eta}(t)\end{aligned} \tag{A.25}$$

Fermionic contributions, NS sector, $\mathcal{O} = \mathbb{1}$

$$\mathrm{Tr} = q^{E_0^{\mathrm{NS},i}} \left[\prod_{r_i>0}^{\infty} \sum_{N_{r_i}=0,1} q^{r_i N_{r_i}} \right] \left[\prod_{s_i>0}^{\infty} \sum_{N_{s_i}=0,1} q^{s_i N_{s_i}} \right] \tag{A.26}$$

- n^{th} twisted sector with $-\frac{1}{2} < nv_i \leqslant \frac{1}{2}$, the untwisted sector is given by $nv_i = 0$:

$$\begin{aligned} \mathrm{Tr} &= q^{\frac{1}{2}(nv_i)^2 - \frac{1}{24}} \prod_{m=1}^{\infty} \left[\left(1 + q^{m-\frac{1}{2}+nv_i}\right)\left(1 + q^{m-\frac{1}{2}-nv_i}\right) \right] \\ &= \frac{\vartheta\left[{nv_i \atop 0}\right]}{\eta}(t) \end{aligned} \tag{A.27}$$

Fermionic contributions, R sector, $\mathcal{O} = (-1)^F$

The bosonic contributions do not differ, if there is a $(-1)^F$ contained in $\mathcal{O}$, or not.

- untwisted sector: now the zero modes ‘contribute’ a factor of $(1-1)$:

$$\begin{aligned} \mathrm{Tr} &= q^{E_0^{\mathrm{R},i}} \left[\prod_{r_i>0}^{\infty} \sum_{N_{r_i}=0,1} (-1)^{N_{r_i}} q^{r_i N_{r_i}} \right] \left[\prod_{s_i>0}^{\infty} \sum_{N_{s_i}=0,1} (-1)^{N_{s_i}} q^{s_i N_{s_i}} \right] \\ &= (1-1) q^{\frac{1}{12}} \left(\prod_{m=1}^{\infty} (1-q^m) \right)^2 = \frac{\vartheta\left[{1/2 \atop 1/2}\right]}{\eta}(t) = 0 \end{aligned} \tag{A.28}$$

- n^{th} twisted sector with $0 < nv_i < 1$:

$$\begin{aligned} \mathrm{Tr} &= e^{\pi i (nv_i - \frac{1}{2})} q^{E_0^{\mathrm{R},i}} \left[\prod_{r_i>0}^{\infty} \sum_{N_{r_i}=0,1} (-1)^{N_{r_i}} q^{r_i N_{r_i}} \right] \left[\prod_{s_i>0}^{\infty} \sum_{N_{s_i}=0,1} (-1)^{N_{s_i}} q^{s_i N_{s_i}} \right] \\ &= e^{\pi i (nv_i - \frac{1}{2})} q^{\frac{1}{2} nv_i (nv_i - 1) + \frac{1}{12}} \prod_{m=1}^{\infty} \left[\left(1 - q^{m-1+nv_i}\right)\left(1 - q^{m-nv_i}\right) \right] \\ &= \frac{\vartheta\left[{1/2+nv_i \atop 1/2}\right]}{\eta}(t) \end{aligned} \tag{A.29}$$

Fermionic contributions, NS sector, $\mathcal{O} = (-1)^F$

$$\mathrm{Tr} = q^{E_0^{\mathrm{NS},i}} \left[\prod_{r_i>0}^{\infty} \sum_{N_{r_i}=0,1} (-1)^{N_{r_i}} q^{r_i N_{r_i}} \right] \left[\prod_{s_i>0}^{\infty} \sum_{N_{s_i}=0,1} (-1)^{N_{s_i}} q^{s_i N_{s_i}} \right] \tag{A.30}$$

- n^{th} twisted sector with $-\frac{1}{2} < nv_i \leqslant \frac{1}{2}$, the untwisted sector is given by $nv_i = 0$:

$$\begin{aligned}\mathrm{Tr} &= e^{\pi i n v_i} q^{\frac{1}{2}(nv_i)^2 - \frac{1}{24}} \prod_{m=1}^{\infty} \left[\left(1 - q^{m-\frac{1}{2}+nv_i}\right)\left(1 - q^{m-\frac{1}{2}-nv_i}\right) \right] \\ &= \frac{\vartheta\left[\substack{nv_i \\ 1/2}\right]}{\eta}(t)\end{aligned} \tag{A.31}$$

Bosonic contributions, $\mathcal{O} = \Theta^k$

For the noncompact directions, one obtains the same results as for $\mathcal{O} = \mathbb{I}$, since Θ^k only acts on the compact directions.

- untwisted sector:

$$\begin{aligned}\mathrm{Tr} &= e^{\pi i k v_i} q^{E_0^i} \left[\prod_{m_i>0}^{\infty} \sum_{N_{m_i}=0}^{\infty} e^{2\pi i k v_i N_{m_i}} q^{m_i N_{m_i}} \right] \left[\prod_{l_i>0}^{\infty} \sum_{N_{l_i}=0}^{\infty} e^{-2\pi i k v_i N_{l_i}} q^{l_i N_{l_i}} \right] \\ &= e^{\pi i k v_i} q^{-\frac{1}{12}} \prod_{m=1}^{\infty} \left[\left(1 - e^{2\pi i k v_i} q^m\right)\left(1 - e^{-2\pi i k v_i} q^m\right) \right]^{-1} \\ &= -2\sin(\pi k v_i) e^{\pi i k v_i} \left(\frac{\vartheta\left[\substack{1/2 \\ 1/2+kv_i}\right]}{\eta}(t) \right)^{-1}\end{aligned} \tag{A.32}$$

- n^{th} twisted sector with $0 < nv_i < 1$:

$$\begin{aligned}\mathrm{Tr} &= e^{\pi i k v_i(1-2nv_i)} q^{E_0^i} \left[\prod_{m_i>0}^{\infty} \sum_{N_{m_i}=0}^{\infty} e^{2\pi i k v_i N_{m_i}} q^{m_i N_{m_i}} \right] \left[\prod_{m_i>0}^{\infty} \sum_{N_{l_i}=0}^{\infty} e^{-2\pi i k v_i N_{l_i}} q^{l_i N_{l_i}} \right] \\ &= e^{\pi i k v_i(1-2nv_i)} q^{-\frac{1}{2}nv_i(nv_i-1)-\frac{1}{12}} \prod_{m=1}^{\infty} \left[\left(1 - e^{2\pi i k v_i} q^{m-1+nv_i}\right)\left(1 - e^{-2\pi i k v_i} q^{m-nv_i}\right) \right]^{-1} \\ &= e^{\pi i (nv_i - \frac{1}{2})} \left(\frac{\vartheta\left[\substack{1/2+nv_i \\ 1/2+kv_i}\right]}{\eta}(t) \right)^{-1}\end{aligned} \tag{A.33}$$

Fermionic contributions, R sector, $\mathcal{O} = \Theta^k$

- n^{th} twisted sector with $0 \leqslant nv_i < 1$, the untwisted sector is given by $nv_i = 0$:

$$\begin{aligned}
\mathrm{Tr} &= e^{2\pi i k v_i (nv_i - \frac{1}{2})} q^{E_0^{\mathrm{R},i}} \left[\prod_{r_i > 0}^{\infty} \sum_{N_{r_i}=0,1} e^{2\pi i k v_i N_{r_i}} q^{r_i N_{r_i}} \right] \left[\prod_{s_i > 0}^{\infty} \sum_{N_{s_i}=0,1} e^{-2\pi i k v_i N_{s_i}} q^{s_i N_{s_i}} \right] \\
&= e^{2\pi i k v_i (nv_i - \frac{1}{2})} q^{\frac{1}{2} nv_i (nv_i - 1) + \frac{1}{12}} \prod_{m=1}^{\infty} \left[\left(1 + e^{2\pi i k v_i} q^{2(m-1+nv_i)}\right) \left(1 + e^{-2\pi i k v_i} q^{m - nv_i}\right) \right] \\
&= \frac{\vartheta \left[{1/2 + nv_i \atop kv_i} \right]}{\eta} (t)
\end{aligned} \tag{A.34}$$

Fermionic contributions, NS sector, $\mathcal{O} = \Theta^k$

- n^{th} twisted sector with $-\frac{1}{2} < nv_i \leqslant \frac{1}{2}$, the untwisted sector is given by $nv_i = 0$:

$$\begin{aligned}
\mathrm{Tr} &= e^{2\pi i k v_i n v_i} q^{E_0^{\mathrm{NS},i}} \left[\prod_{r_i > 0}^{\infty} \sum_{N_{r_i}=0,1} e^{2\pi i k v_i N_{r_i}} q^{r_i N_{r_i}} \right] \left[\prod_{s_i > 0}^{\infty} \sum_{N_{s_i}=0,1} e^{-2\pi i k v_i N_{s_i}} q^{s_i N_{s_i}} \right] \\
&= e^{2\pi i k v_i n v_i} q^{\frac{1}{2}(nv_i)^2 - \frac{1}{24}} \prod_{m=1}^{\infty} \left[\left(1 + e^{2\pi i k v_i} q^{m - \frac{1}{2} + nv_i}\right) \left(1 + e^{-2\pi i k v_i} q^{m - \frac{1}{2} - nv_i}\right) \right] \\
&= \frac{\vartheta \left[{nv_i \atop kv_i} \right]}{\eta} (t)
\end{aligned} \tag{A.35}$$

Fermionic contributions, R sector, $\mathcal{O} = (-1)^F \Theta^k$

The bosonic contributions do not differ, if there is a $(-1)^F$ contained in $\mathcal{O}$, or not. For the noncompact directions, one obtains the same results as for $\mathcal{O} = (-1)^F$, since Θ^k only acts on the compact directions.

- n^{th} twisted sector with $0 \leqslant nv_i < 1$, the untwisted sector is given by

$nv_i = 0$:

$$
\begin{aligned}
\mathrm{Tr} &= e^{2\pi i(\frac{1}{2}+kv_i)(nv_i-\frac{1}{2})} q^{E_0^{\mathrm{R},i}} \left[\prod_{r_i>0}^{\infty} \sum_{N_{r_i}=0,1} (-1)^{N_{r_i}} e^{2\pi i k v_i N_{r_i}} q^{r_i N_{r_i}}\right] \\
&\qquad \left[\prod_{s_i>0}^{\infty} \sum_{N_{s_i}=0,1} (-1)^{N_{s_i}} e^{-2\pi i k v_i N_{s_i}} q^{s_i N_{s_i}}\right] \\
&= e^{2\pi i(\frac{1}{2}+kv_i)(nv_i-\frac{1}{2})} q^{\frac{1}{2}nv_i(nv_i-1)+\frac{1}{12}} \prod_{m=1}^{\infty} \left[\left(1-e^{2\pi i k v_i} q^{m-1+nv_i}\right)\left(1-e^{-2\pi i k v_i} q^{m-nv_i}\right)\right] \\
&= \frac{\vartheta\left[\begin{smallmatrix}1/2+nv_i\\ 1/2+kv_i\end{smallmatrix}\right]}{\eta}(t)
\end{aligned}
\tag{A.36}
$$

Fermionic contributions, NS sector, $\mathcal{O} = (-1)^F \Theta^k$

- n^{th} twisted sector with $-\frac{1}{2} < nv_i \leqslant \frac{1}{2}$, the untwisted sector is given by $nv_i = 0$:

$$
\begin{aligned}
\mathrm{Tr} &= e^{2\pi i(\frac{1}{2}+kv_i)nv_i} q^{E_0^{\mathrm{NS},i}} \left[\prod_{r_i>0}^{\infty} \sum_{N_{r_i}=0,1} (-1)^{N_{r_i}} e^{2\pi i k v_i N_{r_i}} q^{r_i N_{r_i}}\right] \\
&\qquad \left[\prod_{s_i>0}^{\infty} (-1)^{N_{s_i}} \sum_{N_{s_i}=0,1} e^{-2\pi i k v_i N_{s_i}} q^{s_i N_{s_i}}\right] \\
&= e^{2\pi i(\frac{1}{2}+kv_i)nv_i} q^{\frac{1}{2}(nv_i)^2-\frac{1}{24}} \prod_{m=1}^{\infty} \left[\left(1-e^{2\pi i k v_i} q^{m-\frac{1}{2}+nv_i}\right)\left(1-e^{-2\pi i k v_i} q^{m-\frac{1}{2}-nv_i}\right)\right] \\
&= \frac{\vartheta\left[\begin{smallmatrix}nv_i\\ 1/2+kv_i\end{smallmatrix}\right]}{\eta}(t)
\end{aligned}
\tag{A.37}
$$

Appendix B

Computation of tree channel diagrams

In this appendix we will give some details of the computation of the diagrams shown in figure 2.2 in the tree channel. Therefore we have to give a short introduction into the construction of crosscap states, which correspond to the O-planes, and boundary states, which correspond to the D-branes. A comprehensive introduction into the boundary state approach to D-branes is given in [42] and references therein. Appendix A of [8] contains the construction of crosscap states in related models.

B.1 Construction of crosscap states

We denote the crosscap state which corresponds to the orientifold plane invariant under the action of $\Omega\mathcal{R}\Theta^k$ by $|\Omega\mathcal{R}\Theta^k\rangle$. This state has to fulfill

$$X\,|\Omega\mathcal{R}\Theta^k\rangle = \Omega\mathcal{R}\Theta^k\, X\,|\Omega\mathcal{R}\Theta^k\rangle\,, \tag{B.1}$$

where X here can be a non-compact or compact coordinate. Applying world-sheet parity Ω and distinguishing between the non-compact and the compact coordinates, we obtain the equations

$$\left[X^\mu_{L,R}(\sigma,0) - X^\mu_{R,L}(\sigma+\pi,0)\right]|\Omega\mathcal{R}\Theta^k\rangle = 0 \tag{B.2}$$

$$\left[Z^i_{L,R}(\sigma,0) - \Theta^k\mathcal{R}Z^i_{R,L}(\sigma+\pi,0)\right]|\Omega\mathcal{R}\Theta^k\rangle = 0 \tag{B.3}$$

Oscillator contributions

Inserting the mode expansion

$$\begin{aligned} Z^i(\sigma,\tau) = z^i &+ \frac{p^i_L}{2\pi}(\tau+\sigma) + \frac{p^i_R}{2\pi}(\tau-\sigma) \\ &+ \frac{i}{2}\sum_{m\in\mathbb{Z}+k/N}\frac{1}{m}\alpha^i_m e^{-im(\tau+\sigma)} + \frac{i}{2}\sum_{l\in\mathbb{Z}-k/N}\frac{1}{l}\tilde{\alpha}^i_l e^{-il(\tau-\sigma)}\,, \end{aligned} \tag{B.4}$$

(remember (2.12)), the analogous mode expansions for $Z^{\bar{i}}$ and the non-compact coordinates, we obtain the following constraints in terms of bosonic oscillators

$$\begin{aligned}(\alpha^{\mu}_{m} + (-1)^{m}\tilde{\alpha}^{\mu}_{-m})|\Omega\mathcal{R}\Theta^{k}\rangle &= 0\,,\\ (\alpha^{i}_{m} + (-1)^{m}e^{2\pi i k v_i}\tilde{\alpha}^{\bar{i}}_{-m})|\Omega\mathcal{R}\Theta^{k}\rangle &= 0\,,\\ (\alpha^{\bar{i}}_{m} + (-1)^{m}e^{-2\pi i k v_i}\tilde{\alpha}^{i}_{-m})|\Omega\mathcal{R}\Theta^{k}\rangle &= 0\,,\end{aligned} \tag{B.5}$$

together with the fact that m has to be integer (i.e. no twisted crosscap states appear in the tree channel, as expected). In the case of the fermions one obtains similar equations

$$\begin{aligned}(\psi^{\mu}_{r} + i\eta e^{-i\pi r}\tilde{\psi}^{\mu}_{-r})|\Omega\mathcal{R}\Theta^{k},\eta\rangle &= 0\,,\\ (\psi^{i}_{r} + i\eta e^{-i\pi r}e^{2\pi i k v_i}\tilde{\psi}^{\bar{i}}_{-r})|\Omega\mathcal{R}\Theta^{k},\eta\rangle &= 0\,,\\ (\psi^{\bar{i}}_{r} + i\eta e^{-i\pi r}e^{-2\pi i k v_i}\tilde{\psi}^{i}_{-r})|\Omega\mathcal{R}\Theta^{k},\eta\rangle &= 0\,,\end{aligned} \tag{B.6}$$

where ($\eta = \pm 1$) is the usual spin-structure and r has to be (half) integer in the R (NS) sector.

Recalling (A.15), we find as an ansatz for the bosons[1]

$$\begin{aligned}e^{\frac{c_m}{m}\alpha_{-m}\tilde{\alpha}_{-m}}|0\rangle &= \sum_{N=0}^{\infty} c_m^N \frac{1}{N!m^N}(\alpha_{-m}\tilde{\alpha}_{-m})^N|0\rangle\\ &= \sum_{N=0}^{\infty} c_m^N|0,m,N\rangle\end{aligned} \tag{B.7}$$

and for the fermions

$$\begin{aligned}e^{i\eta d_r\psi_{-r}\tilde{\psi}_{-r}}|0,\eta\rangle &= (1 + i\eta d_r\psi_{-r}\tilde{\psi}_{-r})|0,\eta\rangle\\ &= |0,\eta\rangle + i\eta d_r|0,r,\eta\rangle\,,\end{aligned} \tag{B.8}$$

(where $|0,r,\eta\rangle \equiv \psi_{-r}\tilde{\psi}_{-r})|0,\eta\rangle$) which implies e.g. in the compact directions

$$\left(\alpha^{i}_{m} - c_m\tilde{\alpha}^{\bar{i}}_{-m}\right) e^{\frac{c_m}{m}\alpha^{\bar{i}}_{-m}\tilde{\alpha}^{\bar{i}}_{-m}}|0\rangle = 0 \tag{B.9}$$

for the bosons and

$$\left(\psi^{i}_{r} - i\eta d_r\tilde{\psi}^{\bar{i}}_{-r}\right) e^{i\eta d_r\psi^{\bar{i}}_{-r}\tilde{\psi}^{\bar{i}}_{-r}}|0,\eta\rangle = 0 \tag{B.10}$$

for the fermions and thus leads to the solution

$$\begin{aligned}|\Omega\mathcal{R}\Theta^{k},\eta\rangle = \mathcal{N}_C \exp\Big\{&-\sum_m \frac{(-1)^m}{m}\alpha^{\mu}_{-m}\tilde{\alpha}^{\mu}_{-m} - \sum_m \frac{(-1)^m}{m}e^{-2\pi i k v_i}\alpha^{i}_{-m}\tilde{\alpha}^{i}_{-m}\\ &-\sum_m \frac{(-1)^m}{m}e^{2\pi i k v_i}\alpha^{\bar{i}}_{-m}\tilde{\alpha}^{\bar{i}}_{-m} - i\eta\sum_r e^{-i\pi r}\psi^{\mu}_{-r}\tilde{\psi}^{\mu}_{-r}\\ &- i\eta\sum_r e^{-i\pi r}e^{-2\pi i k v_i}\psi^{i}_{-r}\tilde{\psi}^{i}_{-r} - i\eta\sum_r e^{-i\pi r}e^{2\pi i k v_i}\psi^{\bar{i}}_{-r}\tilde{\psi}^{\bar{i}}_{-r}\Big\}|\Omega\mathcal{R}\Theta^{k},\eta\rangle^{(0)}\,,\end{aligned} \tag{B.11}$$

[1] The '0' in the following kets denotes the vacuum, which will be specified later.

where $r \in \mathbb{Z}(\mathbb{Z}+\frac{1}{2})$ in the RR (NSNS) sector and $\mathcal{N}_C$ is some numerical constant to be determined. $|\Omega\mathcal{R}\Theta^k, \eta\rangle^{(0)}$ denotes the ground states[2], which we will discuss in the following. Actually, η appears in the ground state only if the ground state is spinorial. Since only untwisted states propagate in the tree channel in our models, degenerate ground states appear in the RR sector only.

Now we have everything we need to determine the GSO-projection, where the projector is given by

$$\frac{1}{4}\left(1+(-1)^{F_L}\right)\left(1+(-1)^{F_R}\right) . \tag{B.12}$$

We start with the NSNS sector, where the ground state has eigenvalue -1 under both $(-1)^{F_L}$ and $(-1)^{F_R}$. Thus, the NSNS sector of the crosscap state (B.11) behaves like

$$(-1)^{F_{L,R}}|\Omega\mathcal{R}\Theta^k, \eta\rangle_{\mathrm{NSNS}} = -|\Omega\mathcal{R}\Theta^k, -\eta\rangle_{\mathrm{NSNS}} \tag{B.13}$$

Expanding the exponential in (B.11), one easily sees that the sign of η flips under the action of $(-1)^{F_L}$ and $(-1)^{F_R}$. Thus, we find the GSO invariant NSNS crosscap state

$$|\Omega\mathcal{R}\Theta^k\rangle_{\mathrm{NSNS}} = |\Omega\mathcal{R}\Theta^k, +\rangle_{\mathrm{NSNS}} - |\Omega\mathcal{R}\Theta^k, -\rangle_{\mathrm{NSNS}} . \tag{B.14}$$

In the RR sector, we have to take into account the degeneracy of the ground states. On these ground states, the GSO operators take the form

$$\begin{aligned}(-1)^{F_L} &= \prod_{\mu=2}^{9} \sqrt{2}\psi_0^\mu \\ (-1)^{F_R} &= \prod_{\mu=2}^{9} \sqrt{2}\tilde{\psi}_0^\mu .\end{aligned} \tag{B.15}$$

In order to make a link to the conditions (B.6) for the fermionic zero modes, we define

$$\psi_\eta^\mu = \frac{1}{\sqrt{2}}\left(\psi_0^\mu + i\eta\tilde{\psi}_0^\mu\right) \tag{B.16}$$

for the noncompact directions and

$$\begin{aligned}\psi_\eta^{i,k} &= \frac{1}{\sqrt{2}}\left(\psi_0^i + i\eta e^{2\pi i k v_i}\tilde{\psi}_0^{\bar{i}}\right) \\ \psi_\eta^{\bar{i},k} &= \frac{1}{\sqrt{2}}\left(\psi_0^{\bar{i}} + i\eta e^{-2\pi i k v_i}\tilde{\psi}_0^{i}\right)\end{aligned} \tag{B.17}$$

[2]Correctly speaking, $|\Omega\mathcal{R}\Theta^k, \eta\rangle^{(0)}$ in addition contains the momenta, but these will be treated separately.

for the compact directions. Now, expressing (B.15) in terms of (B.16) and (B.17), the conditions (B.6) for the zero modes yield

$$(-1)^{F_{L,R}}|\Omega\mathcal{R}\Theta^k,\eta\rangle^{(0)}_{\mathrm{RR}} = -i\eta|\Omega\mathcal{R}\Theta^k,-\eta\rangle^{(0)}_{\mathrm{RR}} \tag{B.18}$$

for the degenerate ground states, which directly translates to the crosscap states and thus leads to the GSO invariant RR crosscap state

$$|\Omega\mathcal{R}\Theta^k\rangle_{\mathrm{RR}} = |\Omega\mathcal{R}\Theta^k,+\rangle_{\mathrm{RR}} + i|\Omega\mathcal{R}\Theta^k,-\rangle_{\mathrm{RR}}\,. \tag{B.19}$$

The NSNS and RR crosscap state combine

$$|\Omega\mathcal{R}\Theta^k\rangle = |\Omega\mathcal{R}\Theta^k\rangle_{\mathrm{NSNS}} + |\Omega\mathcal{R}\Theta^k\rangle_{\mathrm{RR}}\,. \tag{B.20}$$

In our conventions, the plus sign corresponds to a crosscap which cancels the RR charge of a D-brane, whereas a minus sign corresponds to a crosscap which cancels the RR charge of an anti-D-brane.

The total crosscap state has to be invariant w.r.t. the orbifold group (i.e. it contains the 'complete projector') and is simply given by

$$|C\rangle = \sum_{k=0}^{N-1} |\Omega\mathcal{R}\Theta^k\rangle\,. \tag{B.21}$$

Momenta

From (B.1) we also obtain

$$\left(z^i - e^{2\pi i k v_i}[z^{\bar{i}} + \frac{1}{2}(p_L^{\bar{i}} - p_R^{\bar{i}})]\right)|\Omega\mathcal{R}\Theta^k\rangle = 0 \tag{B.22}$$

by inserting the mode expansion (B.4). From this we can read off that the crosscap state $|\Omega\mathcal{R}\Theta^k\rangle$ is confined to a line on T_i which is tilted by the angle $-\pi k v_i$ w.r.t. the real axis, as is also explained in the text.

Finally, conditions on the momenta arise:

$$\begin{aligned} p^\mu|\Omega\mathcal{R}\Theta^k\rangle &= 0 \\ (p_L^i + e^{2\pi i k v_i}p_R^{\bar{i}})|\Omega\mathcal{R}\Theta^k\rangle &= 0 \\ (p_R^i + e^{2\pi i k v_i}p_L^{\bar{i}})|\Omega\mathcal{R}\Theta^k\rangle &= 0\,. \end{aligned} \tag{B.23}$$

Inserting $p_{L,R} = P \pm W$ for the compact momenta, (B.23) indicates that on each T_i, there are Kaluza-Klein momenta perpendicular and windings parallel to the position of the crosscap state. This is just the opposite of what happens in the loop channel, as expected.

B.2 Construction of boundary states

The construction of the boundary states for the D-branes is similar to the construction of the crosscap states in the previous section. Now, the defining conditions are given by the boundary conditions (2.8), where now the role of τ and σ is interchanged with respect to the loop channel. For details of the construction, see [42].

Similarly to a crosscap state, the boundary state for a D-brane at angle $-\pi k v_i$ on T_i with respect to the horizontal axis is given by

$$\begin{aligned} |\Theta^k, \eta\rangle = \mathcal{N}_B \exp\Big\{ & -\sum_m \frac{1}{m} \alpha^\mu_{-m} \tilde{\alpha}^\mu_{-m} - \sum_m \frac{1}{m} e^{-2\pi i k v_i} \alpha^i_{-m} \tilde{\alpha}^i_{-m} \\ & - \sum_m \frac{1}{m} e^{2\pi i k v_i} \alpha^{\bar{i}}_{-m} \tilde{\alpha}^{\bar{i}}_{-m} - i\eta \sum_r \psi^\mu_{-r} \tilde{\psi}^\mu_{-r} \\ & - i\eta \sum_r e^{-2\pi i k v_i} \psi^i_{-r} \tilde{\psi}^i_{-r} - i\eta \sum_r e^{2\pi i k v_i} \psi^{\bar{i}}_{-r} \tilde{\psi}^{\bar{i}}_{-r} \Big\} |\Theta^k, \eta\rangle^{(0)} \end{aligned} \tag{B.24}$$

Using the analogous equations to (B.14), (B.19) and (B.20), the GSO-invariant boundary state is given by

$$|B\rangle = \sum_{k=0}^{N-1} |\Theta^k\rangle. \tag{B.25}$$

Discrete momenta again exist in the compact directions perpendicular to the position of the boundary state while windings are parallel.

B.3 Tree channel amplitudes

Using equation (B.21) and (B.25), the tree channel amplitudes read

$$\begin{aligned} \tilde{\mathcal{K}} &= \int_0^\infty dl \langle C| e^{-2\pi l (H_L + H_R)} |C\rangle \\ \tilde{\mathcal{A}} &= \int_0^\infty dl \langle B| e^{-2\pi l (H_L + H_R)} |B\rangle \\ \tilde{\mathcal{M}} &= \int_0^\infty dl \left(\langle C| e^{-2\pi l (H_L + H_R)} |B\rangle + h.c. \right) \end{aligned} \tag{B.26}$$

Again we give some details of the calculation of the oscillator contributions to the various tree channel amplitudes.

The oscillator contributions to the Klein bottle tree channel amplitude consist of

$$\begin{aligned}&\langle \Omega\mathcal{R}\Theta^k,\eta|e^{-2\pi l(H_L+H_R)}|\Omega\mathcal{R}\Theta^{k'},\eta'\rangle = \\ &\mathcal{N}_C^2\prod_\mu\prod_r\left(1+\eta\eta' q^{2r}\right)\prod_i\left(1+\eta\eta' e^{2\pi i(k'-k)v_i}q^{2r}\right)\left(1+\eta\eta' e^{-2\pi i(k'-k)v_i}q^{2r}\right)\times \\ &\left[\prod_\mu\prod_m\left(1-\eta\eta' q^{2m}\right)\prod_i\left(1-\eta\eta' e^{2\pi i(k'-k)v_i}q^{2m}\right)\left(1-\eta\eta' e^{-2\pi i(k'-k)v_i}q^{2m}\right)\right]^{-1},\end{aligned} \tag{B.27}$$

with $q = e^{-2\pi l}$ and $r \in \mathbb{Z}(+1/2)$ for the RR (NSNS) exchange. Thus, the RR exchange for $\eta = \eta'$ expressed in theta- and eta-functions reads

$$\begin{aligned}&\langle \Omega\mathcal{R}\Theta^k,\eta|e^{-2\pi l(H_L+H_R)}|\Omega\mathcal{R}\Theta^{k'},\eta\rangle_{\mathrm{RR}} = \mathcal{N}_C^2\left(\frac{\vartheta\left[{1/2 \atop 0}\right]}{\eta^3}\right)^{(d-2)/2}\times \\ &\prod_{(k'-k)v_i\notin\mathbb{Z}}\left[-2\sin\left(\pi(k'-k)v_i\right)\right]e^{\pi i(k'-k)v_i}\frac{\vartheta\left[{1/2 \atop (k'-k)v_i}\right]}{\vartheta\left[{1/2 \atop 1/2+(k'-k)v_i}\right]}\prod_{(k'-k)v_i\in\mathbb{Z}}\frac{\vartheta\left[{1/2 \atop 0}\right]}{\eta^3},\end{aligned} \tag{B.28}$$

where the argument of the theta- and eta-functions is $2l$ and d is the number of non-compact dimensions. Note, that the numbers arising from the factor in square brackets, if one takes the crosscap states corresponding to the various elements of the orbifold group to be equally weighted, as we did in (B.21), exactly lead to the prefactors

$$\prod_{kv_i\notin\mathbb{Z}}\left[-2\sin\left(\pi k v_i\right)\right] \tag{B.29}$$

which appear in the various tree channel amplitudes and thus reflect the insertion of the complete projector. For $\eta \neq \eta'$, the result formally is given by

$$\begin{aligned}&\langle \Omega\mathcal{R}\Theta^k,\eta|e^{-2\pi l(H_L+H_R)}|\Omega\mathcal{R}\Theta^{k'},-\eta\rangle_{\mathrm{RR}} = \mathcal{N}_C^2\left(\frac{\vartheta\left[{1/2 \atop 1/2}\right]}{\eta^3}\right)^{(d-2)/2}\times \\ &\prod_{(k'-k)v_i\notin\mathbb{Z}}\left[-2\sin\left(\pi(k'-k)v_i\right)\right]e^{\pi i(k'-k)v_i}\frac{\vartheta\left[{1/2 \atop 1/2+(k'-k)v_i}\right]}{\vartheta\left[{1/2 \atop 1/2+(k'-k)v_i}\right]}\prod_{(k'-k)v_i\in\mathbb{Z}}\frac{\vartheta\left[{1/2 \atop 1/2}\right]}{\eta^3},\end{aligned} \tag{B.30}$$

which always vanishes.

The calculation of the overlap of two boundary states in the case of the annulus and of a crosscap with a boundary state in the case of the Möbius strip is similar to the calculation above. For the Möbius strip the argument of the theta- and eta functions again is shifted to be $2l + i/2$.

Appendix C

The remaining six dimensional $\Omega\mathcal{R} \times \mathbb{Z}_N$ orientifolds

In this appendix we show the detailed calculations and results for the cases $\mathbb{Z}_{3,4,6}$ for completeness, which were already presented in [20, 7] in some detail.

C.1 $\mathbb{Z}_3$

Now the torus lattices T_1 and T_2 have to be invariant with respect to $\mathcal{R}$ and the orbifold group $\mathbb{Z}_3$. The two possible orientations, again labelled by **A** and **B**, are shown in figure C.1.

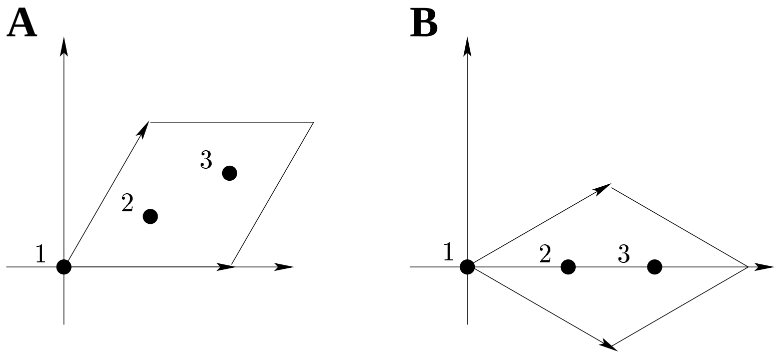

Figure C.1: Lattices for $\mathbb{Z}_3$. Black circles denote the fixed points which are labelled by $1, 2, 3$.

The amplitudes and tadpole cancellation

The Klein bottle 1-loop amplitude (2.22) now is given by

$$\mathcal{K} = \frac{2c}{3}(1_{\mathrm{RR}} - 1_{\mathrm{NSNS}}) \int_0^\infty \frac{dt}{t^4} \mathrm{Tr}_{\mathrm{NSNS}} \left(\Omega\mathcal{R} \left(1 + \Theta + \Theta^2\right) (-1)^F e^{-2\pi t (H_L + H_R)} \right) . \tag{C.1}$$

The basis vectors of the $SU(3)$ lattices in figure C.1 are

$$\vec{e_1}^{\mathbf{A}} = \begin{pmatrix} \sqrt{2} \\ 0 \end{pmatrix}, \qquad \vec{e_2}^{\mathbf{A}} = \begin{pmatrix} 1/\sqrt{2} \\ \sqrt{3/2} \end{pmatrix}, \tag{C.2}$$

$$\vec{e_1}^{\mathbf{B}} = \begin{pmatrix} \sqrt{3/2} \\ -1/\sqrt{2} \end{pmatrix}, \qquad \vec{e_2}^{\mathbf{B}} = \begin{pmatrix} \sqrt{3/2} \\ 1/\sqrt{2} \end{pmatrix}, \tag{C.3}$$

which yield the $\Omega\mathcal{R}$ invariant KK and winding momenta

$$P^{\mathbf{A}} = \frac{2m}{r} \begin{pmatrix} 1 \\ 0 \end{pmatrix}, \qquad W^{\mathbf{A}} = \frac{\sqrt{3}nr}{\alpha'} \begin{pmatrix} 0 \\ 1 \end{pmatrix}, \tag{C.4}$$

$$P^{\mathbf{B}} = \frac{2m}{\sqrt{3}r} \begin{pmatrix} 1 \\ 0 \end{pmatrix}, \qquad W^{\mathbf{B}} = \frac{nr}{\alpha'} \begin{pmatrix} 0 \\ 1 \end{pmatrix}, \tag{C.5}$$

and thus we obtain the lattice contributions $\mathcal{L}_i^{\mathcal{K}} = \mathcal{L}[4,3](t)$ for an $\mathbf{A}$ type torus and $\mathcal{L}_i^{\mathcal{K}} = \mathcal{L}[4/3,1](t)$ for a $\mathbf{B}$ type torus T_i in the untwisted sectors of the Klein bottle 1-loop amplitude.

As in the case of $\mathbb{Z}_2$, the lattice contributions to (C.1) are independent of the insertion from the orbifold group. Using the results of appendix A, we find

$$\begin{aligned} \mathcal{K} = 2c(1_{\mathrm{RR}} - 1_{\mathrm{NSNS}}) \int_0^\infty \frac{dt}{t^4} \frac{\vartheta\left[\begin{smallmatrix} 0 \\ 1/2 \end{smallmatrix}\right]^2}{\eta^6} \times \\ \left\{ \mathcal{L}_1^{\mathcal{K}} \mathcal{L}_2^{\mathcal{K}} \frac{\vartheta\left[\begin{smallmatrix} 0 \\ 1/2 \end{smallmatrix}\right]^2}{\eta^6} + \chi_{\mathcal{K}} \frac{\vartheta\left[\begin{smallmatrix} 1/3 \\ 1/2 \end{smallmatrix}\right] \vartheta\left[\begin{smallmatrix} -1/3 \\ 1/2 \end{smallmatrix}\right]}{\vartheta\left[\begin{smallmatrix} 5/6 \\ 1/2 \end{smallmatrix}\right] \vartheta\left[\begin{smallmatrix} 1/6 \\ 1/2 \end{smallmatrix}\right]} + \chi_{\mathcal{K}} \frac{\vartheta\left[\begin{smallmatrix} 2/3 \\ 1/2 \end{smallmatrix}\right] \vartheta\left[\begin{smallmatrix} -2/3 \\ 1/2 \end{smallmatrix}\right]}{\vartheta\left[\begin{smallmatrix} 7/6 \\ 1/2 \end{smallmatrix}\right] \vartheta\left[\begin{smallmatrix} -1/6 \\ 1/2 \end{smallmatrix}\right]} \right\}, \end{aligned} \tag{C.6}$$

with $2t$ as the argument of the theta and eta functions. Note, that the contributions to the Θ and Θ^2 twisted sectors are identical, as a consequence of $\Theta^2 = \Theta^{-1}$. $\chi_{\mathcal{K}}$ again denotes the multiplicity of $\mathbb{Z}_3$ fixed points which are invariant under $\Omega\mathcal{R}$. In the case of an $\mathbf{A}$ type torus, the fixed point 1 is invariant, whereas 2 and 3 get interchanged, consider figure C.1. In the case of a $\mathbf{B}$ type torus, all three fixed points are invariant. This yields

$$\chi_{\mathcal{K}} = \begin{cases} 1 & (\mathbf{AA}) \\ 3 & (\mathbf{AB}) \\ 9 & (\mathbf{BB}) \end{cases} \tag{C.7}$$

In contrast to the $\mathbb{Z}_2$ model, the contributions from the twisted sectors do not vanish.

To cancel the tadpoles from the Klein bottle, we again introduce D7-branes rotated by half the angles which are given by the elements of the orbifold group, see figure C.2.

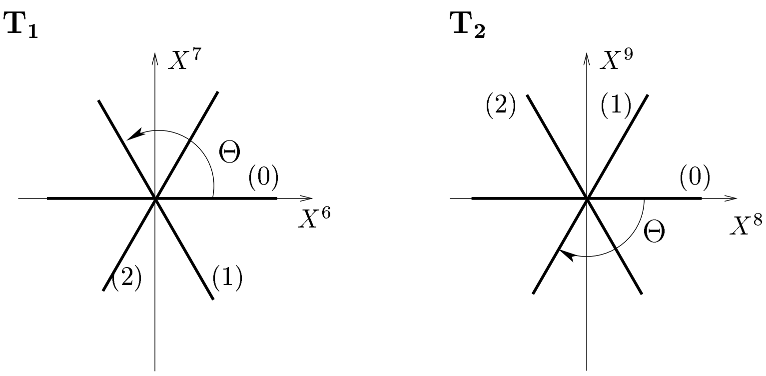

Figure C.2: Location of D7-branes in the case of $\mathbb{Z}_3$. The D-branes are labelled by (0), (1), (2).

In the case of $\mathbb{Z}_3$, the annulus amplitude (2.23) reads

$$\mathcal{A} = \frac{c}{12}(1_{\mathrm{RR}} - 1_{\mathrm{NSNS}}) \int_0^\infty \frac{dt}{t^4} \mathrm{Tr}_{\mathrm{NS}} \left(\left(1 + \Theta + \Theta^2\right)(-1)^F e^{-2\pi t H} \right) . \tag{C.8}$$

Remember, that for the open string the compact momenta p are given by the distance of parallel branes. Figure C.3 shows the location of the D7-branes in the fundamental cells for the two possible lattices. We obtain $p^{\mathbf{A},\mathbf{B}} = \frac{1}{2}P^{\mathbf{A},\mathbf{B}}$ for the

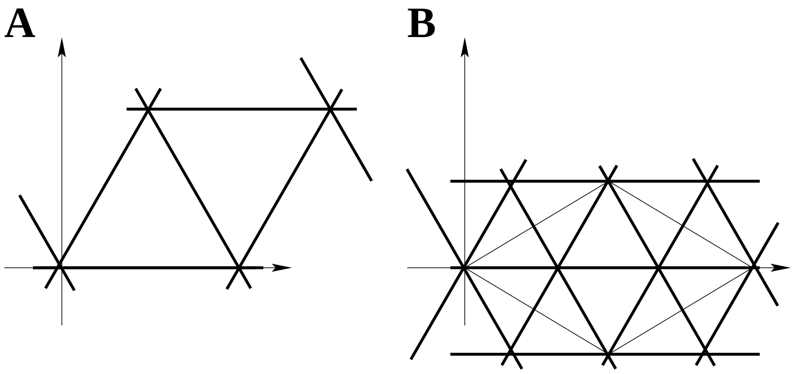

Figure C.3: Location of D-branes in the fundamental cells for $\mathbb{Z}_3$

directions 6 and 8 and $p^{\mathbf{A},\mathbf{B}} = \frac{1}{2}W^{\mathbf{A},\mathbf{B}}$ for the directions 7 and 9. These yield the lattice contributions $\mathcal{L}_i^{\mathcal{A}} = \mathcal{L}[2, 3/2](t)$ for an **A** torus and $\mathcal{L}_i^{\mathcal{A}} = \mathcal{L}[2/3, 1/2](t)$ for a **B** torus.

Now we can calculate the annulus 1-loop amplitude, again using appendix A. The terms with insertions of Θ and Θ^2 do not contribute to the amplitude, since these insertions do not leave the D-branes invariant. This means, that in the case of $\mathbb{Z}_3$ we do not have any twisted sector tadpole cancellation conditions. In other words, if there is an insertion from the orbifold group which squares to the identity, we obtain twisted sector tadpole cancellation conditions displayed in (2.48). For $\mathbb{Z}_{2,4,6}$ this is the case, for $\mathbb{Z}_3$ not. As before, we perform the calculation for strings starting on brane (0) and include an overall factor of three in the end. We obtain

$$\mathcal{A} = \frac{c}{4} M^2 (1_{\mathrm{RR}} - 1_{\mathrm{NSNS}}) \int_0^\infty \frac{dt}{t^4} \frac{\vartheta\left[{0 \atop 1/2}\right]^2}{\eta^6} \times \left\{ \mathcal{L}_1^{\mathcal{A}} \mathcal{L}_2^{\mathcal{A}} \frac{\vartheta\left[{0 \atop 1/2}\right]^2}{\eta^6} + \chi_{\mathcal{A}} \frac{\vartheta\left[{1/3 \atop 1/2}\right] \vartheta\left[{-1/3 \atop 1/2}\right]}{\vartheta\left[{5/6 \atop 1/2}\right] \vartheta\left[{1/6 \atop 1/2}\right]} + \chi_{\mathcal{A}} \frac{\vartheta\left[{2/3 \atop 1/2}\right] \vartheta\left[{-2/3 \atop 1/2}\right]}{\vartheta\left[{7/6 \atop 1/2}\right] \vartheta\left[{-1/6 \atop 1/2}\right]} \right\}, \tag{C.9}$$

with

$$\chi_{\mathcal{A}} = \begin{cases} 1 & (\mathbf{AA}) \\ 3 & (\mathbf{AB}) \\ 9 & (\mathbf{BB}) \end{cases}, \tag{C.10}$$

which one can read off from figure C.3 and t as the argument of the theta- and eta-functions.

The Möbius strip 1-loop amplitude now is given by

$$\mathcal{M} = -\frac{c}{12} (1_{\mathrm{RR}} - 1_{\mathrm{NSNS}}) \int_0^\infty \frac{dt}{t^4} \mathrm{Tr}_{\mathrm{R}} \left(\Omega \mathcal{R} \left(1 + \Theta + \Theta^2 \right) e^{-2\pi t H} \right). \tag{C.11}$$

As one can see in figure C.3, the compact momenta have to be doubled in the 7,9 directions for both types of tori, now. This leads to $\mathcal{L}_i^{\mathcal{M}} = \mathcal{L}[2,6]$ for an $\mathbf{A}$ type torus but $\mathcal{L}_i^{\mathcal{M}} = \mathcal{L}[2/3, 2]$ for a $\mathbf{B}$ type torus.

To find out which strings contribute to the Möbius strip 1-loop amplitude, consider 2.52. For the strings starting on brane (0) this means, that in the untwisted sector the term without insertion contributes, in the Θ-twisted sector the term with insertion of Θ and in the Θ^2-twisted sector the term with insertion of Θ^2. To take into account the strings starting on the other stacks of D-branes, we include a factor of three and obtain

$$\mathcal{M} = \frac{c}{4} (1_{\mathrm{RR}} - 1_{\mathrm{NSNS}}) \int_0^\infty \frac{dt}{t^4} \frac{\vartheta\left[{1/2 \atop 0}\right]^2}{\eta^6} \times \left\{ C_0^0 \mathcal{L}_1^{\mathcal{M}} \mathcal{L}_2^{\mathcal{M}} \frac{\vartheta\left[{1/2 \atop 0}\right]^2}{\eta^6} + C_1^1 \chi_{\mathcal{M}} \frac{\vartheta\left[{5/6 \atop 1/3}\right] \vartheta\left[{1/6 \atop -1/3}\right]}{\vartheta\left[{5/6 \atop 5/6}\right] \vartheta\left[{1/6 \atop 1/6}\right]} + C_2^2 \chi_{\mathcal{M}} \frac{\vartheta\left[{7/6 \atop 2/3}\right] \vartheta\left[{-1/6 \atop -2/3}\right]}{\vartheta\left[{7/6 \atop 7/6}\right] \vartheta\left[{-1/6 \atop -1/6}\right]} \right\}, \tag{C.12}$$

where $\chi_{\mathcal{M}} = \chi_{\mathcal{A}}$, because the intersection points are $\Omega\mathcal{R}$ invariant (see figure C.3) and $t + i/2$ is the argument of the theta- and eta-functions. The Chan-Paton factors are included as well.

The modular transformation of the lattice contributions for the Klein bottle ($lt = 1/4$) reads

$$\begin{aligned} \mathcal{L}[4,3](t) &= \frac{2l}{\sqrt{3}}\tilde{\mathcal{L}}[1,4/3](l) \\ \mathcal{L}[4/3,1](t) &= 2\sqrt{3}l\tilde{\mathcal{L}}[3,4](l)\,, \end{aligned} \tag{C.13}$$

such that we obtain the coefficients

$$c_i^{\mathcal{K}} = \begin{cases} \frac{2}{\sqrt{3}} & (\mathbf{A}) \\ 2\sqrt{3} & (\mathbf{B}) \end{cases} . \tag{C.14}$$

We find the tree channel amplitude

$$\begin{aligned} \tilde{\mathcal{K}} = 8cc_1^{\mathcal{K}}c_2^{\mathcal{K}}(1_{\mathrm{RR}} - 1_{\mathrm{NSNS}}) \int_0^\infty dl \frac{\vartheta\left[\begin{smallmatrix}1/2\\0\end{smallmatrix}\right]^2}{\eta^6} \times \\ \left\{ \tilde{\mathcal{L}}_1^{\mathcal{K}}\tilde{\mathcal{L}}_2^{\mathcal{K}} \frac{\vartheta\left[\begin{smallmatrix}1/2\\0\end{smallmatrix}\right]^2}{\eta^6} - 3\frac{\vartheta\left[\begin{smallmatrix}1/2\\1/3\end{smallmatrix}\right]\vartheta\left[\begin{smallmatrix}1/2\\-1/3\end{smallmatrix}\right]}{\vartheta\left[\begin{smallmatrix}1/2\\5/6\end{smallmatrix}\right]\vartheta\left[\begin{smallmatrix}1/2\\1/6\end{smallmatrix}\right]} - 3\frac{\vartheta\left[\begin{smallmatrix}1/2\\2/3\end{smallmatrix}\right]\vartheta\left[\begin{smallmatrix}1/2\\-2/3\end{smallmatrix}\right]}{\vartheta\left[\begin{smallmatrix}1/2\\7/6\end{smallmatrix}\right]\vartheta\left[\begin{smallmatrix}1/2\\-1/6\end{smallmatrix}\right]} \right\}, \end{aligned} \tag{C.15}$$

where the argument of the theta- and eta-functions is $2l$.

In the case of the annulus, the lattice contributions transform ($lt = 1/2$)

$$\begin{aligned} \mathcal{L}[2,3/2](t) &= \frac{2l}{\sqrt{3}}\tilde{\mathcal{L}}[1,4/3](l) \\ \mathcal{L}[2/3,1/2](t) &= 2\sqrt{3}l\tilde{\mathcal{L}}[3,4](l)\,, \end{aligned} \tag{C.16}$$

and thus $c_i^{\mathcal{A}} = c_i^{\mathcal{K}}$. The annulus tree channel amplitude is

$$\begin{aligned} \tilde{\mathcal{A}} = \frac{c}{8}c_1^{\mathcal{A}}c_2^{\mathcal{A}}M^2(1_{\mathrm{RR}} - 1_{\mathrm{NSNS}}) \int_0^\infty dl \frac{\vartheta\left[\begin{smallmatrix}1/2\\0\end{smallmatrix}\right]^2}{\eta^6} \times \\ \left\{ \tilde{\mathcal{L}}_1^{\mathcal{A}}\tilde{\mathcal{L}}_2^{\mathcal{A}} \frac{\vartheta\left[\begin{smallmatrix}1/2\\0\end{smallmatrix}\right]^2}{\eta^6} - 3\frac{\vartheta\left[\begin{smallmatrix}1/2\\1/3\end{smallmatrix}\right]\vartheta\left[\begin{smallmatrix}1/2\\-1/3\end{smallmatrix}\right]}{\vartheta\left[\begin{smallmatrix}1/2\\5/6\end{smallmatrix}\right]\vartheta\left[\begin{smallmatrix}1/2\\1/6\end{smallmatrix}\right]} - 3\frac{\vartheta\left[\begin{smallmatrix}1/2\\2/3\end{smallmatrix}\right]\vartheta\left[\begin{smallmatrix}1/2\\-2/3\end{smallmatrix}\right]}{\vartheta\left[\begin{smallmatrix}1/2\\7/6\end{smallmatrix}\right]\vartheta\left[\begin{smallmatrix}1/2\\-1/6\end{smallmatrix}\right]} \right\}, \end{aligned} \tag{C.17}$$

with $2l$ as the argument of the theta- and eta-functions.

The lattice contributions for the Möbius strip transform as ($lt = 1/8$)

$$\begin{aligned} \mathcal{L}[2,6](t) &= \frac{4l}{\sqrt{3}}\tilde{\mathcal{L}}[4,4/3](l) \\ \mathcal{L}[2/3,2](t) &= 4\sqrt{3}l\tilde{\mathcal{L}}[12,4](l)\,, \end{aligned} \tag{C.18}$$

i.e. we find the coefficients

$$c_i^{\mathcal{M}} = \begin{cases} \frac{4}{\sqrt{3}} & (\mathbf{A}) \\ 4\sqrt{3} & (\mathbf{B}) \end{cases} \tag{C.19}$$

and the tree channel amplitude

$$\tilde{\mathcal{M}} = -\frac{c}{2} c_1^{\mathcal{M}} c_2^{\mathcal{M}} (1_{\mathrm{RR}} - 1_{\mathrm{NSNS}}) \int_0^\infty dl \frac{\vartheta\left[\begin{smallmatrix}1/2\\0\end{smallmatrix}\right]^2}{\eta^6} \times$$
$$\left\{ C_0^0 \tilde{\mathcal{L}}_1^{\mathcal{M}} \tilde{\mathcal{L}}_2^{\mathcal{M}} \frac{\vartheta\left[\begin{smallmatrix}1/2\\0\end{smallmatrix}\right]^2}{\eta^6} - 3C_2^2 \frac{\vartheta\left[\begin{smallmatrix}1/2\\1/3\end{smallmatrix}\right]\vartheta\left[\begin{smallmatrix}1/2\\-1/3\end{smallmatrix}\right]}{\vartheta\left[\begin{smallmatrix}1/2\\5/6\end{smallmatrix}\right]\vartheta\left[\begin{smallmatrix}1/2\\1/6\end{smallmatrix}\right]} - 3C_1^1 \frac{\vartheta\left[\begin{smallmatrix}1/2\\2/3\end{smallmatrix}\right]\vartheta\left[\begin{smallmatrix}1/2\\-2/3\end{smallmatrix}\right]}{\vartheta\left[\begin{smallmatrix}1/2\\7/6\end{smallmatrix}\right]\vartheta\left[\begin{smallmatrix}1/2\\-1/6\end{smallmatrix}\right]} \right\}, \tag{C.20}$$

with the argument $2l + i/2$. Note that the role of the Θ and Θ^2 twisted sectors in the loop channel has interchanged from the tree channel point of view.

The asymptotic behaviour yields the tadpole cancellation conditions

$$C_0^0 = C_1^1 = C_2^2 = M \tag{C.21}$$

and

$$M = 8 \qquad (\mathbf{AA}, \mathbf{AB}, \mathbf{BB}), \tag{C.22}$$

i.e. the same for each model. Note, that in the case of $\mathbb{Z}_3$ there are no twisted sector tadpole cancellation conditions. As a consequence, we can choose the representation matrices of the orientifold and orbifold group on the Chan-Paton factors to be the $M \times M$ (i.e. 8×8) unit matrix.

The closed string spectrum

In the untwisted NSNS sector, the invariant states are the ones from (2.100) and (2.101) and the first two lines of (2.103), which yield seven scalars and the graviton of $\mathcal{N} = 1$, $d = 6$ SUGRA. In the untwisted RR sector, we have the anti-self-dual 2-form and three scalars from (2.104) as well as two scalars from the last two lines of (2.105). Actually, these states are the model independent ones and therefore will constitute the untwisted closed string spectrum for $\mathbb{Z}_{4,6}$ as well, which is given by the $\mathcal{N} = 1$, $d = 6$ SUGRA multiplet and 3 hypermultiplets altogether.

In the Θ twisted NSNS sector, we begin with the state corresponding to q_L, i.e. $|0, 0, +\frac{1}{3}, -\frac{1}{3}\rangle_L$. Note, that only integer and half-integer entries have an interpretation as a spin. This state has the wrong GSO projection and is tachyonic. Applying the oscillator $\psi^{\bar{1}}_{-1/6}$ yields the state $|0, 0, -\frac{2}{3}, -\frac{1}{3}\rangle_L$ which is massless and has the correct GSO projection. Altogether, we find

$$\begin{aligned}
\psi^2_{-1/6}|0,0,+\frac{1}{3},-\frac{1}{3}\rangle_L &= |0,0,+\frac{1}{3},+\frac{2}{3}\rangle_L \equiv |1\rangle_{\rm NS} , \\
\psi^{\bar 1}_{-1/6}|0,0,+\frac{1}{3},-\frac{1}{3}\rangle_L &= |0,0,-\frac{2}{3},-\frac{1}{3}\rangle_L \equiv |2\rangle_{\rm NS} , \\
\tilde\psi^{\bar 2}_{-1/6}|0,0,-\frac{1}{3},+\frac{1}{3}\rangle_R &= |0,0,-\frac{1}{3},-\frac{2}{3}\rangle_R \equiv |\tilde 1\rangle_{\rm NS} , \\
\psi^{1}_{-1/6}|0,0,-\frac{1}{3},+\frac{1}{3}\rangle_R &= |0,0,+\frac{2}{3},+\frac{1}{3}\rangle_R \equiv |\tilde 2\rangle_{\rm NS} .
\end{aligned} \tag{C.23}$$

Tensorizing[1] and symmetrizing these states with respect to $\Omega\mathcal{R}$ leads to combinations similar to (2.110). i.e. 3 scalars for an invariant fixed point and 4 scalars for a pair of fixed points, consider figure C.1. For an **A** torus, the fixed point 1 is invariant and 2 and 3 get interchanged. For **B**, all three fixed points are invariant, i.e.

AA : 11 is invariant; 12-13, 21-31, 23-32, 22-33 form 4 pairs under $\Omega\mathcal{R}$,
AB : 21-31, 22-32, 23-33 form 3 pairs under $\Omega\mathcal{R}$, the remaining 3 fixed points are invariant
BB : all 9 fixed points are invariant

This gives 19 (21,27) scalars for the **AA** (**AB**,**BB**) model in the Θ twisted NSNS sector. The Θ^2 twisted sector obviously yields the same result.

In the Θ twisted RR sector, we find the massless GSO-even ground states

$$\begin{array}{ll}
|+\frac{1}{2},-\frac{1}{2},-\frac{1}{6},+\frac{1}{6}\rangle_L \equiv |1\rangle_{\rm R} , & |-\frac{1}{2},+\frac{1}{2},-\frac{1}{6},+\frac{1}{6}\rangle_L \equiv |2\rangle_{\rm R} , \\
|+\frac{1}{2},-\frac{1}{2},+\frac{1}{6},-\frac{1}{6}\rangle_R \equiv |\tilde 1\rangle_{\rm R} , & |-\frac{1}{2},+\frac{1}{2},+\frac{1}{6},-\frac{1}{6}\rangle_R \equiv |\tilde 2\rangle_{\rm R} ,
\end{array} \tag{C.24}$$

where again each state produces a minus sign under Θ, which is eliminated by tensorizing and we find states similar to (2.112). From this, we can immediately conclude that each invariant fixed point yields one scalar and each pair one tensor multiplet[2]. Again, the Θ^2 twisted sector contributes the same amount.

To summarize the closed string spectrum of the $\mathbb{Z}_3$ model

twist sector	**AA**	**AB**	**BB**
untwisted	SUGRA + 3H		
$\Theta + \Theta^2$	10H + 8T	12H + 6T	18H

(C.25)

[1] Note, that the left moving states in (C.23) have eigenvalue $e^{2\pi i/3}$ under Θ and the right moving states have eigenvalue $e^{4\pi i/3}$. Thus, tensorizing always yields states invariant under Θ.

[2] Actually, a pair of fixed points contributes two halves of tensor multiplets and the other two halves are provided by the Θ^2 twisted sector, but this does not change the counting.

The open string spectrum

We start with the untwisted NS sector. The $(0,0)$, $(1,1)$ and $(2,2)$ strings are mapped onto each other under Θ and Θ^2. Therefore, we only have to count e.g. the degrees of freedom for the $(0,0)$ strings. The only symmetry of the $(0,0)$ strings is $\Omega\mathcal{R}$. Remember, that we found out that each element of the orbifold and orientifold group can be represented by the $M \times M$ unit matrix ($M = 8$ for each of the three models). Thus we find the only constraint

$$\lambda^{(0,0)} = -\lambda^{(0,0)T} . \tag{C.26}$$

In the non-compact directions, this yields the gauge group $SO(8)$ and in the compact directions we obtain 1H in the adjoint, i.e. the **28** of $SO(8)$. As always, the fermionic content of the multiplets is found in the R sector.

Similarly, in the Θ twisted NS sector, the only strings we have to consider are the $(0,2)$ strings. The state for this string is described by the first line of (C.23), which corresponds to half a hypermultiplet. The other half is provided by the Θ^2 twisted sector. For these strings, $\Omega\mathcal{R}\Theta$ is a symmetry and leads to the same constraint as (C.26) for $\lambda^{(0,2)}$. Together with the multiplicities for the $\Omega\mathcal{R}$ invariant intersections (C.10), we obtain the open string spectrum

twist sector	**AA**	**AB**	**BB**	rep. of $SO(8)$
untwisted		1V		**28**
		1H		**28**
$\Theta + \Theta^2$	1H	3H	9H	**28**

(C.27)

The closed and open string massless spectrum satisfies the anomaly constraint (2.128) and the results are in agreement with [20, 7].

C.2 $\mathbb{Z}_4$

The lattices are the same as in the case of $\mathbb{Z}_2$, but now the fixed point structure is slightly different, see figure C.4. In the **B** lattice, the fixed points 3 and 4 get interchanged under $\Omega\mathcal{R}$. Under the action of Θ, the fixed points 3 and 4 get interchanged in both lattices.

The amplitudes and tadpole cancellation

For the KK and W momenta invariant under $\Omega\mathcal{R}$ and $\Omega\mathcal{R}\Theta^2$ we find, in analogy to the $\mathbb{Z}_2$ model, the lattice contribution $\mathcal{L}_i^{\mathcal{K}} = \mathcal{L}[1,1](t)$ for an **A** type torus and $\mathcal{L}_i^{\mathcal{K}} = \mathcal{L}[2,2](t)$ for a **B** type torus T_i. But for the KK and W momenta invariant under $\Omega\mathcal{R}\Theta$ and $\Omega\mathcal{R}\Theta^3$, the results get interchanged, i.e. $\mathcal{L}_i^{\mathcal{K}} = \mathcal{L}[2,2](t)$ for

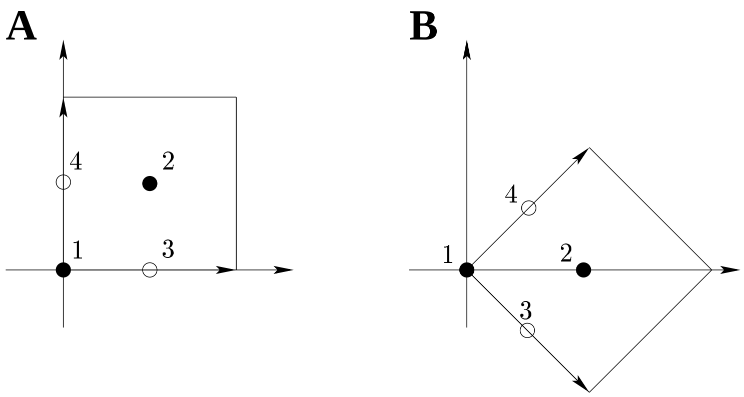

Figure C.4: Lattices for $\mathbb{Z}_4$. Black circles denote the fixed points under Θ and white circles the additional fixed points under Θ^2.

an **A** type torus and $\mathcal{L}_i^{\mathcal{K}} = \mathcal{L}[1,1](t)$ for a **B** type torus T_i. Consider e.g. an **AA** model in the case of $\mathbb{Z}_4$. The contribution from the untwisted sector is proportional to

$$\left(\mathcal{L}[1,1](t)^2 + \mathcal{L}[2,2](t)^2\right) \mathcal{K}^{(0)}(2t)\,, \tag{C.28}$$

where the first term within the brackets stems from the insertions $\Omega\mathcal{R}$ and $\Omega\mathcal{R}\Theta^2$ and the second term from the insertions $\Omega\mathcal{R}\Theta$ and $\Omega\mathcal{R}\Theta^3$, according to the statements above. $\mathcal{K}^{(0)}$ denotes the oscillator contributions to the untwisted sector. Modular transformation ($lt = 1/4$) of (C.28) leads to a term proportional to

$$\left(4\tilde{\mathcal{L}}[4,4](l)^2 + \tilde{\mathcal{L}}[2,2](l)^2\right) \tilde{\mathcal{K}}^{(0)}(2l)\,. \tag{C.29}$$

Calculating the tree channel amplitude directly from the crosscap states, we obtain a result proportional to

$$\left(\tilde{\mathcal{L}}[4,4](l)^2 + \tilde{\mathcal{L}}[2,2](l)^2\right) \tilde{\mathcal{K}}^{(0)}(2l)\,, \tag{C.30}$$

where the first (second) term arises from the overlaps of crosscaps with even (odd) powers of Θ. This means that the $\mathbb{Z}_4$ **AA** and **BB** models do not respect worldsheet duality and therefore are inconsistent. This leaves us with the **AB** model (which gets mapped to **BA**, and therefore to itself) for the case of $\mathbb{Z}_4$. The same applies for the $\mathbb{Z}_6$ model.

Also the multiplicities of the invariant fixed points get more involved. The following table shows the multiplicities $\chi_{\mathcal{K}}$ of the fixed points invariant under the different insertions. $\chi_{\mathcal{K}}^{(1)}$ is the multiplicity in the Θ twisted sector, which is the same as the multiplicity in the Θ^3 twisted sector, of course. $\chi_{\mathcal{K}}^{(2)}$ is the multiplicity in the Θ^2 twisted sector. Invariance under $\Omega\mathcal{R}$ ($\Omega\mathcal{R}\Theta$) of course

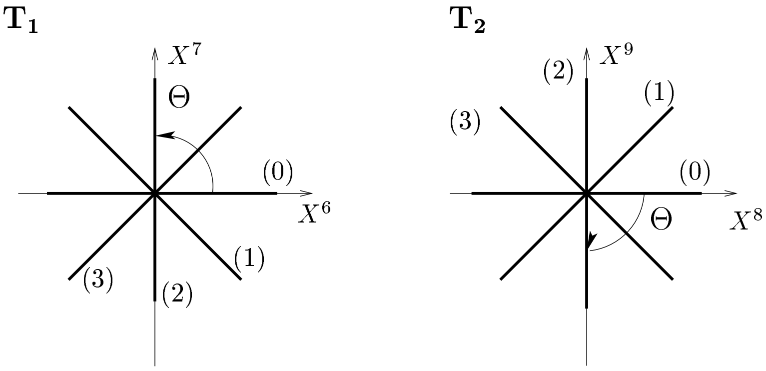

Figure C.5: Location of D7-branes for $\mathbb{Z}_4$ labelled by $(0), \ldots, (3)$.

implies invariance under $\Omega\mathcal{R}\Theta^2$ ($\Omega\mathcal{R}\Theta^3$).

$$
\begin{array}{c||c|c||c|c}
 & \multicolumn{2}{c||}{\mathbf{A}} & \multicolumn{2}{c}{\mathbf{B}} \\
 & \multicolumn{4}{c}{\text{invariant under}\ldots} \\
 & \Omega\mathcal{R} & \Omega\mathcal{R}\Theta & \Omega\mathcal{R} & \Omega\mathcal{R}\Theta \\
\hline
\chi_{\mathcal{K}}^{(1)} = \chi_{\mathcal{K}}^{(1)} & 2 & 2 & 2 & 2 \\
\chi_{\mathcal{K}}^{(2)} & 4 & 2 & 2 & 4
\end{array}
\tag{C.31}
$$

We obtain the 1-loop amplitude for the **AB** model

$$
\mathcal{K} = 2c(1_{\mathrm{RR}} - 1_{\mathrm{NSNS}}) \int_0^\infty \frac{dt}{t^4} \frac{\vartheta\left[{0 \atop 1/2}\right]^2}{\eta^6} \times
$$
$$
\left\{ \mathcal{L}[1,1]\mathcal{L}[2,2] \frac{\vartheta\left[{0 \atop 1/2}\right]^2}{\eta^6} + 4 \frac{\vartheta\left[{1/4 \atop 1/2}\right]\vartheta\left[{-1/4 \atop 1/2}\right]}{\vartheta\left[{3/4 \atop 1/2}\right]\vartheta\left[{1/4 \atop 1/2}\right]} + 8 \frac{\vartheta\left[{1/2 \atop 1/2}\right]^2}{\vartheta\left[{0 \atop 1/2}\right]^2} + 4 \frac{\vartheta\left[{3/4 \atop 1/2}\right]\vartheta\left[{-3/4 \atop 1/2}\right]}{\vartheta\left[{5/4 \atop 1/2}\right]\vartheta\left[{-1/4 \atop 1/2}\right]} \right\} . \tag{C.32}
$$

For the arguments of the various functions, see above.

The D7-branes at angles we introduce in the case of $\mathbb{Z}_4$ are shown in figure C.5. Terms with insertions of Θ and Θ^3 do not contribute to the amplitude, because they do not leave the D-branes invariant. Terms with insertion of Θ^2 again lead to the twisted sector tadpole cancellation condition (2.48) and therefore do not show up in the following. The location of the D7-branes in the fundamental cells is shown in figure C.6. From this figure we can see that the compact momenta for the stack of branes (0) are the same as in the case of $\mathbb{Z}_2$. For the stack of branes (1) the role of **A** and **B** gets interchanged, but this does not matter, since we are only dealing with the **AB** model. Therefore we can proceed as always, namely perform the calculation for the stack of D-branes (0) and include a factor of N in the end. The invariant intersection points are the

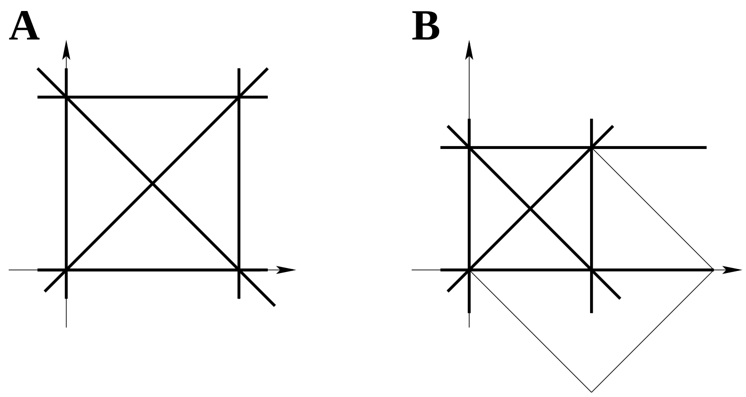

Figure C.6: Location of D-branes in the fundamental cells for $\mathbb{Z}_4$

same as in the case of $\mathbb{Z}_2$, namely only in the case of a Θ^2 twisted string (starting on brane (0)) on a **B** torus, we find an intersection number of 2, all the other cases yield a factor of one. Including the Chan-Paton factors, we obtain

$$\begin{aligned}\mathcal{A} = {} & \frac{c}{4} M^2 (1_{\mathrm{RR}} - 1_{\mathrm{NSNS}}) \int_0^\infty \frac{dt}{t^4} \frac{\vartheta\left[{0 \atop 1/2}\right]^2}{\eta^6} \times \\ & \left\{ \mathcal{L}[2,2]\mathcal{L}[1,1]\frac{\vartheta\left[{0 \atop 1/2}\right]^2}{\eta^6} + \frac{\vartheta\left[{1/4 \atop 1/2}\right]\vartheta\left[{-1/4 \atop 1/2}\right]}{\vartheta\left[{3/4 \atop 1/2}\right]\vartheta\left[{1/4 \atop 1/2}\right]} + 2\frac{\vartheta\left[{1/2 \atop 1/2}\right]^2}{\vartheta\left[{0 \atop 1/2}\right]^2} + \frac{\vartheta\left[{3/4 \atop 1/2}\right]\vartheta\left[{-3/4 \atop 1/2}\right]}{\vartheta\left[{5/4 \atop 1/2}\right]\vartheta\left[{-1/4 \atop 1/2}\right]} \right\},\end{aligned} \tag{C.33}$$

where the factor of two in the third term within the braces is the intersection number discussed above.

We perform the calculation for a string starting on the stack of branes (0). The lattice contributions are the same as in the case of $\mathbb{Z}_2$ and only appear for untwisted sectors without insertion from the orbifold group. From (2.53) we learn that only untwisted strings without insertion and with insertion of Θ^2 as well as Θ^2 twisted strings with insertion of Θ and Θ^3 contribute, i.e.

$$\begin{aligned}\mathcal{M} = {} & -\frac{c}{4} M (1_{\mathrm{RR}} - 1_{\mathrm{NSNS}}) \int_0^\infty \frac{dt}{t^4} \frac{\vartheta\left[{1/2 \atop 0}\right]^2}{\eta^6} \times \\ & \left\{ C_0^0 \mathcal{L}[2,2]\mathcal{L}[1,4]\frac{\vartheta\left[{1/2 \atop 0}\right]^2}{\eta^6} + 2C_1^2 \frac{\vartheta\left[{1 \atop 1/4}\right]\vartheta\left[{0 \atop -1/4}\right]}{\vartheta\left[{1 \atop 3/4}\right]\vartheta\left[{0 \atop 1/4}\right]} \right. \\ & \left. -4C_2^0 \frac{\vartheta\left[{1/2 \atop 1/2}\right]^2}{\vartheta\left[{1/2 \atop 0}\right]^2} + 2C_3^2 \frac{\vartheta\left[{1 \atop 3/4}\right]\vartheta\left[{0 \atop -3/4}\right]}{\vartheta\left[{1 \atop 5/4}\right]\vartheta\left[{0 \atop -1/4}\right]} \right\}.\end{aligned} \tag{C.34}$$

The intersection numbers are the same as in the case of the annulus, because the intersection points for the strings starting on stack (0) are $\Omega\mathcal{R}$ invariant. This leads to the factors of two in the second and fourth term within the braces. The factor -4 in the third term again arises from (A.32).

For the coefficients of the modular transformation of the lattice contributions and further details, remember section 2.2.4. Modular transformation of the 1-loop amplitudes leads to

$$\begin{aligned}\tilde{\mathcal{K}} &= 64c(1_{\mathrm{RR}}-1_{\mathrm{NSNS}})\int_0^\infty dl \frac{\vartheta\left[{1/2 \atop 0}\right]^2}{\eta^6}\times \\ &\left\{\tilde{\mathcal{L}}[4,4]\tilde{\mathcal{L}}[2,2]\frac{\vartheta\left[{1/2 \atop 0}\right]^2}{\eta^6} - 2\frac{\vartheta\left[{1/2 \atop 1/4}\right]\vartheta\left[{1/2 \atop -1/4}\right]}{\vartheta\left[{1/2 \atop 3/4}\right]\vartheta\left[{1/2 \atop 1/4}\right]} - 4\frac{\vartheta\left[{1/2 \atop 1/2}\right]^2}{\vartheta\left[{1/2 \atop 0}\right]^2} - 2\frac{\vartheta\left[{1/2 \atop 3/4}\right]\vartheta\left[{1/2 \atop -3/4}\right]}{\vartheta\left[{1/2 \atop 5/4}\right]\vartheta\left[{1/2 \atop -1/4}\right]}\right\},\end{aligned} \tag{C.35}$$

$$\begin{aligned}\tilde{\mathcal{A}} &= \frac{c}{4}M^2(1_{\mathrm{RR}}-1_{\mathrm{NSNS}})\int_0^\infty dl \frac{\vartheta\left[{1/2 \atop 0}\right]^2}{\eta^6}\times \\ &\left\{\tilde{\mathcal{L}}[1,1]\tilde{\mathcal{L}}[2,2]\frac{\vartheta\left[{1/2 \atop 0}\right]^2}{\eta^6} - 2\frac{\vartheta\left[{1/2 \atop 1/4}\right]\vartheta\left[{1/2 \atop -1/4}\right]}{\vartheta\left[{1/2 \atop 3/4}\right]\vartheta\left[{1/2 \atop 1/4}\right]} - 4\frac{\vartheta\left[{1/2 \atop 1/2}\right]^2}{\vartheta\left[{1/2 \atop 0}\right]^2} - 2\frac{\vartheta\left[{1/2 \atop 3/4}\right]\vartheta\left[{1/2 \atop -3/4}\right]}{\vartheta\left[{1/2 \atop 5/4}\right]\vartheta\left[{1/2 \atop -1/4}\right]}\right\},\end{aligned} \tag{C.36}$$

$$\begin{aligned}\tilde{\mathcal{M}} &= -8c(1_{\mathrm{RR}}-1_{\mathrm{NSNS}})\int_0^\infty dl \frac{\vartheta\left[{1/2 \atop 0}\right]^2}{\eta^6}\times \\ &\left\{C_0^0\tilde{\mathcal{L}}[4,4]\tilde{\mathcal{L}}[8,2]\frac{\vartheta\left[{1/2 \atop 0}\right]^2}{\eta^6} - 2C_3^2\frac{\vartheta\left[{1/2 \atop 1/4}\right]\vartheta\left[{1/2 \atop -1/4}\right]}{\vartheta\left[{1/2 \atop 3/4}\right]\vartheta\left[{1/2 \atop 1/4}\right]}\right. \\ &\left. +4C_2^0\frac{\vartheta\left[{1/2 \atop 1/2}\right]^2}{\vartheta\left[{1/2 \atop 0}\right]^2} - 2C_1^2\frac{\vartheta\left[{1/2 \atop 3/4}\right]\vartheta\left[{1/2 \atop -3/4}\right]}{\vartheta\left[{1/2 \atop 5/4}\right]\vartheta\left[{1/2 \atop -1/4}\right]}\right\},\end{aligned} \tag{C.37}$$

which imply the tadpole cancellation conditions

$$M = 16 \tag{C.38}$$

and

$$C_0^0 = C_3^2 = -C_2^0 = C_1^2 = M\,. \tag{C.39}$$

Recalling the abbreviation (2.56), this means

$$\gamma^{(0)-T}_{\Omega\mathcal{R}0}\gamma^{(0)}_{\Omega\mathcal{R}0} = \gamma^{(2)-T}_{\Omega\mathcal{R}3}\gamma^{(0)}_{\Omega\mathcal{R}3} = -\gamma^{(0)-T}_{\Omega\mathcal{R}2}\gamma^{(0)}_{\Omega\mathcal{R}2} = \gamma^{(2)-T}_{\Omega\mathcal{R}1}\gamma^{(0)}_{\Omega\mathcal{R}1} = \mathbb{1}_M\,. \tag{C.40}$$

Redoing the calculation with strings starting on brane (1), we obtain

$$\gamma^{(1)-T}_{\Omega\mathcal{R}1}\gamma^{(1)}_{\Omega\mathcal{R}1} = \gamma^{(3)-T}_{\Omega\mathcal{R}0}\gamma^{(1)}_{\Omega\mathcal{R}0} = -\gamma^{(1)-T}_{\Omega\mathcal{R}3}\gamma^{(1)}_{\Omega\mathcal{R}3} = \gamma^{(3)-T}_{\Omega\mathcal{R}2}\gamma^{(1)}_{\Omega\mathcal{R}2} = \mathbb{1}_M \tag{C.41}$$

and so on. The rule is, if one raises the label of the starting brane by one, one has to raise the power of the insertion Θ by one as well. To satisfy these relations, we can choose

$$\gamma^{(0)}_{\Omega\mathcal{R}2} = \gamma^{(1)}_{\Omega\mathcal{R}3} = \gamma^{(2)}_{\Omega\mathcal{R}0} = \gamma^{(3)}_{\Omega\mathcal{R}1} = I\,, \tag{C.42}$$

with I from (2.97). If we choose in addition

$$\gamma^{(0)}_{\Omega\mathcal{R}1} = \gamma^{(1)}_{\Omega\mathcal{R}0} = \gamma^{(2)}_{\Omega\mathcal{R}1} = \gamma^{(3)}_{\Omega\mathcal{R}0} = I\,, \tag{C.43}$$

up to signs, and the remaining $\Omega\mathcal{R}$ matrices to be the unit matrix, it follows from (2.92) that this choice is consistent and that the twisted tadpole cancellation conditions (2.48) are satisfied, i.e.

$$\gamma^{(a)}_2 = I\,. \tag{C.44}$$

The closed string spectrum

As shown in the case of $\mathbb{Z}_3$, the untwisted sector consists of one $\mathcal{N}=1$, $d=6$ SUGRA multiplet and 3 hypermultiplets.

In the Θ twisted NSNS sector, proceeding in analogy to the $\mathbb{Z}_3$ model, we find the massless states with correct GSO projection

$$\begin{aligned}
\psi^2_{-1/4}|0,0,+\tfrac{1}{4},-\tfrac{1}{4}\rangle_L &= |0,0,+\tfrac{1}{4},+\tfrac{3}{4}\rangle_L \equiv |1\rangle_{\mathrm{NS}}\,,\\
\psi^{\bar{1}}_{-1/4}|0,0,+\tfrac{1}{4},-\tfrac{1}{4}\rangle_L &= |0,0,-\tfrac{3}{4},-\tfrac{1}{4}\rangle_L \equiv |2\rangle_{\mathrm{NS}}\,,\\
\tilde{\psi}^{\bar{2}}_{-1/4}|0,0,-\tfrac{1}{4},+\tfrac{1}{4}\rangle_R &= |0,0,-\tfrac{1}{4},-\tfrac{3}{4}\rangle_R \equiv |\tilde{1}\rangle_{\mathrm{NS}}\,,\\
\psi^{1}_{-1/4}|0,0,-\tfrac{1}{4},+\tfrac{1}{4}\rangle_R &= |0,0,+\tfrac{3}{4},+\tfrac{1}{4}\rangle_R \equiv |\tilde{2}\rangle_{\mathrm{NS}}\,.
\end{aligned} \tag{C.45}$$

Tensorizing and symmetrizing these states with respect to $\Omega\mathcal{R}$ again leads to combinations similar to (2.110), but now the fixed point structure is different from the case of $\mathbb{Z}_2$, see figure C.4. The fixed points of the Θ twisted sector are given by the points 11, 12, 21 and 22 which are all invariant under the elements from the orientifold and the orbifold group. Thus each fixed point contributes three scalars and therefore we find 12 scalars (i.e. 6 half-hypermultiplets; the other halves again are supplied by the Θ^3 twisted sector) in the Θ twisted NSNS sector.

The states in the Θ^2 twisted NSNS sector are completely analogous to the states in the Θ twisted sector of the $\mathbb{Z}_2$ model and thus given by (2.109). The fixed points, however, behave differently. In addition to the interchange of the fixed points 3 and 4 of the **B** lattice under $\Omega\mathcal{R}$, the fixed points 3 and 4 of both types of lattices are interchanged under Θ (and Θ^3). Remember, that we deal with the **AB** lattice only in the $\mathbb{Z}_4$ model. The fixed points 11, 12, 21 and 22 are invariant; the fixed points 13-14 and 23-24 form pairs under $\Omega\mathcal{R}$ and Θ; the fixed points 31-41 and 32-42 form pairs under Θ; the fixed points 33-34-43-44 form a quartet under $\Omega\mathcal{R}$ and Θ. The invariant fixed points, the pairs under $\Omega\mathcal{R}$ and Θ and the pairs under Θ each contribute three scalars, whereas the quartet contributes four scalars. This can easily be seen by symmetrizing with respect to $\Omega\mathcal{R}$ and Θ. Altogether, the Θ^2 twisted NSNS contains 28 scalars, i.e. 7 hypermultiplets.

In the Θ twisted RR sector, again proceeding similar to the case of $\mathbb{Z}_3$, we find massless states in analogy to (2.112). The 4 invariant fixed points each contribute one scalar to give 2 half-hypermultiplets. The remaining halves again come from the Θ^3 twisted sector.

The states in the Θ^2 twisted RR sector are similar to the Θ twisted sector of the $\mathbb{Z}_2$ model and thus given by (2.111). The invariant fixed points, the pairs under $\Omega\mathcal{R}$ and Θ and the pairs under Θ each contribute one scalar, i.e. two hypermultiplets and the quartet contributes one tensor multiplet.

The content of the closed string spectrum of the $\mathbb{Z}_4$ model is shown in the following table

twist sector	**AB**
untwisted	SUGRA + 3H
$\Theta + \Theta^3$	8H
Θ^2	9H + 1T

(C.46)

The open string spectrum

We obtain the gauge group in the untwisted NS sector from the states $\psi^{\mu}_{-1/2}|0,ij\rangle\lambda^{(a,a)}_{ji}$. The string $(0,0)$ is invariant under $\Omega\mathcal{R}$ and $\Omega\mathcal{R}\Theta^2$ and mapped to the $(2,2)$ string under Θ. The string $(1,1)$ is invariant under $\Omega\mathcal{R}\Theta$ and $\Omega\mathcal{R}\Theta^3$ and mapped to the $(3,3)$ string under Θ. Thus we expect to obtain one factor of the gauge group from the $(0,0)$ string and another factor as a copy from the $(1,1)$ string. Applying the symmetries on the $(0,0)$ string and using the matrix representations we found above, we obtain

$$\lambda^{(0,0)} = -\lambda^{(0,0)T} = -I\lambda^{(0,0)T}I\,, \tag{C.47}$$

i.e. a matrix of the form (2.118) and thus $U(M/2)$ as the gauge group in analogy to the case of the $\mathbb{Z}_2$ model. The $(1,1)$ string yields another factor of $U(M/2)$ and thus, since $M=16$ in this model, we find the gauge group

$$U(8)\times U(8)\,. \tag{C.48}$$

Similarly, for $\psi^{i,\bar{i}}_{-1/2}|0,ij\rangle\lambda^{(a,a)}_{ji}$, we find the constraints

$$\lambda^{(0,0)} = -\lambda^{(0,0)T} = I\lambda^{(0,0)T}I\,, \tag{C.49}$$

i.e. a matrix of the form (2.123) and therefore 2 hypermultiplets in the antisymmetric representation, i.e. 2H in the $(\mathbf{28},\mathbf{1})+(\mathbf{1},\mathbf{28})$ of the gauge group.

The Θ twisted sector consists of the $(0,3)$ strings and the Θ^3 twisted sector consists of the $(0,1)$ strings. The other Θ and Θ^3 twisted strings can be reached by symmetries. The states corresponding to the Θ twisted strings are given by the first two lines in (C.45). The only symmetry is Θ^2, i.e.

$$\lambda^{(0,3)} = \pm I \lambda^{(0,3)} I \,, \tag{C.50}$$

which leads to a matrix of the form (2.126) and we find, in analogy to the Θ twisted sector of $\mathbb{Z}_2$, 1H in the bifundamental $(\mathbf{8},\mathbf{8})$ from the Θ twisted sector and another one from the Θ^3 twisted sector. In contrast to the Θ twisted sector of $\mathbb{Z}_2$, the multiplicity is just one.

It remains to determine the content of the Θ^2 twisted sector, which consists of the $(0,2)$ and the $(1,3)$ strings. The corresponding states are given by the first lines of (2.109). In comparison to the Θ twisted sector, there are additional symmetries. The $(0,2)$ strings are symmetric under $\Omega\mathcal{R}\Theta$ and $\Omega\mathcal{R}\Theta^3$, i.e.

$$\lambda^{(0,2)} = -\left(\gamma^{(2)}_{\Omega\mathcal{R}1}\lambda^{(0,2)}\gamma^{(0)-1}_{\Omega\mathcal{R}1}\right)^T = -\left(\gamma^{(2)}_{\Omega\mathcal{R}3}\lambda^{(0,2)}\gamma^{(0)-1}_{\Omega\mathcal{R}3}\right)^T \,, \tag{C.51}$$

Using the matrix representations we found, these constraints read

$$\lambda^{(0,2)} = I\lambda^{(0,2)T} I = -\lambda^{(0,2)T} \,, \tag{C.52}$$

leading to a matrix of the form (2.123) and therefore to 1H in the antisymmetric $(\mathbf{28},\mathbf{1})$. The $(1,3)$ strings yield 1H in the antisymmetric $(\mathbf{1},\mathbf{28})$. In addition, we have a multiplicity of 2 from the intersections in the **B** lattice.

Altogether, we find the open string spectrum of the $\mathbb{Z}_4$ model

twist sector	**AB**	rep. of $[U(8)]^2$
untwisted	1V	$(\mathbf{64},\mathbf{1})+(\mathbf{1},\mathbf{64})$
	2H	$(\mathbf{28},\mathbf{1})+(\mathbf{1},\mathbf{28})$
$\Theta+\Theta^3$	2H	$(\mathbf{8},\mathbf{8})$
Θ^2	2H	$(\mathbf{28},\mathbf{1})+(\mathbf{1},\mathbf{28})$

(C.53)

The massless spectrum again satisfies the anomaly constraint (2.128) and is in agreement with [20].

C.3 $\mathbb{Z}_6$

The lattice of the $\mathbb{Z}_6$ model is the same as in the case of $\mathbb{Z}_3$, but the fixed point structure is slightly more complicated now, see figure C.7. Under $\Omega\mathcal{R}$, the points 2 and 3 as well as 5 and 6 are interchanged in the **A** lattice; in the **B** lattice, the points 2 and 3 are interchanged. Under Θ, Θ^2 and Θ^3, the points 4, 5 and 6 are rotated onto each other circularly in both lattices. In addition, under Θ and Θ^3, the points 2 and 3 are interchanged in both lattices.

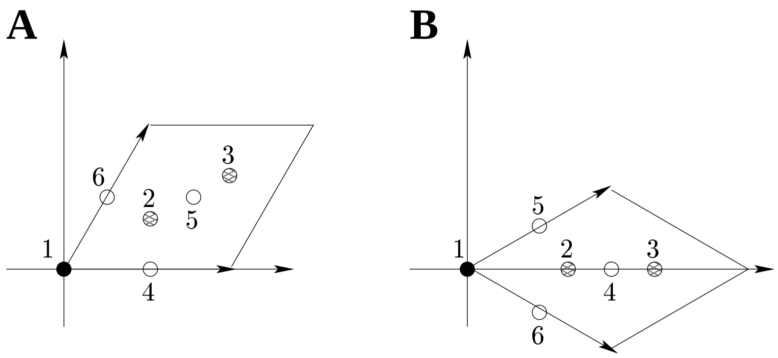

Figure C.7: Lattices for $\mathbb{Z}_6$. The black circle, labelled by 1, denotes the fixed point under Θ. The grey circles 2 and 3 denote the additional fixed points under Θ^2 and the white circles 4,5 and 6 the additional fixed points under Θ^3 (additional with respect to point 1).

The amplitudes and tadpole cancellation

Since an insertion of Θ (and Θ^3) interchanges the lattice contributions of an **A** and a **B** lattice, in analogy to the case of $\mathbb{Z}_4$, worldsheet duality leads to the fact that only the **AB** model is consistent. The actual lattice contributions are similar to the $\mathbb{Z}_3$ model.

The following table shows the multiplicities $\chi_\mathcal{K}$ of the fixed points invariant under the different insertions. $\chi_\mathcal{K}^{(n)}$ is the multiplicity in the Θ^n twisted sector.

	A				**B**			
	invariant under ...							
	$\Omega\mathcal{R}$	$\Omega\mathcal{R}\Theta$	$\Omega\mathcal{R}\Theta^2$	$\Omega\mathcal{R}\Theta^3$	$\Omega\mathcal{R}$	$\Omega\mathcal{R}\Theta$	$\Omega\mathcal{R}\Theta^2$	$\Omega\mathcal{R}\Theta^3$
$\chi_\mathcal{K}^{(1)} = \chi_\mathcal{K}^{(5)}$	1	1	1	1	1	1	1	1
$\chi_\mathcal{K}^{(2)} = \chi_\mathcal{K}^{(4)}$	1	3	1	3	3	1	3	1
$\chi_\mathcal{K}^{(3)}$	2	2	2	2	2	2	2	2

(C.54)

Thus we find the Klein bottle amplitude

$$
\begin{aligned}
\mathcal{K} = 2c(1_{\rm RR} - 1_{\rm NSNS}) \int_0^\infty \frac{dt}{t^4} \frac{\vartheta\left[{0 \atop 1/2}\right]^2}{\eta^6} \times \\
\Bigg\{ \mathcal{L}[4,3]\mathcal{L}[4/3,1] \frac{\vartheta\left[{0 \atop 1/2}\right]^2}{\eta^6} + \frac{\vartheta\left[{1/6 \atop 1/2}\right]\vartheta\left[{-1/6 \atop 1/2}\right]}{\vartheta\left[{2/3 \atop 1/2}\right]\vartheta\left[{1/3 \atop 1/2}\right]} + 3\frac{\vartheta\left[{1/3 \atop 1/2}\right]\vartheta\left[{-1/3 \atop 1/2}\right]}{\vartheta\left[{5/6 \atop 1/2}\right]\vartheta\left[{1/6 \atop 1/2}\right]} \qquad \text{(C.55)} \\
+4\frac{\vartheta\left[{1/2 \atop 1/2}\right]\vartheta\left[{-1/2 \atop 1/2}\right]}{\vartheta\left[{1 \atop 1/2}\right]\vartheta\left[{0 \atop 1/2}\right]} + 3\frac{\vartheta\left[{2/3 \atop 1/2}\right]\vartheta\left[{-2/3 \atop 1/2}\right]}{\vartheta\left[{7/6 \atop 1/2}\right]\vartheta\left[{-1/6 \atop 1/2}\right]} + \frac{\vartheta\left[{5/6 \atop 1/2}\right]\vartheta\left[{-5/6 \atop 1/2}\right]}{\vartheta\left[{4/3 \atop 1/2}\right]\vartheta\left[{-1/3 \atop 1/2}\right]} \Bigg\} .
\end{aligned}
$$

In figure C.8 we show the rotated stacks of D7-branes we introduce in the

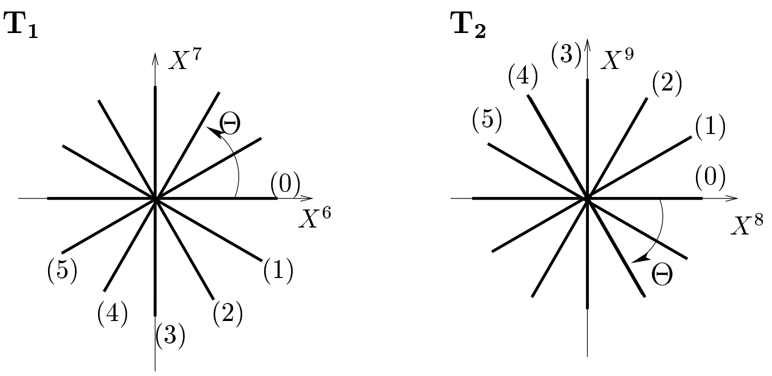

Figure C.8: Location of D7-branes in the case of $\mathbb{Z}_6$. The D-branes are labelled by $(0), \ldots, (5)$.

$\mathbb{Z}_6$ model to cancel the tadpoles from the Klein bottle. From figure C.9, one can read off the intersection numbers. For a string starting on stack (0), the intersection numbers are 1, 2, 1 (1, 2, 3) in the Θ, Θ^2, Θ^3 twisted sector on the **A** (**B**) lattice, respectively. In the case of the annulus, we do not have to care about the invariance of the intersection points under the various insertions, because only the insertion of $\mathbb{1}$ contributes, since insertions of Θ, Θ^2, Θ^4 and Θ^5 do not leave the D-branes invariant and the term with insertion of Θ^3 vanishes due to the twisted tadpole cancellation condition. We calculate the annulus

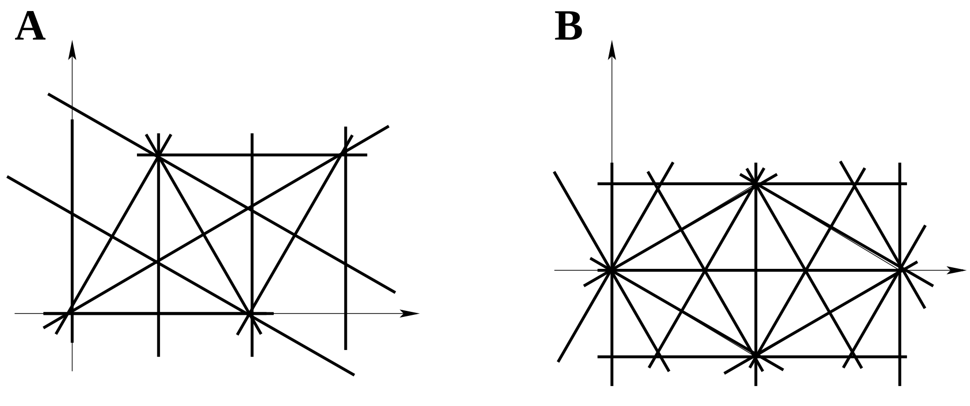

Figure C.9: Location of D-branes in the fundamental cells for $\mathbb{Z}_6$

amplitude from the strings starting on brane (0) and include a factor of 6 in the end

$$\mathcal{A} = \frac{c}{4}M^2(1_{\rm RR} - 1_{\rm NSNS}) \int_0^\infty \frac{dt}{t^4} \frac{\vartheta\left[{0 \atop 1/2}\right]^2}{\eta^6} \times$$
$$\left\{ \mathcal{L}[2,3/2]\mathcal{L}[2/3,1/2] \frac{\vartheta\left[{0 \atop 1/2}\right]^2}{\eta^6} + \frac{\vartheta\left[{1/6 \atop 1/2}\right]\vartheta\left[{-1/6 \atop 1/2}\right]}{\vartheta\left[{2/3 \atop 1/2}\right]\vartheta\left[{1/3 \atop 1/2}\right]} + 3\frac{\vartheta\left[{1/3 \atop 1/2}\right]\vartheta\left[{-1/3 \atop 1/2}\right]}{\vartheta\left[{5/6 \atop 1/2}\right]\vartheta\left[{1/6 \atop 1/2}\right]} \right.$$
$$\left. +4\frac{\vartheta\left[{1/2 \atop 1/2}\right]\vartheta\left[{-1/2 \atop 1/2}\right]}{\vartheta\left[{1 \atop 1/2}\right]\vartheta\left[{0 \atop 1/2}\right]} + 3\frac{\vartheta\left[{2/3 \atop 1/2}\right]\vartheta\left[{-2/3 \atop 1/2}\right]}{\vartheta\left[{7/6 \atop 1/2}\right]\vartheta\left[{-1/6 \atop 1/2}\right]} + \frac{\vartheta\left[{5/6 \atop 1/2}\right]\vartheta\left[{-5/6 \atop 1/2}\right]}{\vartheta\left[{4/3 \atop 1/2}\right]\vartheta\left[{-1/3 \atop 1/2}\right]} \right\}. \tag{C.56}$$

From equation (2.53) we find, that for strings starting on brane (0), the untwisted sector with insertion of $\Omega\mathcal{R}$ and $\Omega\mathcal{R}\Theta^3$, the Θ twisted sector with insertion of $\Omega\mathcal{R}\Theta^2$ and $\Omega\mathcal{R}\Theta^5$ and the Θ^4 twisted sector with insertion of $\Omega\mathcal{R}\Theta$ and $\Omega\mathcal{R}\Theta^4$ contribute to the Möbius strip. Furthermore, figure C.9 tells us the multiplicities of the invariant intersection points

	A		**B**	
	invariant under . . .			
	$\Omega\mathcal{R}\Theta^{1,5}$	$\Omega\mathcal{R}\Theta^{2,4}$	$\Omega\mathcal{R}\Theta^{1,5}$	$\Omega\mathcal{R}\Theta^{2,4}$
$\chi^{(2)}_{\mathcal{M}} = \chi^{(4)}_{\mathcal{M}}$	1	1	1	3

(C.57)

We obtain the Möbius strip 1-loop amplitude

$$\mathcal{M} = \frac{c}{4}(1_{\rm RR} - 1_{\rm NSNS}) \int_0^\infty \frac{dt}{t^4} \frac{\vartheta\left[{1/2 \atop 0}\right]^2}{\eta^6} \times$$
$$\left\{ C_0^0\mathcal{L}[2,3]\mathcal{L}[2/3,2] \frac{\vartheta\left[{1/2 \atop 0}\right]^2}{\eta^6} + C_5^2\frac{\vartheta\left[{5/6 \atop 5/6}\right]\vartheta\left[{1/6 \atop -5/6}\right]}{\vartheta\left[{5/6 \atop 4/3}\right]\vartheta\left[{1/6 \atop -1/3}\right]} + 3C_4^4\frac{\vartheta\left[{7/6 \atop 2/3}\right]\vartheta\left[{-1/6 \atop -2/3}\right]}{\vartheta\left[{7/6 \atop 7/6}\right]\vartheta\left[{-1/6 \atop -1/6}\right]} \right.$$
$$\left. -4C_3^0\frac{\vartheta\left[{1/2 \atop 1/2}\right]\vartheta\left[{1/2 \atop -1/2}\right]}{\vartheta\left[{1/2 \atop 1}\right]\vartheta\left[{1/2 \atop 0}\right]} + 3C_2^2\frac{\vartheta\left[{5/6 \atop 1/3}\right]\vartheta\left[{1/6 \atop -1/3}\right]}{\vartheta\left[{5/6 \atop 5/6}\right]\vartheta\left[{1/6 \atop 1/6}\right]} + C_1^4\frac{\vartheta\left[{7/6 \atop 2/3}\right]\vartheta\left[{-1/6 \atop -2/3}\right]}{\vartheta\left[{7/6 \atop 7/6}\right]\vartheta\left[{-1/6 \atop -1/6}\right]} \right\}. \tag{C.58}$$

The factor -4 again arises from (A.32).

Modular transformation of the amplitudes yields

$$\tilde{\mathcal{K}} = 32c(1_{\rm RR} - 1_{\rm NSNS}) \int_0^\infty dl \frac{\vartheta\left[{1/2 \atop 0}\right]^2}{\eta^6} \times$$
$$\left\{ \tilde{\mathcal{L}}[1,4/3]\tilde{\mathcal{L}}[3,4] \frac{\vartheta\left[{1/2 \atop 0}\right]^2}{\eta^6} - \frac{\vartheta\left[{1/2 \atop 1/6}\right]\vartheta\left[{1/2 \atop -1/6}\right]}{\vartheta\left[{1/2 \atop 2/3}\right]\vartheta\left[{1/2 \atop 1/3}\right]} - 3\frac{\vartheta\left[{1/2 \atop 1/3}\right]\vartheta\left[{1/2 \atop -1/3}\right]}{\vartheta\left[{1/2 \atop 5/6}\right]\vartheta\left[{1/2 \atop 1/6}\right]} \right. \tag{C.59}$$
$$\left. -4\frac{\vartheta\left[{1/2 \atop 1/2}\right]\vartheta\left[{1/2 \atop -1/2}\right]}{\vartheta\left[{1/2 \atop 1}\right]\vartheta\left[{1/2 \atop 0}\right]} - 3\frac{\vartheta\left[{1/2 \atop 2/3}\right]\vartheta\left[{1/2 \atop -2/3}\right]}{\vartheta\left[{1/2 \atop 7/6}\right]\vartheta\left[{1/2 \atop -1/6}\right]} - \frac{\vartheta\left[{1/2 \atop 5/6}\right]\vartheta\left[{1/2 \atop -5/6}\right]}{\vartheta\left[{1/2 \atop 4/3}\right]\vartheta\left[{1/2 \atop -1/3}\right]} \right\},$$

$$
\begin{aligned}
\tilde{\mathcal{A}} = \frac{c}{2} M^2 (1_{\mathrm{RR}} - 1_{\mathrm{NSNS}}) \int_0^\infty dl \frac{\vartheta\left[{1/2 \atop 0}\right]^2}{\eta^6} \times & \\
\Bigg\{ \tilde{\mathcal{L}}[1,4/3]\tilde{\mathcal{L}}[3,4] \frac{\vartheta\left[{1/2 \atop 0}\right]^2}{\eta^6} - \frac{\vartheta\left[{1/2 \atop 1/6}\right]\vartheta\left[{1/2 \atop -1/6}\right]}{\vartheta\left[{1/2 \atop 2/3}\right]\vartheta\left[{1/2 \atop 1/3}\right]} - 3\frac{\vartheta\left[{1/2 \atop 1/3}\right]\vartheta\left[{1/2 \atop -1/3}\right]}{\vartheta\left[{1/2 \atop 5/6}\right]\vartheta\left[{1/2 \atop 1/6}\right]} & \qquad \text{(C.60)} \\
-4\frac{\vartheta\left[{1/2 \atop 1/2}\right]\vartheta\left[{1/2 \atop -1/2}\right]}{\vartheta\left[{1/2 \atop 1}\right]\vartheta\left[{1/2 \atop 0}\right]} - 3\frac{\vartheta\left[{1/2 \atop 2/3}\right]\vartheta\left[{1/2 \atop -2/3}\right]}{\vartheta\left[{1/2 \atop 7/6}\right]\vartheta\left[{1/2 \atop -1/6}\right]} - \frac{\vartheta\left[{1/2 \atop 5/6}\right]\vartheta\left[{1/2 \atop -5/6}\right]}{\vartheta\left[{1/2 \atop 4/3}\right]\vartheta\left[{1/2 \atop -1/3}\right]} \Bigg\} ,&
\end{aligned}
$$

$$
\begin{aligned}
\tilde{\mathcal{M}} = 8c (1_{\mathrm{RR}} - 1_{\mathrm{NSNS}}) \int_0^\infty dl \frac{\vartheta\left[{1/2 \atop 0}\right]^2}{\eta^6} \times & \\
\Bigg\{ C_0^0 \tilde{\mathcal{L}}[4,4/3]\tilde{\mathcal{L}}[12,4] \frac{\vartheta\left[{1/2 \atop 0}\right]^2}{\eta^6} - C_5^2 \frac{\vartheta\left[{1/2 \atop 1/6}\right]\vartheta\left[{1/2 \atop -1/6}\right]}{\vartheta\left[{1/2 \atop 2/3}\right]\vartheta\left[{1/2 \atop 1/3}\right]} - 3C_4^4 \frac{\vartheta\left[{1/2 \atop 1/3}\right]\vartheta\left[{1/2 \atop -1/3}\right]}{\vartheta\left[{1/2 \atop 5/6}\right]\vartheta\left[{1/2 \atop 1/6}\right]} & \\
+4C_3^0 \frac{\vartheta\left[{1/2 \atop 1/2}\right]\vartheta\left[{1/2 \atop -1/2}\right]}{\vartheta\left[{1/2 \atop 1}\right]\vartheta\left[{1/2 \atop 0}\right]} - 3C_2^2 \frac{\vartheta\left[{1/2 \atop 2/3}\right]\vartheta\left[{1/2 \atop -2/3}\right]}{\vartheta\left[{1/2 \atop 7/6}\right]\vartheta\left[{1/2 \atop -1/6}\right]} - C_1^4 \frac{\vartheta\left[{1/2 \atop 5/6}\right]\vartheta\left[{1/2 \atop -5/6}\right]}{\vartheta\left[{1/2 \atop 4/3}\right]\vartheta\left[{1/2 \atop -1/3}\right]} \Bigg\} .&
\end{aligned}
\qquad \text{(C.61)}
$$

We obtain the tadpole cancellation conditions

$$
M = 8 \qquad \text{(C.62)}
$$

and

$$
C_0^0 = C_5^2 = C_4^4 = -C_3^0 = C_2^2 = C_1^4 = M \qquad \text{(C.63)}
$$

together with (2.48). Calculating the Möbius strip starting from the other stacks of D-branes, we can find further sets of relations for the representation matrices of the Chan-Paton factors in the same way as we did for $\mathbb{Z}_4$.

The closed string spectrum

The untwisted sector consists of one $\mathcal{N} = 1$, $d = 6$ SUGRA multiplet and 3 hypermultiplets.

In the Θ twisted sector, there is only one fixed point, namely the point 11, which is invariant. In analogy to e.g. (C.23) and (C.24), with the corresponding moding for $\mathbb{Z}_6$, we find 3 scalars in the NSNS and 1 scalar in the RR sector, resulting in 2H together with the Θ^5 twisted sector.

In the Θ^2 twisted sector, 11 is invariant, 12-13 is a pair under Θ, 21-31 is a pair under $\Omega\mathcal{R}$ and Θ and 22-32-23-33 a quartet under $\Omega\mathcal{R}$ and Θ. From the RR and NSNS sector, the invariant point and the pairs each contribute 1H and the quartet 1H and 1T. Altogether, the Θ^2 and Θ^4 twisted sectors contribute 8H plus 2T.

In the Θ^3 twisted sector, 11 is invariant, 14-15-16, 41-51-61 and 44-55-66 form triplets under Θ and 45-56-64-46-54-65 are connected by $\Omega\mathcal{R}$ and Θ. The invariant point and the pairs each contribute 1H and the six connected points 1H and 1T, i.e. 5H and 1T, altogether

twist sector	**AB**
untwisted	SUGRA + 3H
$\Theta + \Theta^5$	2H
$\Theta^2 + \Theta^4$	8H + 2T
Θ^3	5H + 1T

(C.64)

The open string spectrum

In the untwisted NS sector the strings $(0,0)$, $(2,2)$ and $(4,4)$ as well as $(1,1)$, $(3,3)$ and $(5,5)$ are mapped onto each other by Θ. Thus the gauge group is obtained similar to $\mathbb{Z}_{2,4}$ and reads

$$U(4) \times U(4)\,. \tag{C.65}$$

Furthermore, we find 2H in the antisymmetric $(\mathbf{6},\mathbf{1}) + (\mathbf{1},\mathbf{6})$ in the untwisted sector.

The Θ twisted sector consists of the $(0,5)$ strings and the Θ^5 twisted sector consists of the $(0,1)$ strings, giving 2H in the bifundamental $(\mathbf{4},\mathbf{4})$.

The Θ^2 twisted sector contains some subtleties. The $(0,4)$ strings are located at the fixed points 11, 12 and 13, consider the figures C.8 and C.9. The $(0,4)$ string is invariant under $\Omega\mathcal{R}\Theta^2$ and $\Omega\mathcal{R}\Theta^5$, but only the fixed point 11 is invariant under both of these operations. The fixed points are invariant under $\Omega\mathcal{R}\Theta^2$ only and are interchanged under $\Omega\mathcal{R}\Theta^5$. Thus, the $(0,4)$ strings at fixed point 11 are constrained by

$$\lambda^{(0,4)} = I\lambda^{(0,4)T}I = -\lambda^{(0,4)T}\,, \tag{C.66}$$

leading to a matrix of the form (2.123) and therefore to 1H in the antisymmetric $(\mathbf{6},\mathbf{1})$. The $(1,5)$ strings yield 1H in the antisymmetric $(\mathbf{1},\mathbf{6})$. Of course, we find the same content in the Θ^4 twisted sector. The $(0,4)$ strings located at the fixed point 12 get mapped to strings located at the fixed point 13, as stated above and the invariance under $\Omega\mathcal{R}\Theta^2$ leads to the constraint

$$\lambda^{(0,4)} = -\lambda^{(0,4)T}\,, \tag{C.67}$$

which implies

$$\lambda^{(0,0)} = \begin{pmatrix} A_1 & X \\ -X^T & A_2 \end{pmatrix}\,, \tag{C.68}$$

and leads to 1H in the antisymmetric $(\mathbf{6},\mathbf{1})$ and $\frac{1}{2}$H in the adjoint $(\mathbf{16},\mathbf{1})$. The $(1,5)$ strings yield the same for the other factor of the gauge group and the same content is found in the Θ^4 twisted sector.

The symmetry in the Θ^3 twisted sector, i.e. the $(0,3)$ strings, is given by Θ^3 and thus

$$\lambda^{(0,3)} = \pm I \lambda^{(0,3)} I \,, \tag{C.69}$$

leading to (2.126). This gives 1H in the bifundamental $(\mathbf{4},\mathbf{4})$. From figure C.9 we can read off a multiplicity of 4 for this sector.

Altogether, we have found

twist sector	**AB**	rep. of $[U(4)]^2$
untwisted	1V	$(\mathbf{16},\mathbf{1})+(\mathbf{1},\mathbf{16})$
	2H	$(\mathbf{6},\mathbf{1})+(\mathbf{1},\mathbf{6})$
$\Theta+\Theta^5$	2H	$(\mathbf{4},\mathbf{4})$
$\Theta^2+\Theta^4$	4H	$(\mathbf{6},\mathbf{1})+(\mathbf{1},\mathbf{6})$
	1H	$(\mathbf{16},\mathbf{1})+(\mathbf{1},\mathbf{16})$
Θ^3	4H	$(\mathbf{4},\mathbf{4})$

(C.70)

The massless spectrum again satisfies the anomaly constraint (2.128) and is in agreement with [20].

Bibliography

[1] G. Aldazabal, A. Font, L. E. Ibáñez, and G. Violero, *$D = 4$, $N = 1$, type IIB orientifolds*, Nucl. Phys. **B536** (1998), 29–68, hep-th/9804026.

[2] G. Aldazabal, S. Franco, L. E. Ibáñez, R. Rabadan, and A. M. Uranga, *$D = 4$ chiral string compactifications from intersecting branes*, (2000), hep-th/0011073.

[3] G. Aldazabal, S. Franco, L. E. Ibáñez, R. Rabadan, and A. M. Uranga, *Intersecting brane worlds*, JHEP **02** (2001), 047, hep-ph/0011132.

[4] G. Aldazabal, L. E. Ibáñez, and F. Quevedo, *Standard-like models with broken supersymmetry from type I string vacua*, JHEP **01** (2000), 031, hep-th/9909172.

[5] G. Aldazabal and A. M. Uranga, *Tachyon-free non-supersymmetric type IIB orientifolds via brane-antibrane systems*, JHEP **10** (1999), 024, hep-th/9908072.

[6] C. Angelantonj, M. Bianchi, G. Pradisi, A. Sagnotti, and Y. S. Stanev, *Chiral asymmetry in four-dimensional open-string vacua*, Phys. Lett. **B385** (1996), 96–102, hep-th/9606169.

[7] C. Angelantonj and R. Blumenhagen, *Discrete deformations in type I vacua*, Phys. Lett. **B473** (2000), 86–93, hep-th/9911190.

[8] C. Angelantonj, R. Blumenhagen, and M. R. Gaberdiel, *Asymmetric orientifolds, brane supersymmetry breaking and non-BPS branes*, Nucl. Phys. **B589** (2000), 545–576, hep-th/0006033.

[9] I. Antoniadis, *A possible new dimension at a few TeV*, Phys. Lett. **B246** (1990), 377–384.

[10] I. Antoniadis, N. Arkani-Hamed, S. Dimopoulos, and G. R. Dvali, *New dimensions at a millimeter to a Fermi and superstrings at a TeV*, Phys. Lett. **B436** (1998), 257–263, hep-ph/9804398.

[11] N. Arkani-Hamed, S. Dimopoulos, and G. R. Dvali, *The hierarchy problem and new dimensions at a millimeter*, Phys. Lett. **B429** (1998), 263–272, hep-ph/9803315.

[12] C. Bachas, *A way to break supersymmetry*, (1995), hep-th/9503030.

[13] C. P. Bachas, *Lectures on D-branes*, (1998), hep-th/9806199.

[14] M. Berkooz, M. R. Douglas, and R. G. Leigh, *Branes intersecting at angles*, Nucl. Phys. **B480** (1996), 265–278, hep-th/9606139.

[15] M. Berkooz and R. G. Leigh, *A $D = 4$ $N = 1$ orbifold of type I strings*, Nucl. Phys. **B483** (1997), 187–208, hep-th/9605049.

[16] M. Bianchi, G. Pradisi, and A. Sagnotti, *Toroidal compactification and symmetry breaking in open string theories*, Nucl. Phys. **B376** (1992), 365–386.

[17] M. Bianchi and A. Sagnotti, *On the systematics of open string theories*, Phys. Lett. **B247** (1990), 517–524.

[18] M. Bianchi and A. Sagnotti, *Twist symmetry and open string wilson lines*, Nucl. Phys. **B361** (1991), 519–538.

[19] R. Blumenhagen, L. Görlich, and B. Körs, *Supersymmetric 4d orientifolds of type IIA with D6-branes at angles*, JHEP **01** (2000), 040, hep-th/9912204.

[20] R. Blumenhagen, L. Görlich, and B. Körs, *Supersymmetric orientifolds in 6d with D-branes at angles*, Nucl. Phys. **B569** (2000), 209–228, hep-th/9908130.

[21] R. Blumenhagen, L. Görlich, B. Körs, and D. Lüst, *Asymmetric orbifolds, noncommutative geometry and type I string vacua*, Nucl. Phys. **B582** (2000), 44–64, hep-th/0003024.

[22] R. Blumenhagen, L. Görlich, B. Körs, and D. Lüst, *Noncommutative compactifications of type I strings on tori with magnetic background flux*, JHEP **10** (2000), 006, hep-th/0007024.

[23] R. Blumenhagen, B. Körs, and D. Lüst, *Type I strings with F- and B-flux*, JHEP **02** (2001), 030, hep-th/0012156.

[24] R. Blumenhagen, B. Körs, D. Lüst, and T. Ott, *The standard model from stable intersecting brane world orbifolds*, (2001), hep-th/0107138.

[25] P. Candelas, Gary T. Horowitz, A. Strominger, and E. Witten, *Vacuum configurations for superstrings*, Nucl. Phys. **B258** (1985), 46–74.

[26] J. O. Conrad, *Brane tensions and coupling constants from within M- theory*, Phys. Lett. **B421** (1998), 119–124, hep-th/9708031.

[27] E. Cremmer, B. Julia, and J. Scherk, *Supergravity theory in 11 dimensions*, Phys. Lett. **B76** (1978), 409–412.

[28] M. Cvetič, M. Plumacher, and J. Wang, *Three family type IIB orientifold string vacua with non- abelian wilson lines*, JHEP **04** (2000), 004, hep-th/9911021.

[29] M. Cvetič, G. Shiu, and A. M. Uranga, *Chiral four-dimensional $N = 1$ supersymmetric type IIA orientifolds from intersecting D6-branes*, (2001), hep-th/0107166.

[30] A. Dabholkar and J. Park, *An orientifold of type-IIB theory on $K3$*, Nucl. Phys. **B472** (1996), 207–220, hep-th/9602030.

[31] A. Dabholkar and J. Park, *Strings on orientifolds*, Nucl. Phys. **B477** (1996), 701–714, hep-th/9604178.

[32] J. Dai, R. G. Leigh, and J. Polchinski, *New connections between string theories*, Mod. Phys. Lett. **A4** (1989), 2073–2083.

[33] K. R. Dienes, E. Dudas, and T. Gherghetta, *Extra spacetime dimensions and unification*, Phys. Lett. **B436** (1998), 55–65, hep-ph/9803466.

[34] L. J. Dixon, Jeffrey A. Harvey, C. Vafa, and E. Witten, *Strings on orbifolds*, Nucl. Phys. **B261** (1985), 678–686.

[35] L. J. Dixon, Jeffrey A. Harvey, C. Vafa, and E. Witten, *Strings on orbifolds. 2*, Nucl. Phys. **B274** (1986), 285–314.

[36] M. J. Duff, R. R. Khuri, and J. X. Lu, *String solitons*, Phys. Rept. **259** (1995), 213–326, hep-th/9412184.

[37] W. Fischler and L. Susskind, *Dilaton tadpoles, string condensates and scale invariance. 2*, Phys. Lett. **B173** (1986), 262.

[38] A. Font, Luis E. Ibáñez, H.-P. Nilles, and F. Quevedo, *Yukawa couplings in degenerate orbifolds: Towards a realistic $SU(3) \times SU(2) \times U(1)$ superstring*, Phys. Lett. **210B** (1988), 101.

[39] A. Font, Luis E. Ibáñez, F. Quevedo, and A. Sierra, *The construction of 'realistic' four-dimensional strings through orbifolds*, Nucl. Phys. **B331** (1990), 421–474.

[40] S. Förste, G. Honecker, and R. Schreyer, *Orientifolds with branes at angles*, JHEP **06** (2001), 004, hep-th/0105208.

[41] S. Förste, G. Honecker, and R. Schreyer, *Supersymmetric $\mathbb{Z}_N \times \mathbb{Z}_M$ orientifolds in 4d with D-branes at angles*, Nucl. Phys. **B593** (2001), 127–154, hep-th/0008250.

[42] M. R. Gaberdiel, *Lectures on non-BPS dirichlet branes*, Class. Quant. Grav. **17** (2000), 3483–3520, hep-th/0005029.

[43] E. G. Gimon and C. V. Johnson, *$K3$ orientifolds*, Nucl. Phys. **B477** (1996), 715–745, hep-th/9604129.

[44] E. G. Gimon and J. Polchinski, *Consistency conditions for orientifolds and D-manifolds*, Phys. Rev. **D54** (1996), 1667–1676, hep-th/9601038.

[45] A. Giveon, M. Porrati, and E. Rabinovici, *Target space duality in string theory*, Phys. Rept. **244** (1994), 77–202, hep-th/9401139.

[46] F. Gliozzi, J. Scherk, and David I. Olive, *Supersymmetry, supergravity theories and the dual spinor model*, Nucl. Phys. **B122** (1977), 253–290.

[47] J. Govaerts, *Quantum consistency of open string theories*, Phys. Lett. **B220** (1989), 77.

[48] M. B. Green and J. H. Schwarz, *Anomaly cancellation in supersymmetric $d = 10$ gauge theory and superstring theory*, Phys. Lett. **B149** (1984), 117–122.

[49] M. B. Green, J. H. Schwarz, and E. Witten, *Superstring theory. Vol. 1: Introduction*, Cambridge, Uk: Univ. Pr. (1987) 469 P. (Cambridge Monographs On Mathematical Physics).

[50] M. B. Green, J. H. Schwarz, and E. Witten, *Superstring theory. Vol. 2: Loop amplitudes, anomalies and phenomenology*, Cambridge, Uk: Univ. Pr. (1987) 596 P. (Cambridge Monographs On Mathematical Physics).

[51] D. J. Gross, J. A. Harvey, E. J. Martinec, and R. Rohm, *Heterotic string theory. 1. The free heterotic string*, Nucl. Phys. **B256** (1985), 253.

[52] D. J. Gross, J. A. Harvey, E. J. Martinec, and R. Rohm, *Heterotic string theory. 2. The interacting heterotic string*, Nucl. Phys. **B267** (1986), 75.

[53] D. J. Gross, J. A. Harvey, E. J. Martinec, and Ryan Rohm, *The heterotic string*, Phys. Rev. Lett. **54** (1985), 502–505.

[54] P. Hořava, *Background duality of open string models*, Phys. Lett. **B231** (1989), 251.

[55] P. Horava, *Strings on world sheet orbifolds*, Nucl. Phys. **B327** (1989), 461.

[56] P. Hořava and E. Witten, *Eleven-dimensional supergravity on a manifold with boundary*, Nucl. Phys. **B475** (1996), 94–114, hep-th/9603142.

[57] P. Hořava and E. Witten, *Heterotic and type I string dynamics from eleven dimensions*, Nucl. Phys. **B460** (1996), 506–524, hep-th/9510209.

[58] L. E. Ibáñez, F. Marchesano, and R. Rabadan, *Getting just the standard model at intersecting branes*, (2001), hep-th/0105155.

[59] Luis E. Ibáñez, Jihn E. Kim, H.-P. Nilles, and F. Quevedo, *Orbifold compactifications with three families of $SU(3) \times SU(2) \times U(1)^n$*, Phys. Lett. **B191** (1987), 282–286.

[60] Z. Kakushadze, *Aspects of $N = 1$ type I-heterotic duality in four dimensions*, Nucl. Phys. **B512** (1998), 221–236, hep-th/9704059.

[61] Z. Kakushadze, *On four dimensional $N = 1$ type I compactifications*, Nucl. Phys. **B535** (1998), 311–334, hep-th/9806008.

[62] Z. Kakushadze and G. Shiu, *A chiral $N = 1$ type I vacuum in four dimensions and its heterotic dual*, Phys. Rev. **D56** (1997), 3686–3697, hep-th/9705163.

[63] D. Lüst and S. Theisen, *Lectures on string theory*, Lect. Notes Phys. **346** (1989), 1–346.

[64] W. Nahm, *Supersymmetries and their representations*, Nucl. Phys. **B135** (1978), 149.

[65] H.-P. Nilles, M. Olechowski, and M. Yamaguchi, *Supersymmetry breaking and soft terms in M-theory*, Phys. Lett. **B415** (1997), 24–30, hep-th/9707143.

[66] H.-P. Nilles, M. Olechowski, and M. Yamaguchi, *Supersymmetry breakdown at a hidden wall*, Nucl. Phys. **B530** (1998), 43–72, hep-th/9801030.

[67] J. Polchinski, *String theory. Vol. 1: An introduction to the bosonic string*, Cambridge, UK: Univ. Pr. (1998) 402 p.

[68] J. Polchinski, *String theory. Vol. 2: Superstring theory and beyond*, Cambridge, UK: Univ. Pr. (1998) 531 p.

[69] J. Polchinski, *Dirichlet-branes and Ramond-Ramond charges*, Phys. Rev. Lett. **75** (1995), 4724–4727, hep-th/9510017.

[70] J. Polchinski, *TASI lectures on D-branes*, (1996), hep-th/9611050.

[71] J. Polchinski and Y. Cai, *Consistency of open superstring theories*, Nucl. Phys. **B296** (1988), 91.

[72] J. Polchinski and E. Witten, *Evidence for heterotic - type I string duality*, Nucl. Phys. **B460** (1996), 525–540, hep-th/9510169.

[73] G. Pradisi and A. Sagnotti, *Open string orbifolds*, Phys. Lett. **B216** (1989), 59.

[74] R. Rabadán and A. M. Uranga, *Type IIB orientifolds without untwisted tadpoles, and non- BPS D-branes*, JHEP **01** (2001), 029, hep-th/0009135.

[75] A. Sagnotti, *Open strings and their symmetry groups*, Talk presented at the Cargese Summer Institute on Non- Perturbative Methods in Field Theory, Cargese, France, Jul 16-30, 1987.

[76] J. H. Schwarz, *Superstring theory*, Phys. Rept. **89** (1982), 223–322.

[77] A. Sen, *Stable non-BPS bound states of BPS D-branes*, JHEP **08** (1998), 010, hep-th/9805019.

[78] A. Sen, *Stable non-BPS states in string theory*, JHEP **06** (1998), 007, hep-th/9803194.

[79] A. Sen, *Tachyon condensation on the brane antibrane system*, JHEP **08** (1998), 012, hep-th/9805170.

[80] A. Sen and B. Zwiebach, *Tachyon condensation in string field theory*, JHEP **03** (2000), 002, hep-th/9912249.

[81] A. Strominger and E. Witten, *New manifolds for superstring compactification*, Commun. Math. Phys. **101** (1985), 341.

[82] P. K. Townsend, *The eleven-dimensional supermembrane revisited*, Phys. Lett. **B350** (1995), 184–187, hep-th/9501068.

[83] P. K. Townsend, *Four lectures on M-theory*, (1996), hep-th/9612121.

[84] E. Witten, *String theory dynamics in various dimensions*, Nucl. Phys. **B443** (1995), 85–126, hep-th/9503124.

[85] G. Zwart, *Four-dimensional $N = 1$ $\mathbb{Z}_N \times \mathbb{Z}_M$ orientifolds*, Nucl. Phys. **B526** (1998), 378–392, hep-th/9708040.